



Supplement of

The SPARC water vapour assessment II: biases and drifts of water vapour satellite data records with respect to frost point hygrometer records

Michael Kiefer et al.

Correspondence to: Michael Kiefer (michael.kiefer@kit.edu)

The copyright of individual parts of the supplement might differ from the article licence.

Contents

1	Introduction	2
2	Individual comparisons between satellite data records and stations	5
2.1	ACE-FTS H2O_v3.5tg (ACE)	5
2.2	GOMOS H2O_v6 (GOM)	9
2.3	HALOE H2O_V19 (HAL)	14
2.4	HIRDLS H2O_V7 (HIR)	17
2.5	ILAS_II v3.0 (ILA)	21
2.6	MAESTRO v30 (MST)	22
2.7	MIPAS-BOL H2O_FR2.3 (MBH)	25
2.8	MIPAS-BOL H2O_MA2.3 (MBM)	28
2.9	MIPAS-BOL H2O_RR2.3 (MBR)	32
2.10	MIPAS-ESA V7H_H2O_NOM (MEH)	38
2.11	MIPAS-ESA V7R_H2O_MA (MEM)	41
2.12	MIPAS-ESA V7R_H2O_NOM (MER)	45
2.13	MIPAS-IMK V5H_H2O_20 (MIH)	51
2.14	MIPAS-IMK V5R_H2O_220 (MIR)	54
2.15	MIPAS-IMK V5R_H2O_522 (MIM)	60
2.16	MIPAS-OXF H2O_FR1.30 (MOH)	64
2.17	MIPAS-OXF H2O_MA1.30 (MOM)	67
2.18	MIPAS-OXF H2O_RR1.30 (MOR)	71
2.19	MLS-Aura H2O_V4.2 (MLS)	77
2.20	POAM_III H2O_v4 (POM)	83
2.21	SAGE_II v7.0 (SG2)	85
2.22	SAGE_III H2O_v4 (SG3)	88
2.23	SCIAMACHY H2O_LO_V1.0 (SCL)	90
2.24	SCIAMACHY H2O_SOOE_V1.0 (SC1)	91
2.25	SCIAMACHY H2O_SOOP_V4.21 (SC4)	93
2.26	SCIAMACHY H2O_V3.01 (SC3)	95
2.27	SMILES H2O_A.2.9.2 (SLA)	100
2.28	SMILES H2O_B.2.9.2 (SLB)	102
2.29	SMR H2O_020_544 (SM5)	104
2.30	SMR H2O_021_489 (SM4)	111
2.31	SOFIE H2O_v01.3 (SOF)	114

1 Introduction

In this supplement we collect the results of the individual comparisons between satellite (SAT) data records and frost point hygrometer (NOAA FPH or CFH, short: FP) balloon soundings of stratospheric water vapour. For each pair of SAT and FP measurements within the coincidence criteria (see Section 2.2 of the main paper) the respective means, standard deviations, mean differences and their standard errors of the mean (SEM) were calculated according to Eqs. (7,8) (see main paper). Mean profiles, mean differences with their SEM, and the number of coincident measurements, are shown respectively in the three panels of each figure.

For identification of the FP and SAT data sets we mostly use the three letter codes as given in Tables S1 and S2.

Table S1: Overview of NOAA frost point hygrometer (NOAA FPH) and cryogenic frost point hygrometer (CFH) stations used for comparisons with satellite data.

Code	Site	Period	Instr. type	Lat / deg	Long / deg
BND	Bandung	2003 – 2004	CFH	-6.9	107.6
BEL	Beltsville	2006 – 2011	CFH	39.0	-76.9
BIK	Biak	2006 – 2015	CFH	-1.2	136.1
BLD	Boulder	1980 – present	CFH/NOAA FPH	40.0	-105.2
FTS	Fort Sumner	1996 – 2004	NOAA FPH	34.5	-104.3
HAN	Hanoi	2007 – 2011	CFH	21.0	105.8
HIL	Hilo	2002 – present	CFH/NOAA FPH	19.7	-155.1
HOU	Houston	2011, 2013	CFH/NOAA FPH	29.6	-95.2
HUN	Huntsville	2002	NOAA FPH	34.7	-86.7
KIR	Kiruna	1991 – 2003	NOAA FPH	67.8	20.2
KTB	Kototabang	2007 – 2008	CFH	-0.2	100.3
KMG	Kunming	2009 – 2012	CFH/NOAA FPH	25.0	102.7
LRN	La Reunion	2005 – 2011	CFH	-20.9	55.5
LDR	Lauder	2003 – present	NOAA FPH	-45.0	169.7
LSA	Lhasa	2010, 2013	CFH	29.7	91.1
LIN	Lindenberg	2006 – present	CFH	52.2	14.1
NYA	Ny Alesund	2002 – 2004, 2013 – present	CFH/NOAA FPH	78.9	11.9
RVM	Research Vessel Mirai ^a	2011	CFH	-8.0/1.2	80.5/136.1
SCR	San Cristobal	1998 – 2007	CFH/NOAA FPH	-0.9	-89.6
SJC	San Jose ^b	2005 – present	CFH	9.9	-84.1
SOD	Sodankyla	1995 – present	CFH/NOAA FPH	67.4	26.6
SGP	Southern Great Plains	2003	CFH	36.6	-97.5
TMF	Table Mountain	2006 – 2009, 2013	CFH/NOAA FPH	34.4	-117.7
TRW	Tarawa	2005 – 2010	CFH	1.4	172.9
TNG	Tengchong	2010	CFH	25.0	98.5
WTK	Watukosek	2001 – 2003	NOAA FPH	-7.6	112.7
YAN	Yangjiang	2010	CFH	21.9	112.0

a) ship cruise

b) includes Alajuela, HerediaSan Pedro, and San Jose

Table S2: Overview of the water vapour data sets from satellites used in this study. Column Ret. type indicates whether the retrieval result was number density $n_{\text{H}_2\text{O}}$ (marked ND) instead of vmr, and whether the retrieval was done in the $\log(\text{vmr})$ or $\log(n_{\text{H}_2\text{O}})$ domain. The numbers in the last column indicate the frost point hygrometer stations the data records of which have been used for the drift analysis of the satellite data (compare to Table S1).

Code	Instrument	Data set version	Label	Ret. type	Kernel type
ACE	ACE-FTS	3.5	ACE-FTS v3.5		SK
GOM	GOMOS	LATMOS v6	GOMOS		SK
HAL	HALOE	v19	HALOE		SK
HIR	HIRDLS	v7	HIRDLS		SK
ILA	ILAS-II	v3/3.01	ILAS-II		SK
MST	MAESTRO	Research	MAESTRO		SK
MBH	MIPAS	Bologna V5H v2.3 NOM	MIPAS-Bologna V5H		AK
MBR		Bologna V5R v2.3 NOM	MIPAS-Bologna V5R NOM		AK
MBM		Bologna V5R v2.3 MA	MIPAS-Bologna V5R MA		AK
MEH		ESA V7H v7 NOM	MIPAS-ESA V7H		AK
MER		ESA V7R v7 NOM	MIPAS-ESA V7R NOM		AK
MEM		ESA V7R v7 MA	MIPAS-ESA V7R MA		AK
MIH		IMK/IAA V5H v20 NOM	MIPAS-IMKIAA V5H	log	AK
MIR		IMK/IAA V5R v220/1 NOM	MIPAS-IMKIAA V5R NOM	log	AK
MIM		IMK/IAA V5R v522 MA	MIPAS-IMKIAA V5R MA	log	AK
MOH		Oxford V5H v1.30 NOM	MIPAS-Oxford V5H	log	SK
MOR		Oxford V5R v1.30 NOM	MIPAS-Oxford V5R NOM	log	AK
MOM		Oxford V5R v1.30 MA	MIPAS-Oxford V5R MA	log	SK
MLS		MLS	v4.2	MLS	log
POM	POAM III	v4	POAM III		SK
SG2	SAGE II	v7.00	SAGE II		SK
SG3	SAGE III	Solar occ. v4	SAGE III		SK
SC3	SCIAMACHY	Limb v3.01	SCIAMACHY limb	ND/log	AK
SCL		Lunar occultation v1.0	SCIAMACHY lunar	ND/log	SK
SC1		Solar occ. - OEM v1.0	SCIAMACHY solar OEM	ND/log	AK
SC4		Solar occ. - OP v4.2.1	SCIAMACHY solar OP	ND	SK
SLA	SMILES	NICT v2.9.2 band A	SMILES-NICT band A		SK
SLB		NICT v2.9.2 band B	SMILES-NICT band B		SK
SM5	SMR	v2.0 544 GHz	SMR 544 GHz	log	AK
SM4		v2.1 489 GHz	SMR 489 GHz		AK
SOF	SOFIE	v1.3	SOFIE		SK

2 Individual comparisons between satellite data records and stations

2.1 ACE-FTS H2O_v3.5tg (ACE)

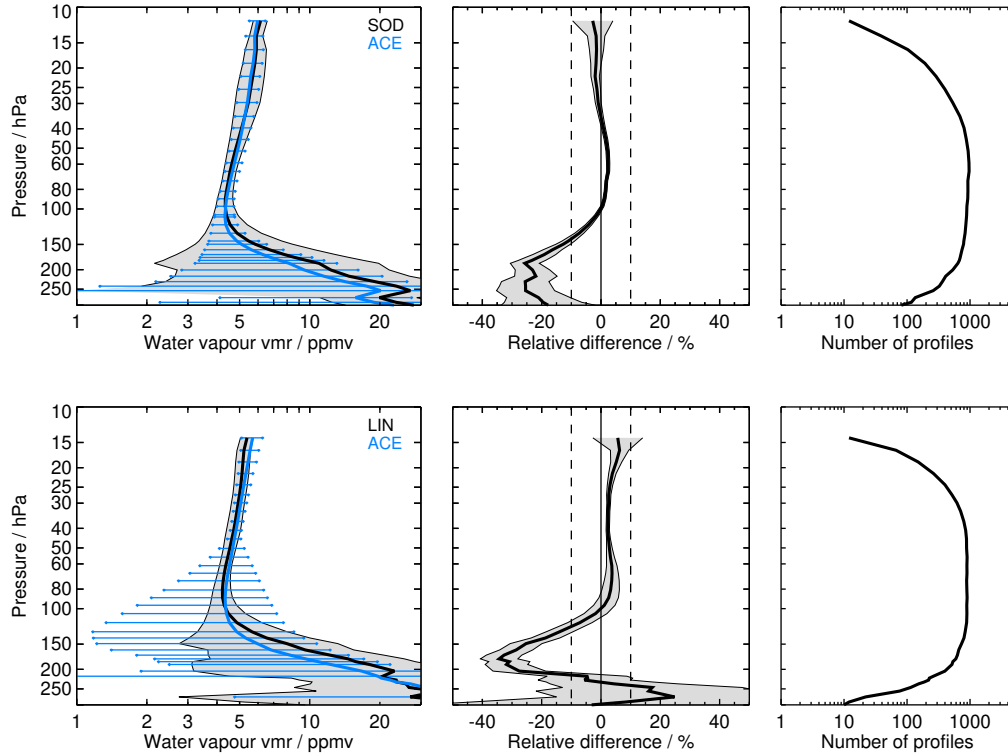


Figure S1: Comparison of ACE water vapour profiles with FP profiles at SOD, LIN, BLD, BEL, TMF, LSA, HOU, TNG, KMG, HIL, SJC, SCR, BIK, and BIK balloon sites. Mean profiles over all coincidences of the respective pairings are shown. The individual profiles were cut at the respective local tropopause before averaging. Left panels: mean profiles (FP: black, SAT: blue) and their standard deviations (FP: grey shading, SAT: horizontal blue lines). Middle panel: Relative mean bias and twice its standard error of the mean (grey shading, $\pm 2\sigma_{\text{bias}}$), calculated as the mean differences SAT-FP divided by the mean FP profile and multiplied by 100; the vertical dashed lines enclose the $\pm 10\%$ range. Right panel: number of data points along the vertical grid. This number can vary over the vertical range, depending on the altitude coverage of the individual coincident SAT and FP profiles, respectively.

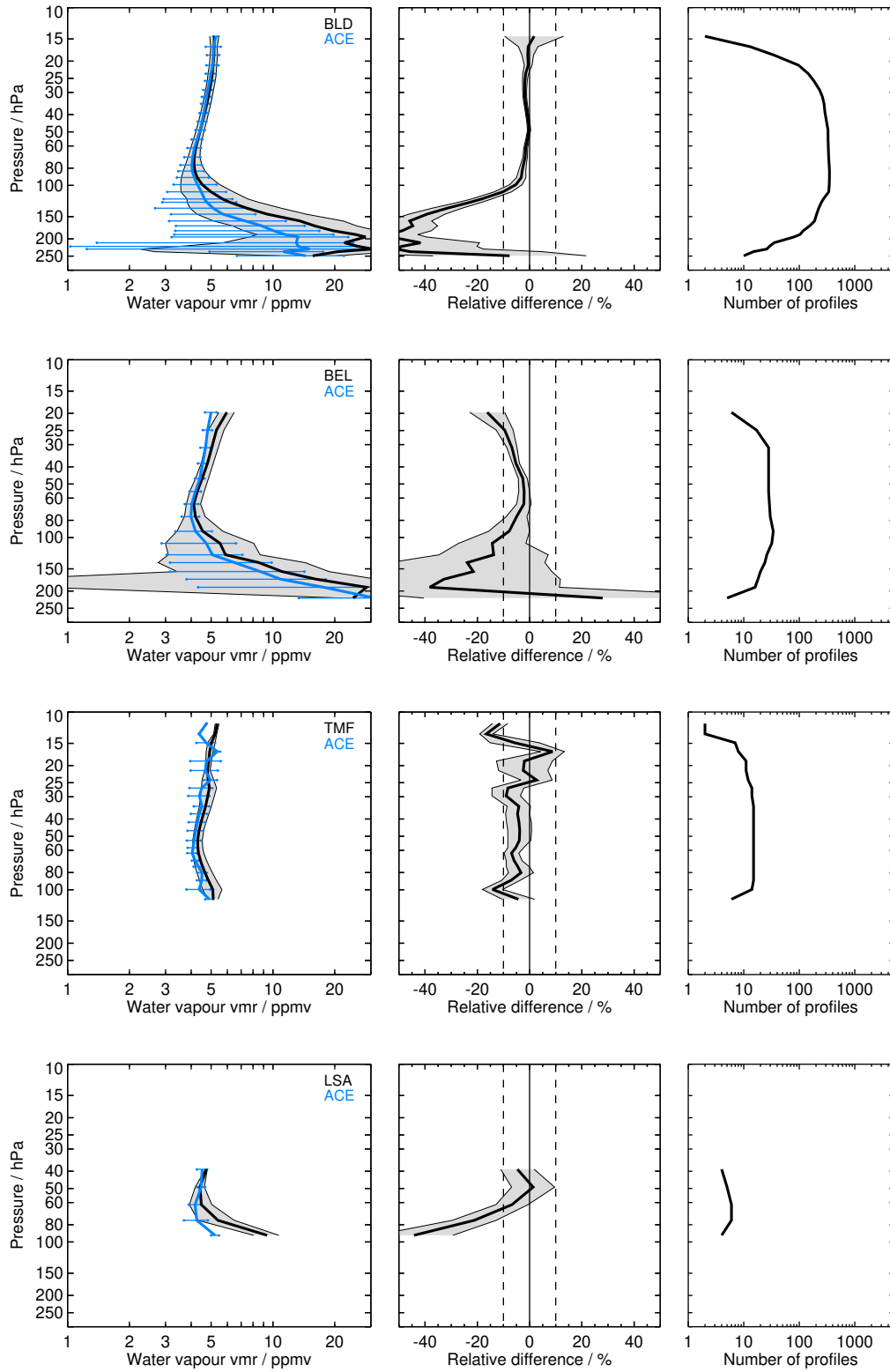


Figure S1: Continued.

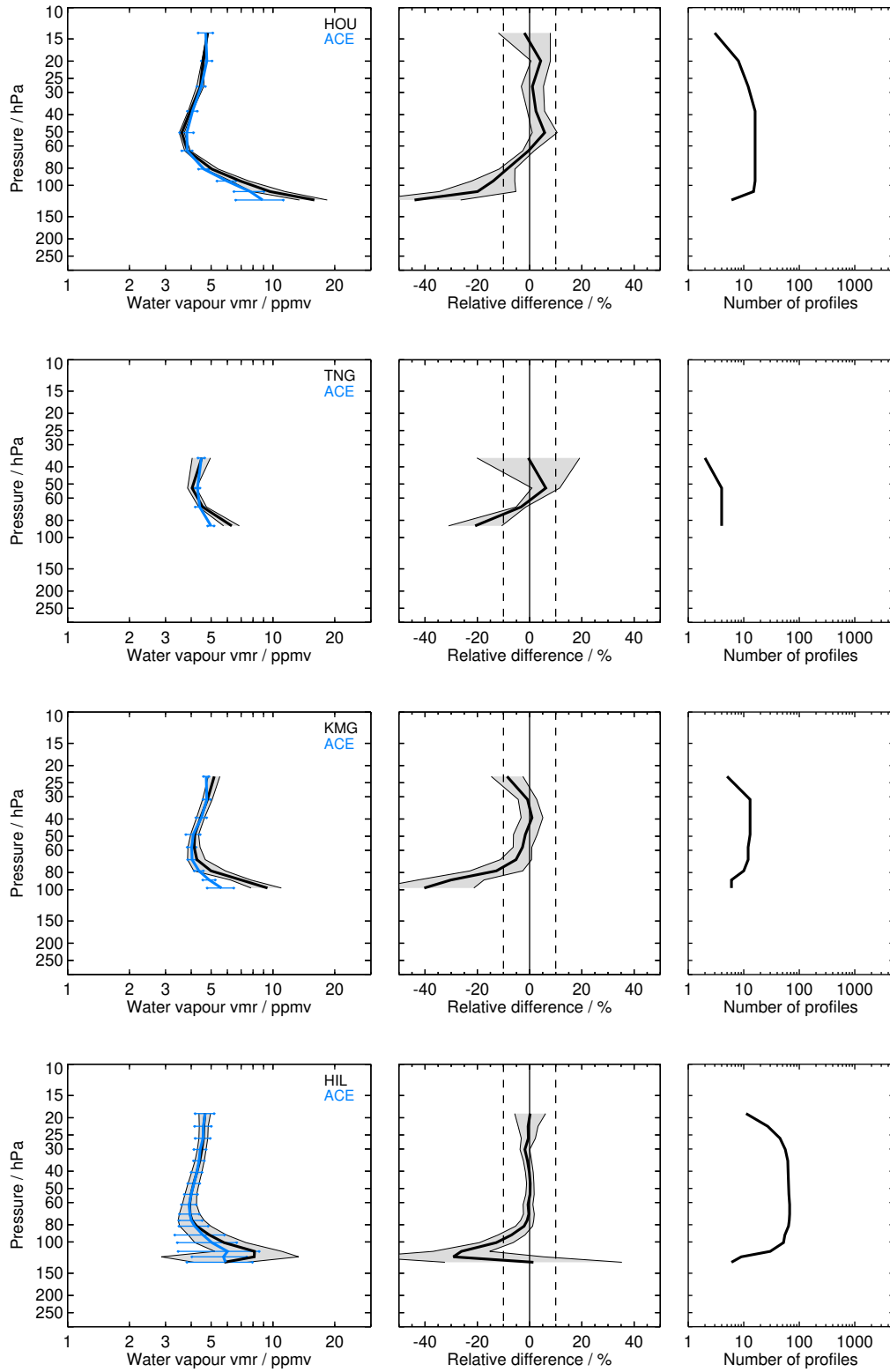


Figure S1: Continued.

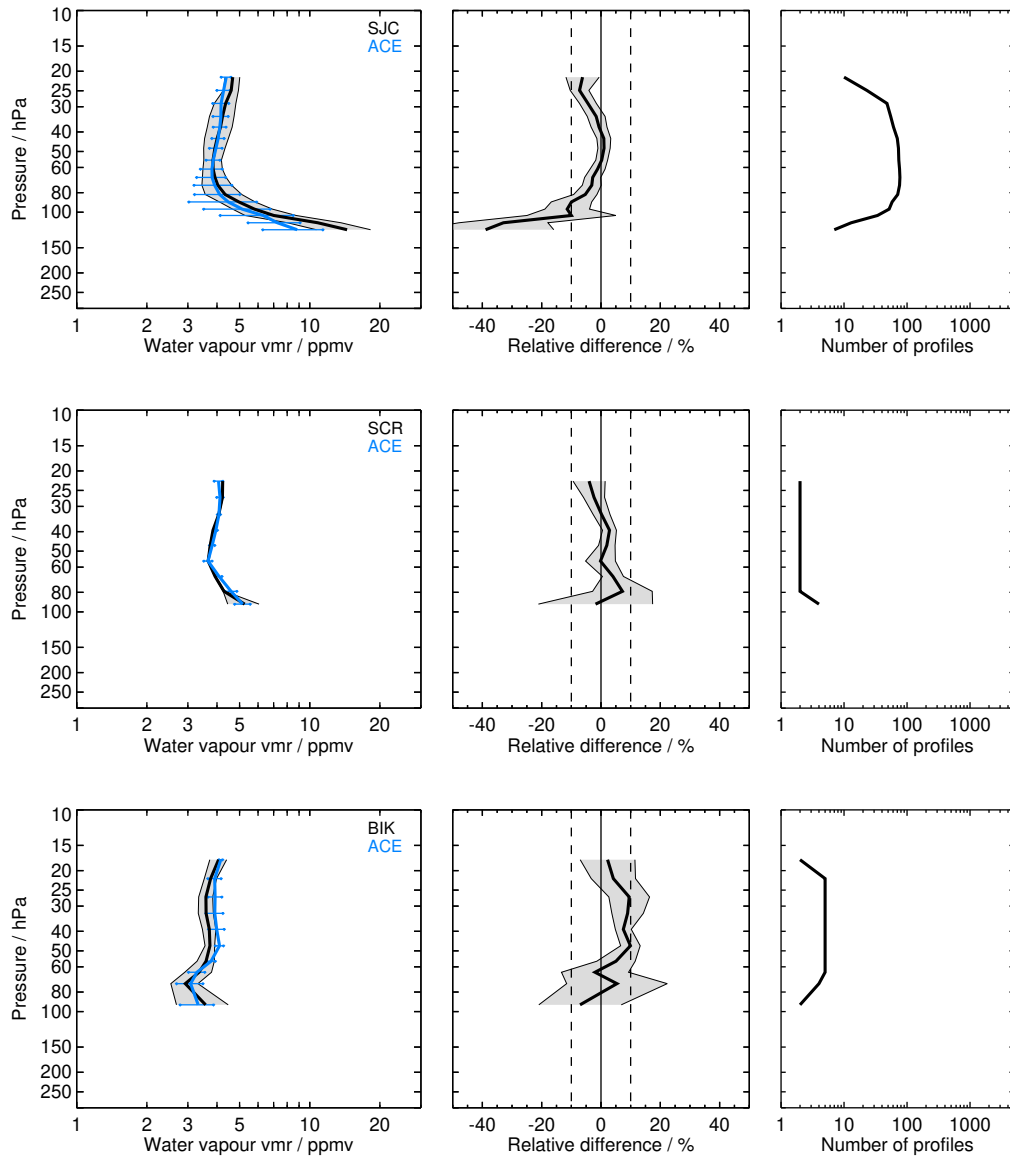


Figure S1: Continued.

2.2 GOMOS H2O_v6 (GOM)

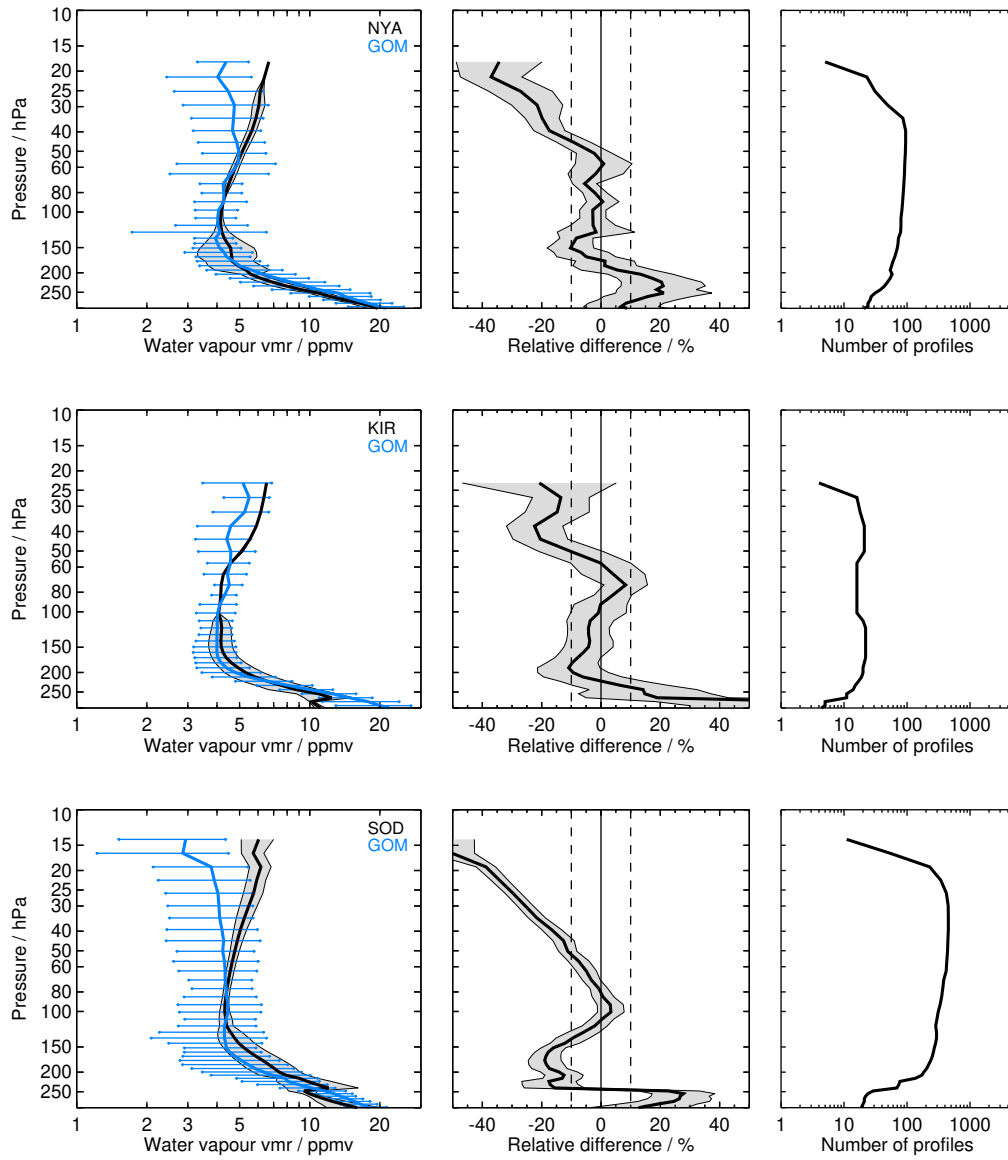


Figure S2: Same as Fig. S1 but for GOM and the NYA, KIR, SOD, LIN, BLD, BEL, FTS, LSA, TNG, KMG, YAN, HAN, HIL, SJC, SCR, LDR, and LDR balloon sites.

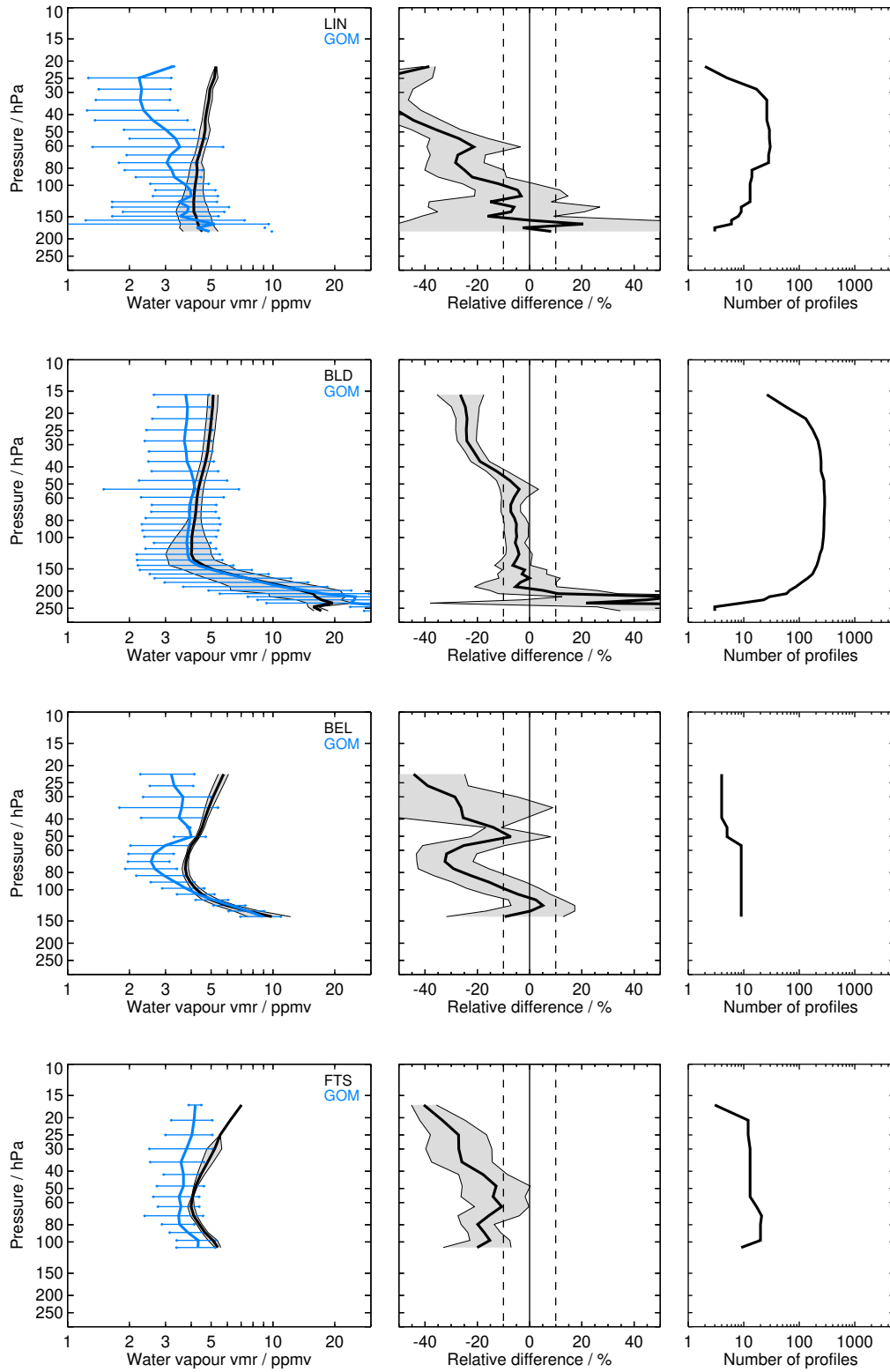


Figure S2: Continued.

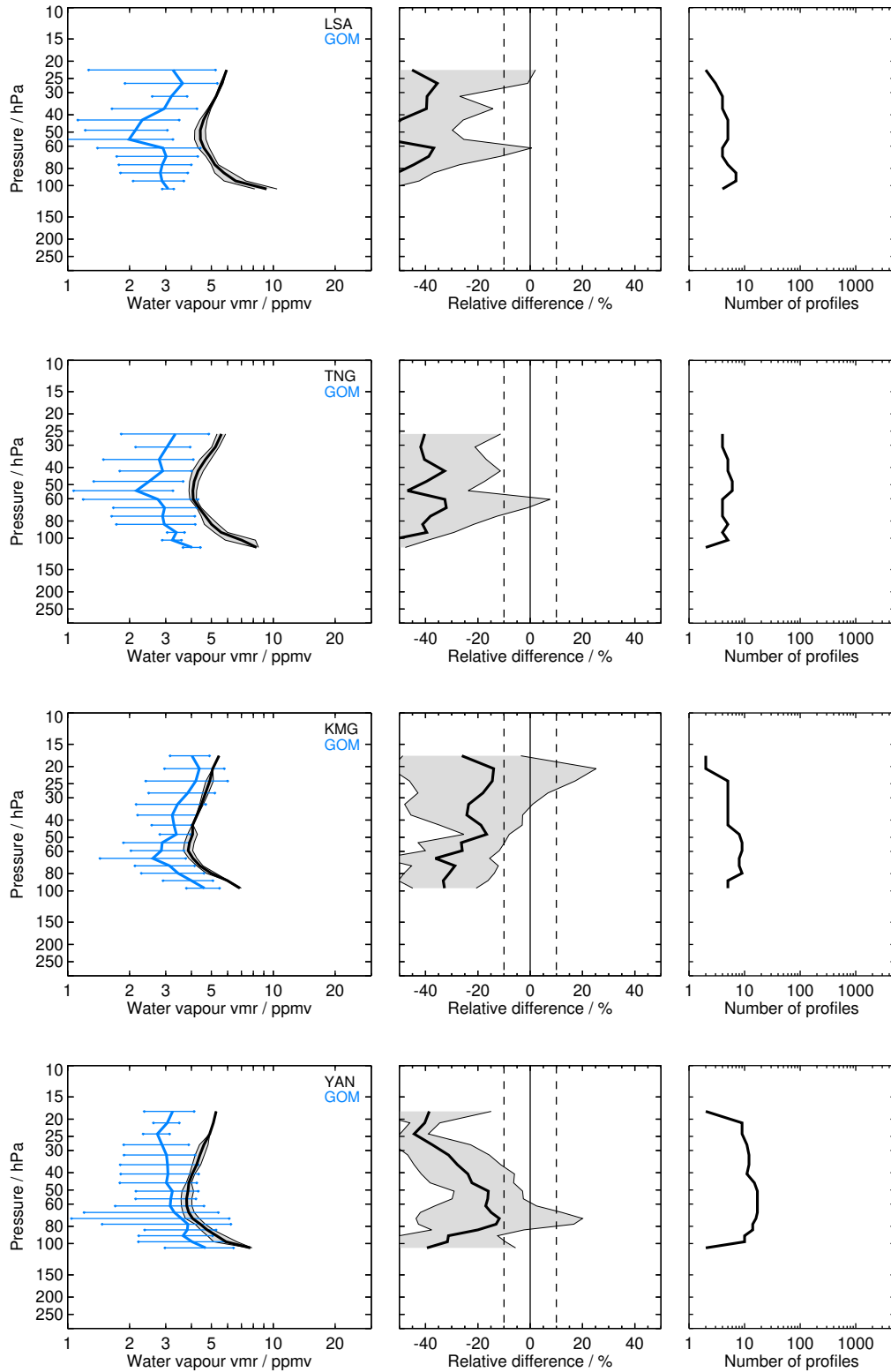


Figure S2: Continued.

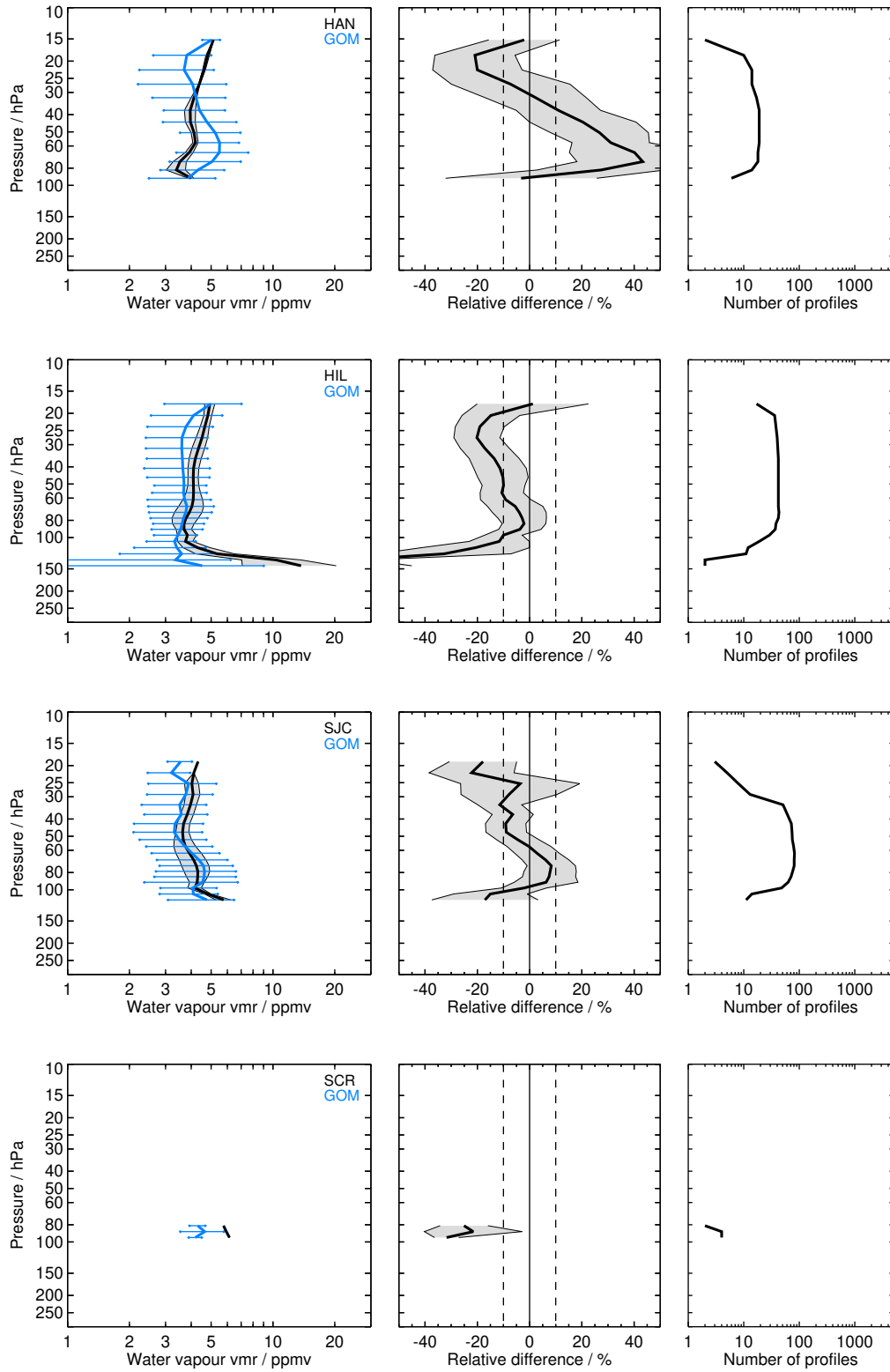


Figure S2: Continued.

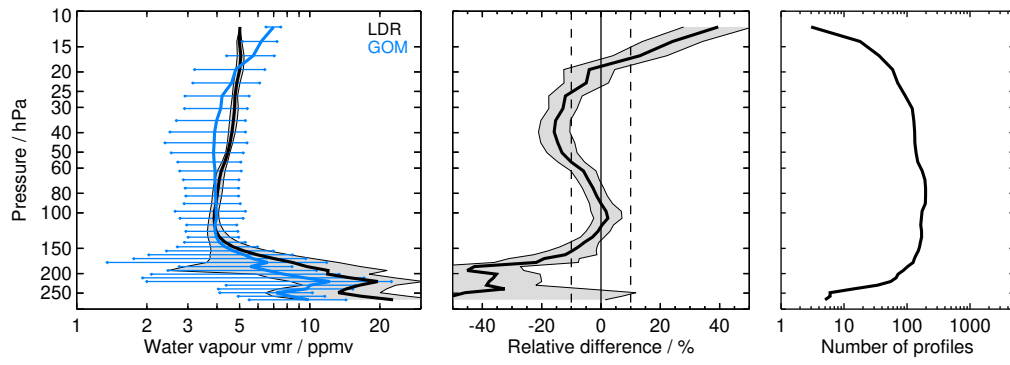


Figure S2: Continued.

2.3 HALOE H2O_V19 (HAL)

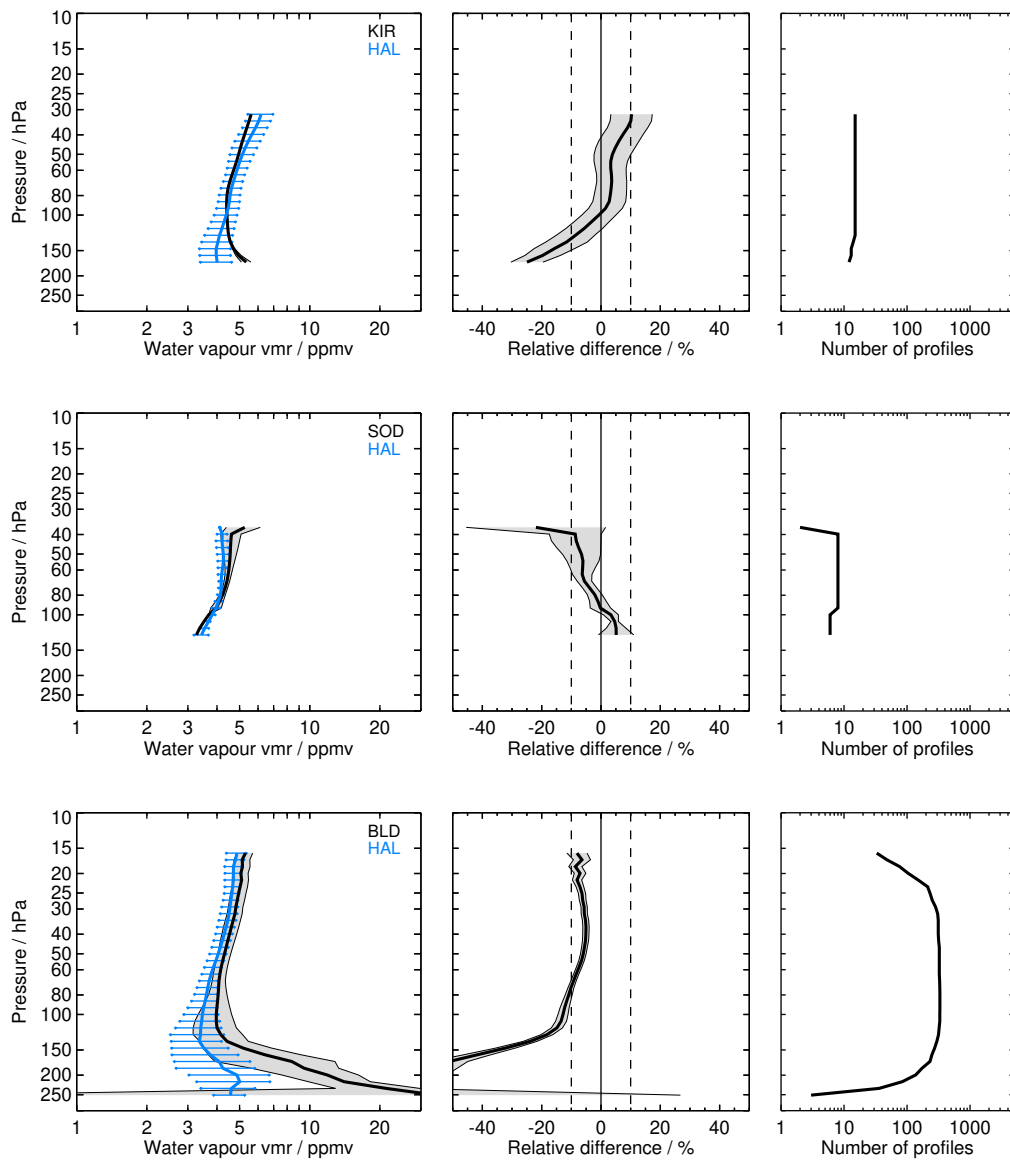


Figure S3: Same as Fig. S1 but for HAL and the KIR, SOD, BLD, SGP, HUN, FTS, HIL, SJC, SCR, LDR, and LDR balloon sites.

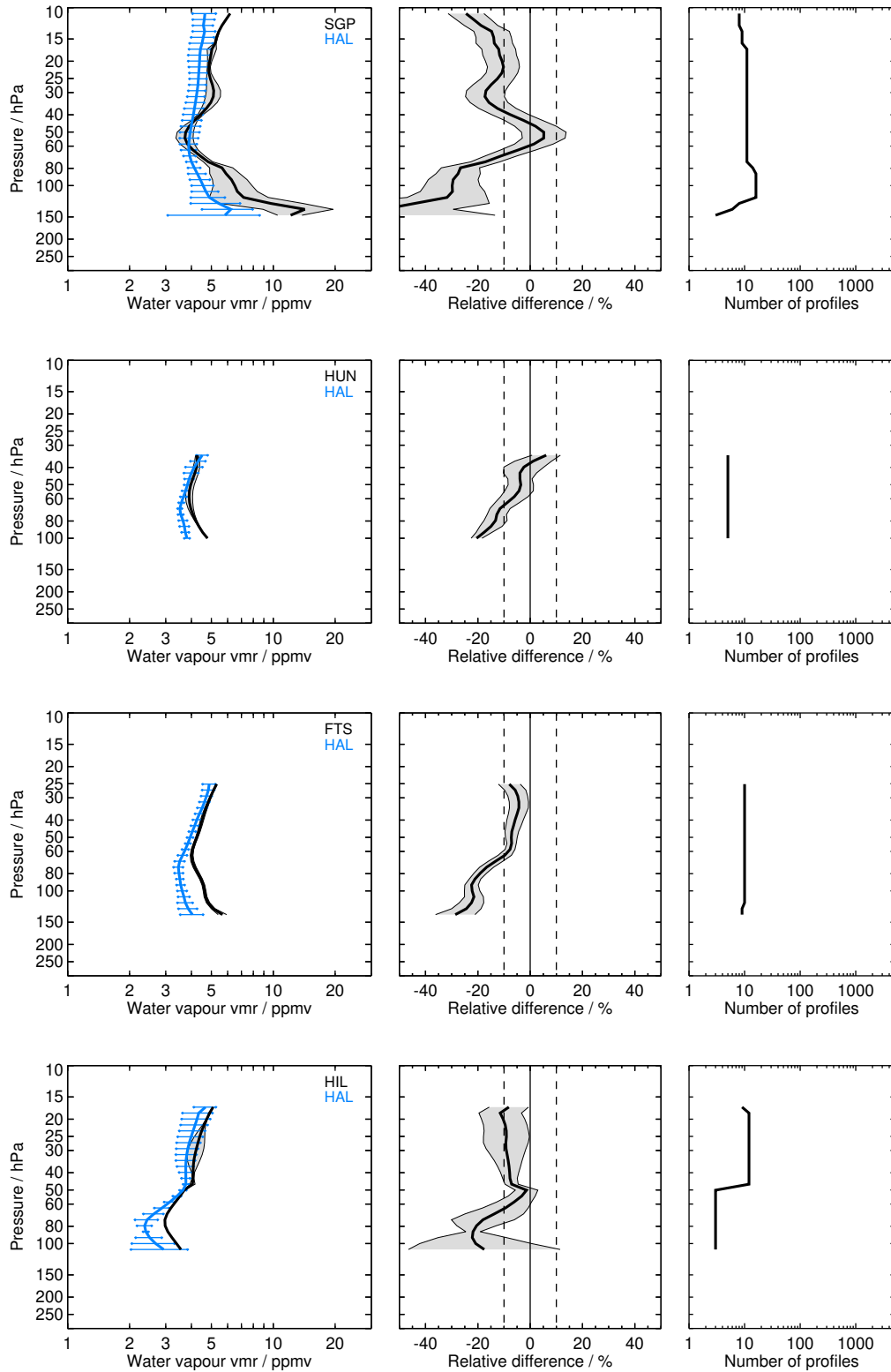


Figure S3: Continued.

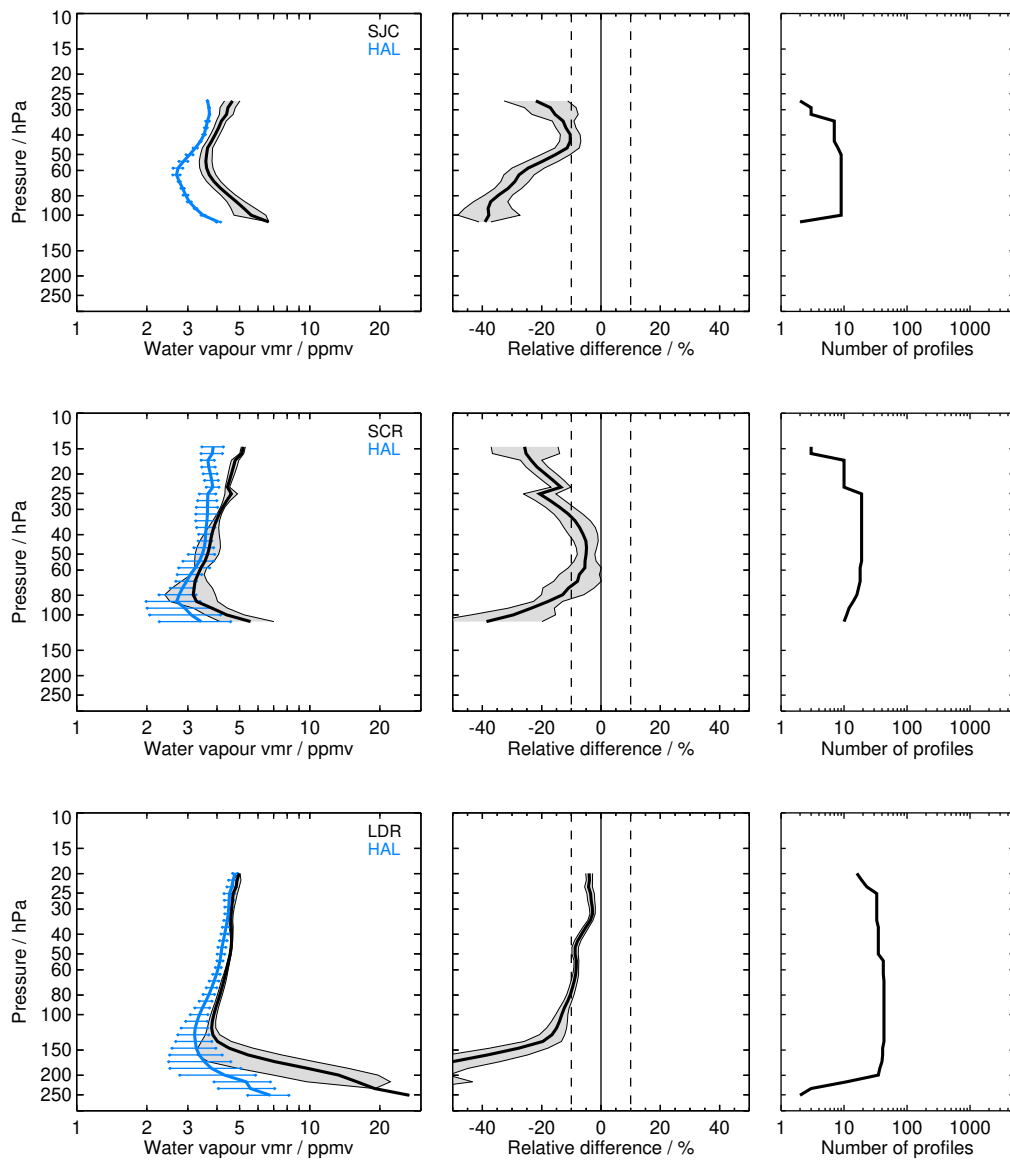


Figure S3: Continued.

2.4 HIRDLS H2O_V7 (HIR)

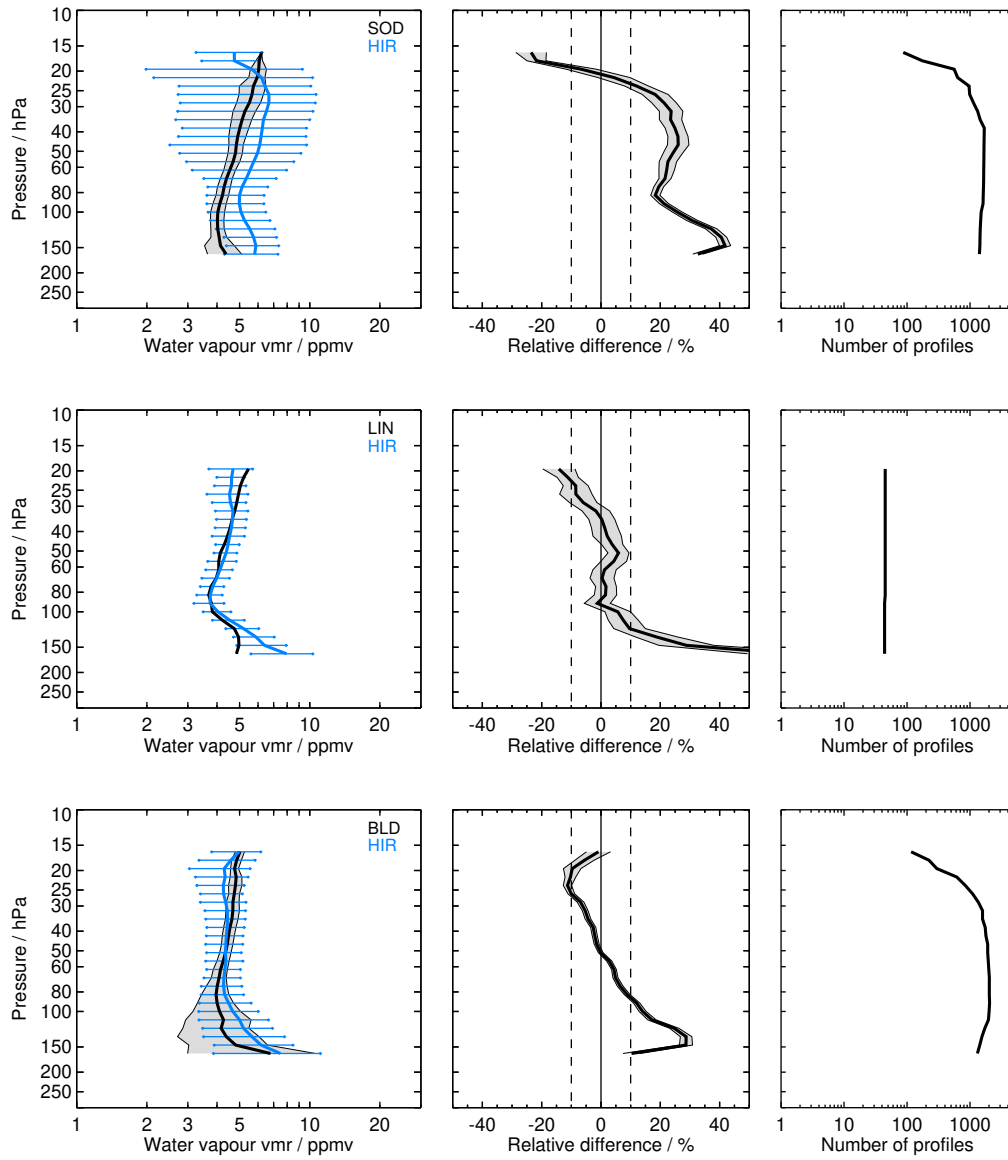


Figure S4: Same as Fig. S1 but for HIR and the SOD, LIN, BLD, BEL, TMF, HAN, SJC, TRW, KTB, SCR, BIK, LRN, LDR, and LDR balloon sites.

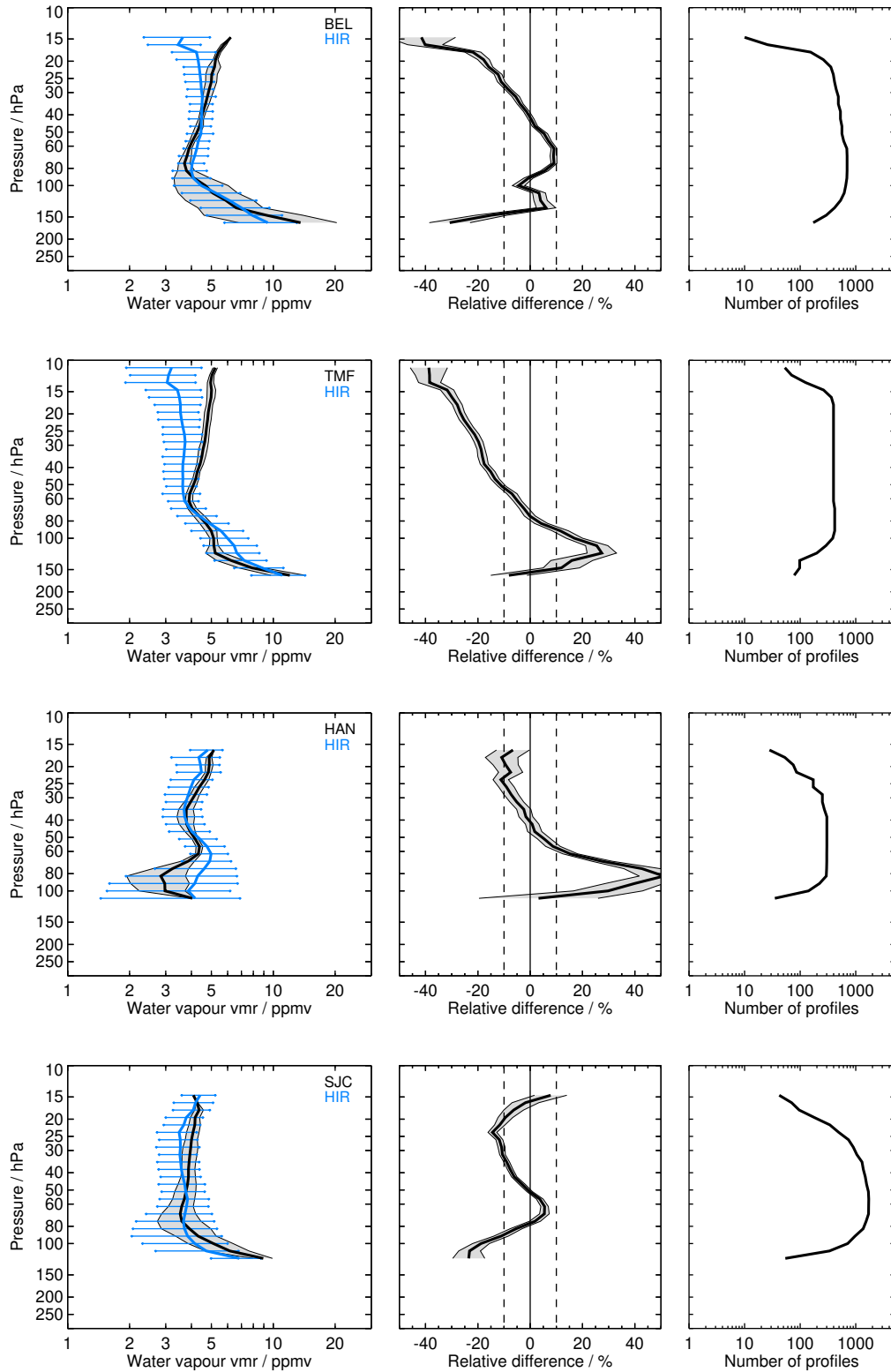


Figure S4: Continued.

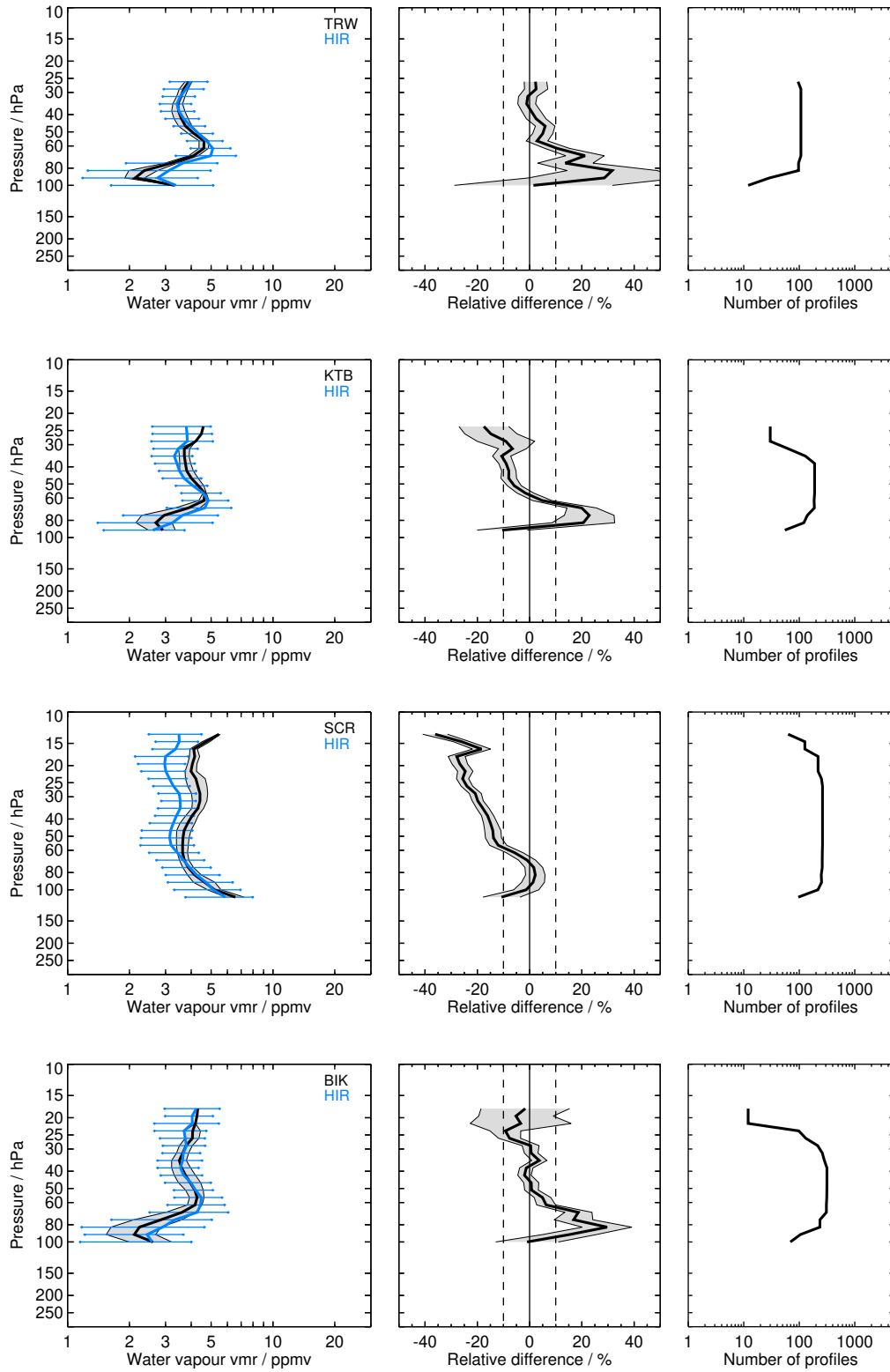


Figure S4: Continued.

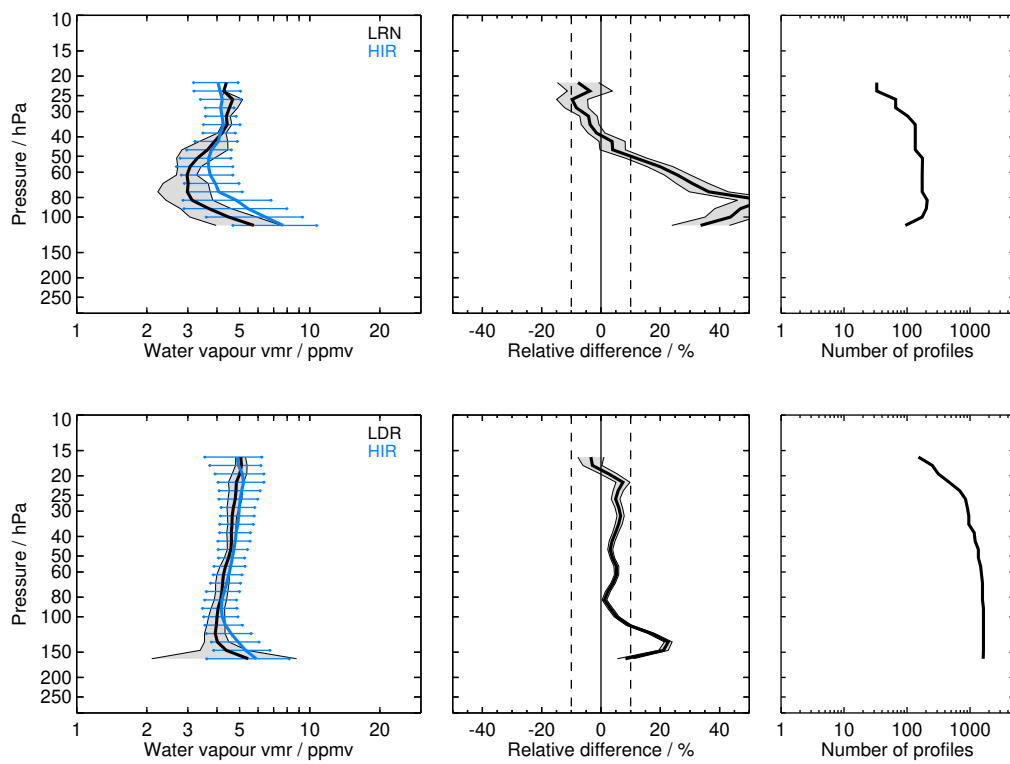


Figure S4: Continued.

2.5 ILAS_II v3.0 (ILA)

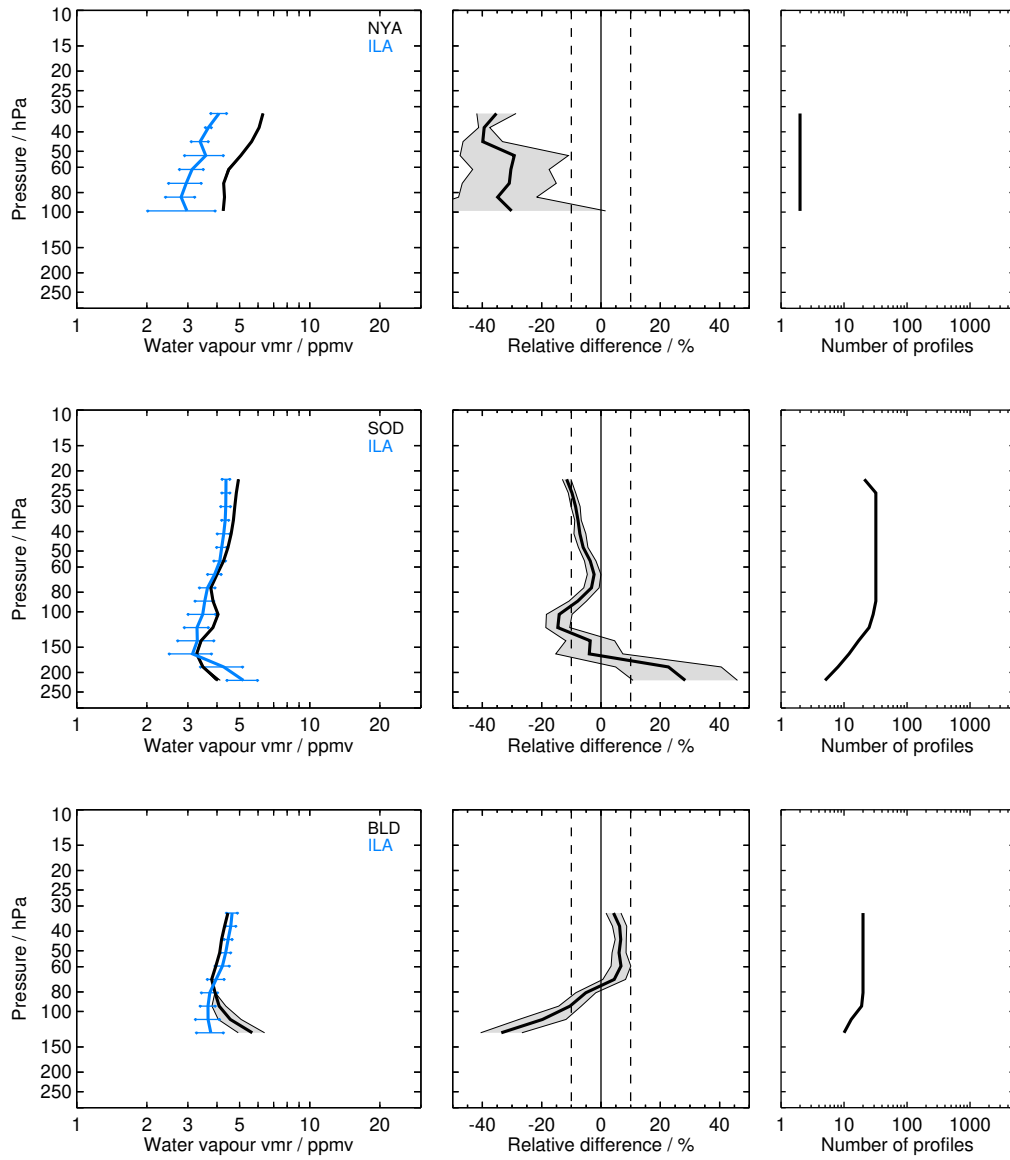


Figure S5: Same as Fig. S1 but for ILA and the NYA, SOD, BLD, and BLD balloon sites.

2.6 MAESTRO v30 (MST)

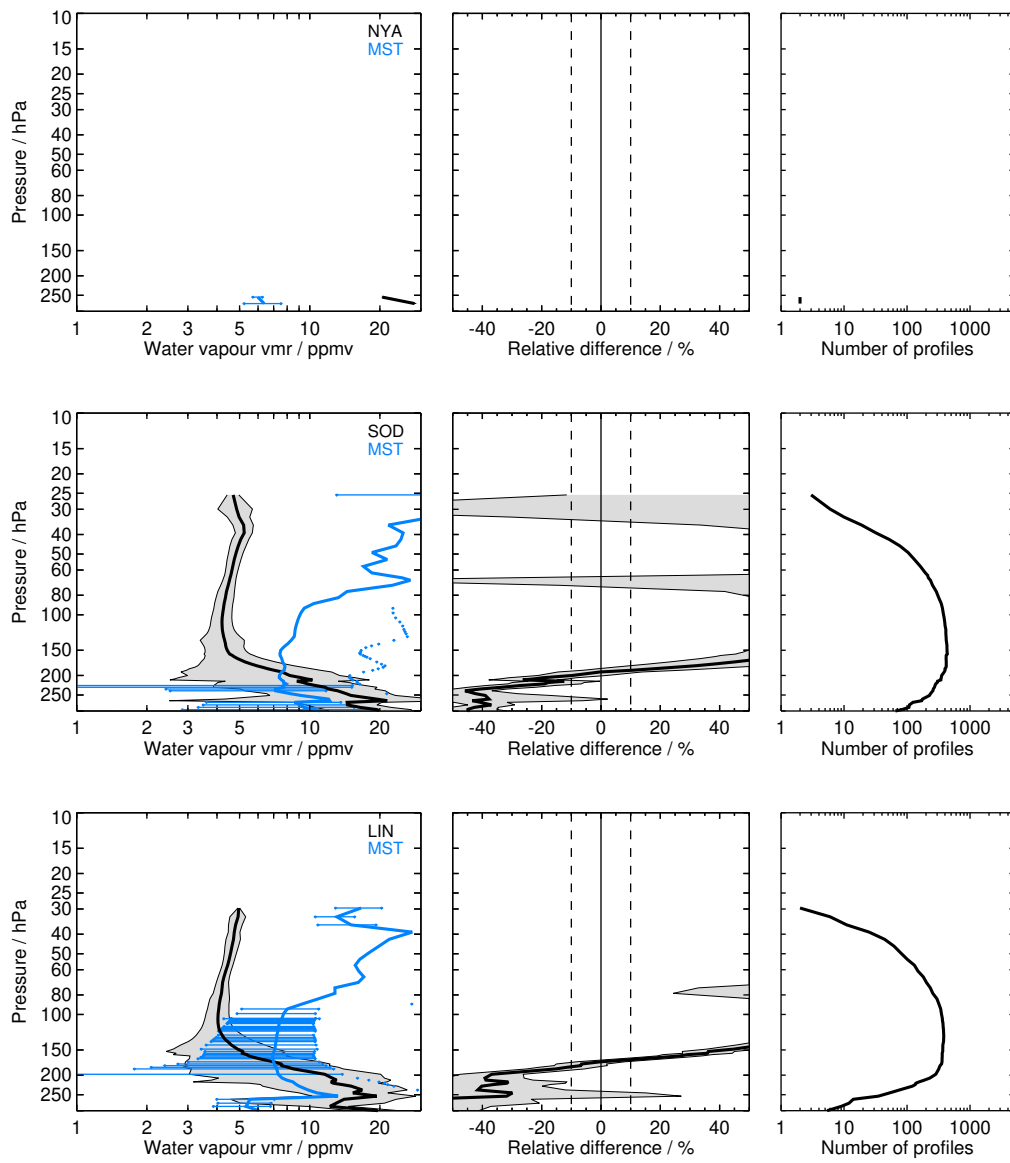


Figure S6: Same as Fig. S1 but for MST and the NYA, SOD, LIN, BLD, BEL, LSA, HOU, KMG, HIL, SJC, LDR, and LDR balloon sites.

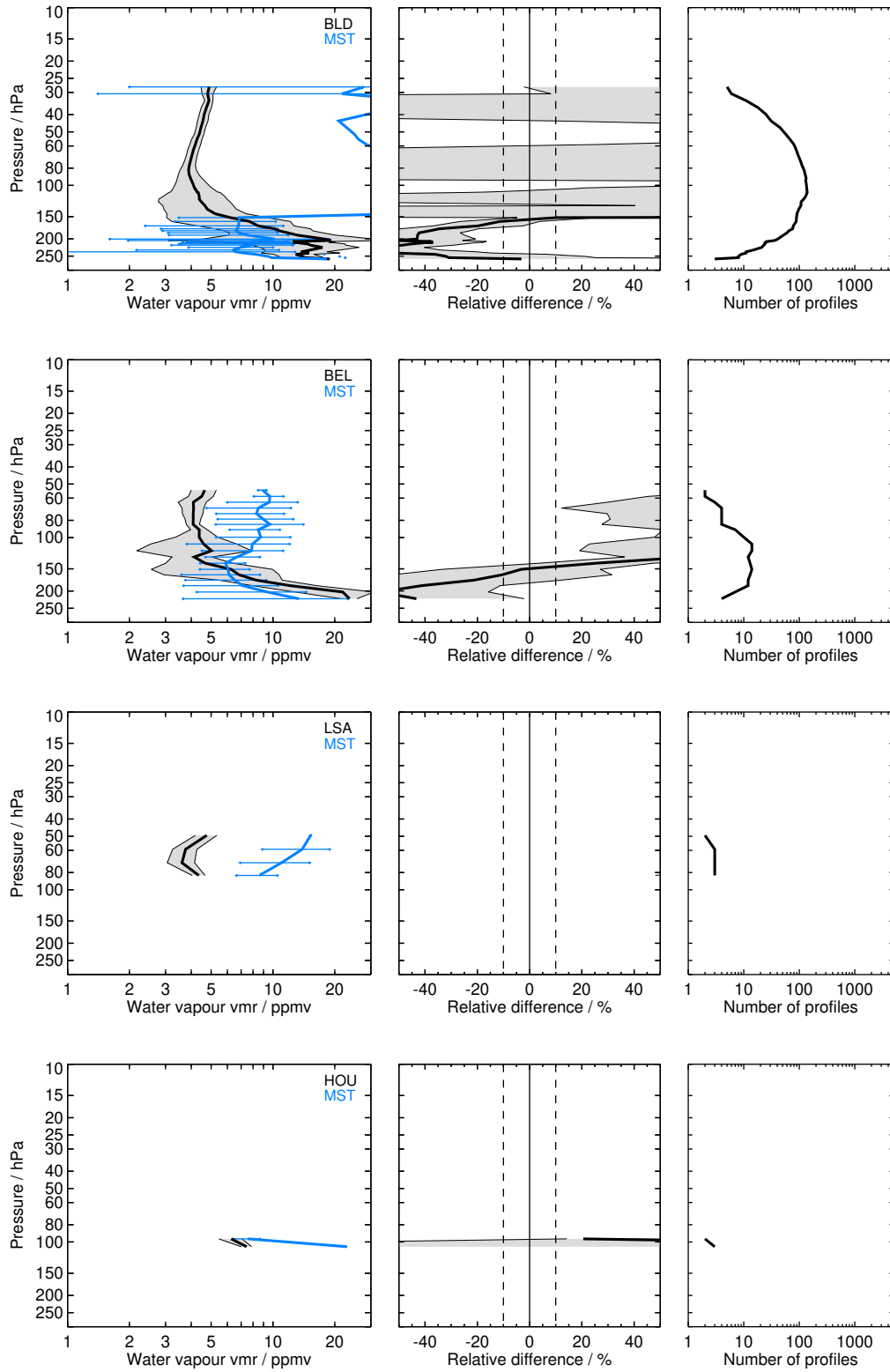


Figure S6: Continued.

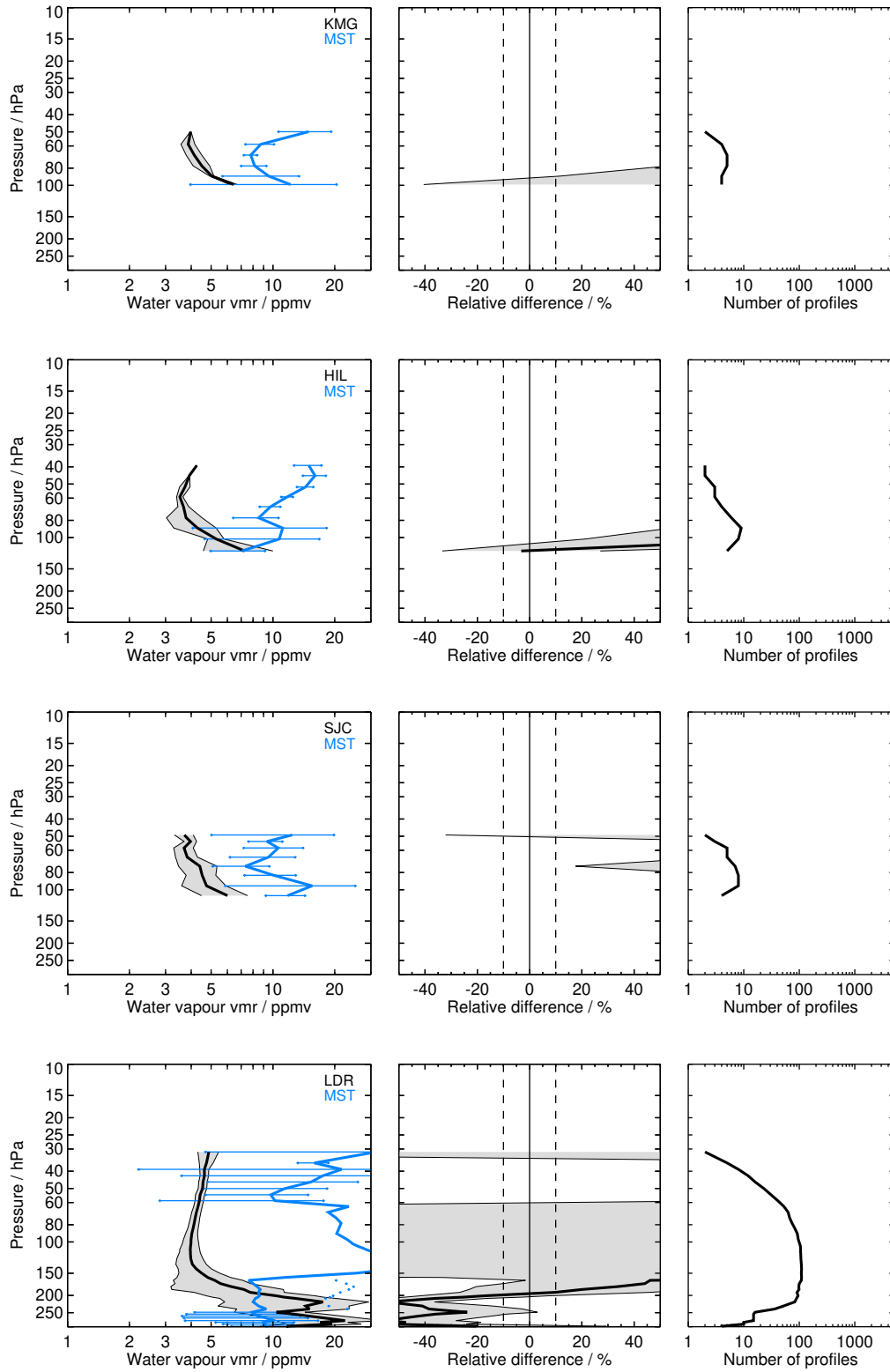


Figure S6: Continued.

2.7 MIPAS-BOL H2O_FR2.3 (MBH)

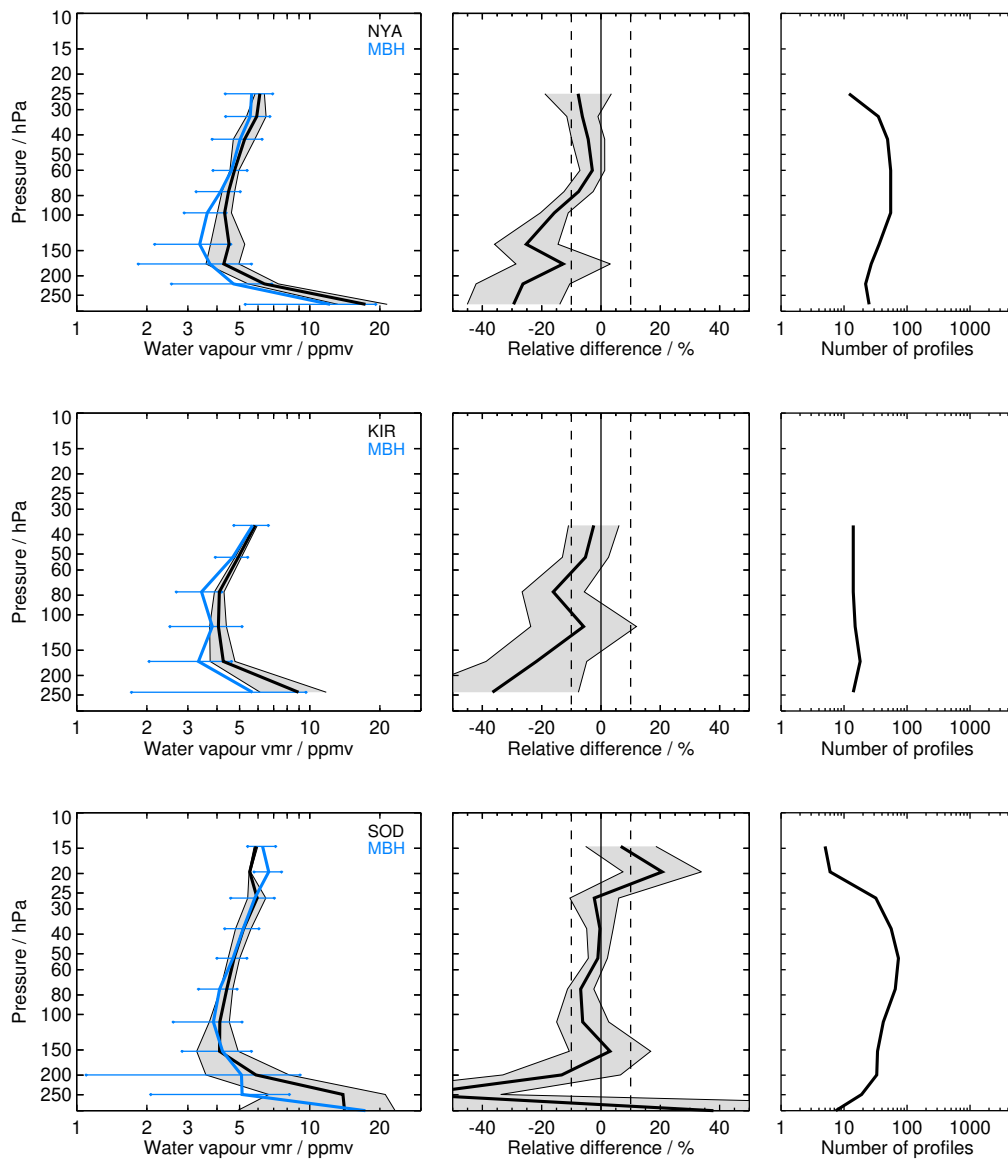


Figure S7: Same as Fig. S1 but for MBH and the NYA, KIR, SOD, BLD, SGP, HUN, FTS, HIL, SCR, WTK, LDR, and LDR balloon sites.

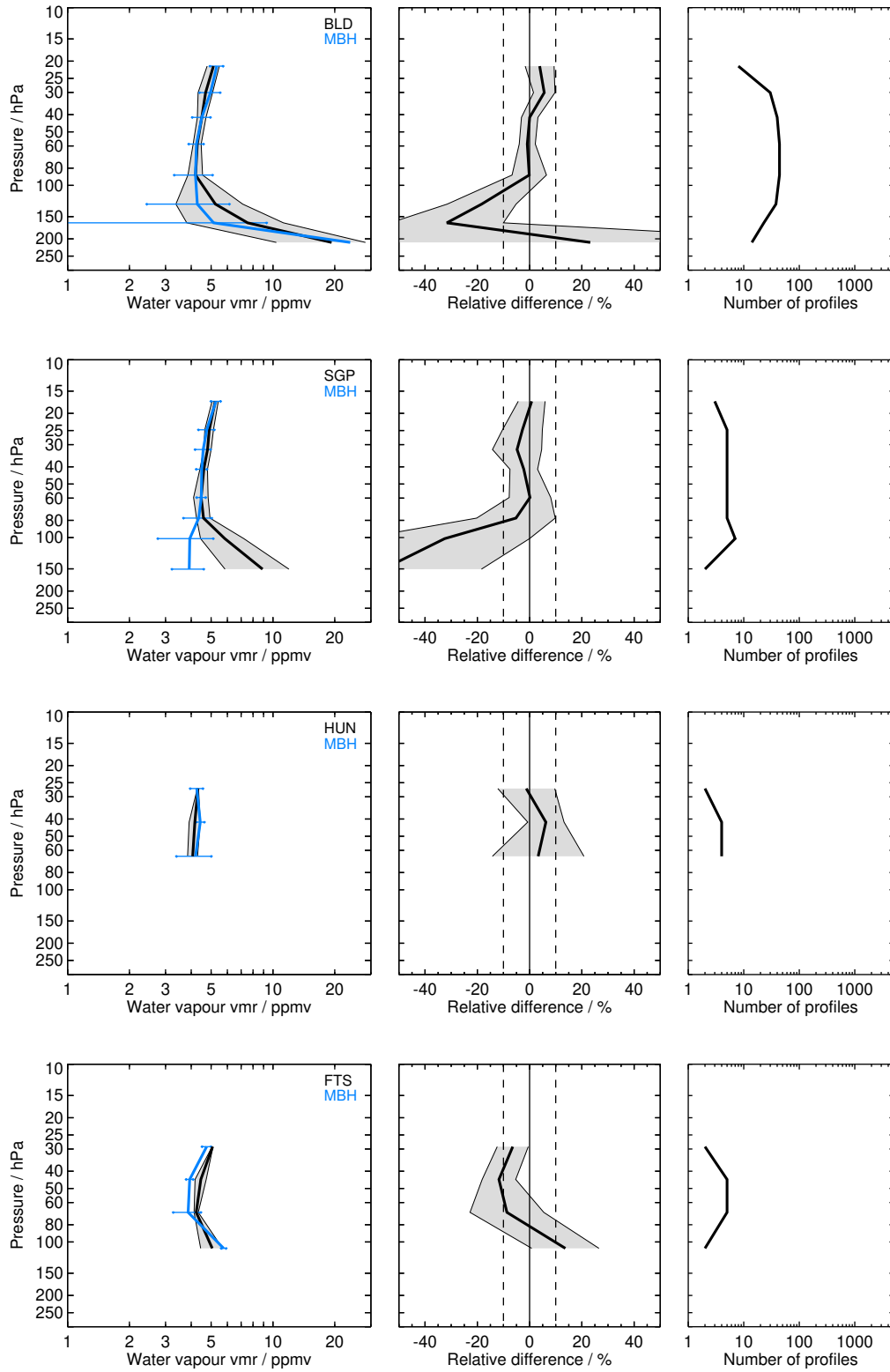


Figure S7: Continued.

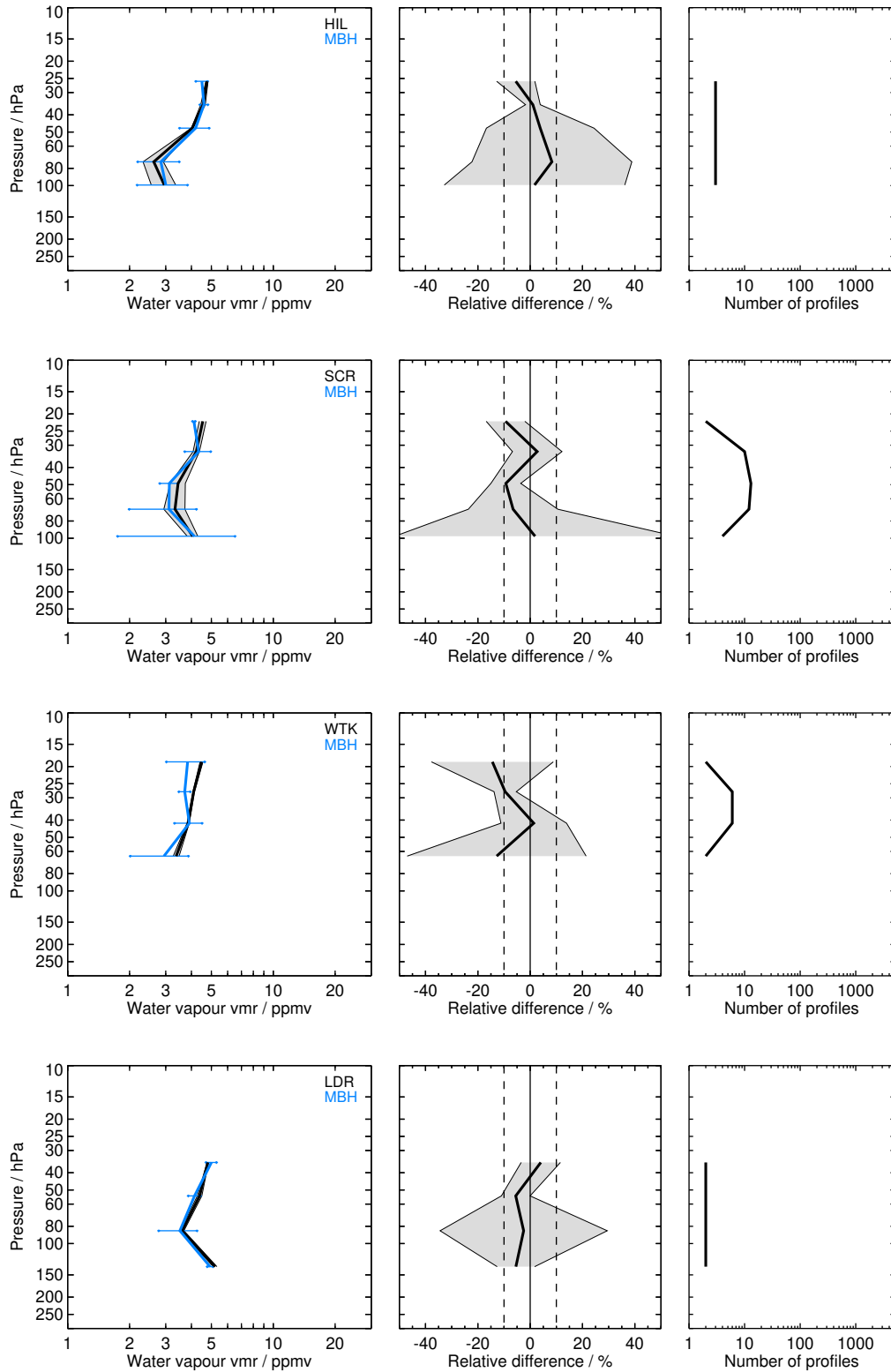


Figure S7: Continued.

2.8 MIPAS-BOL H2O_MA2.3 (MBM)

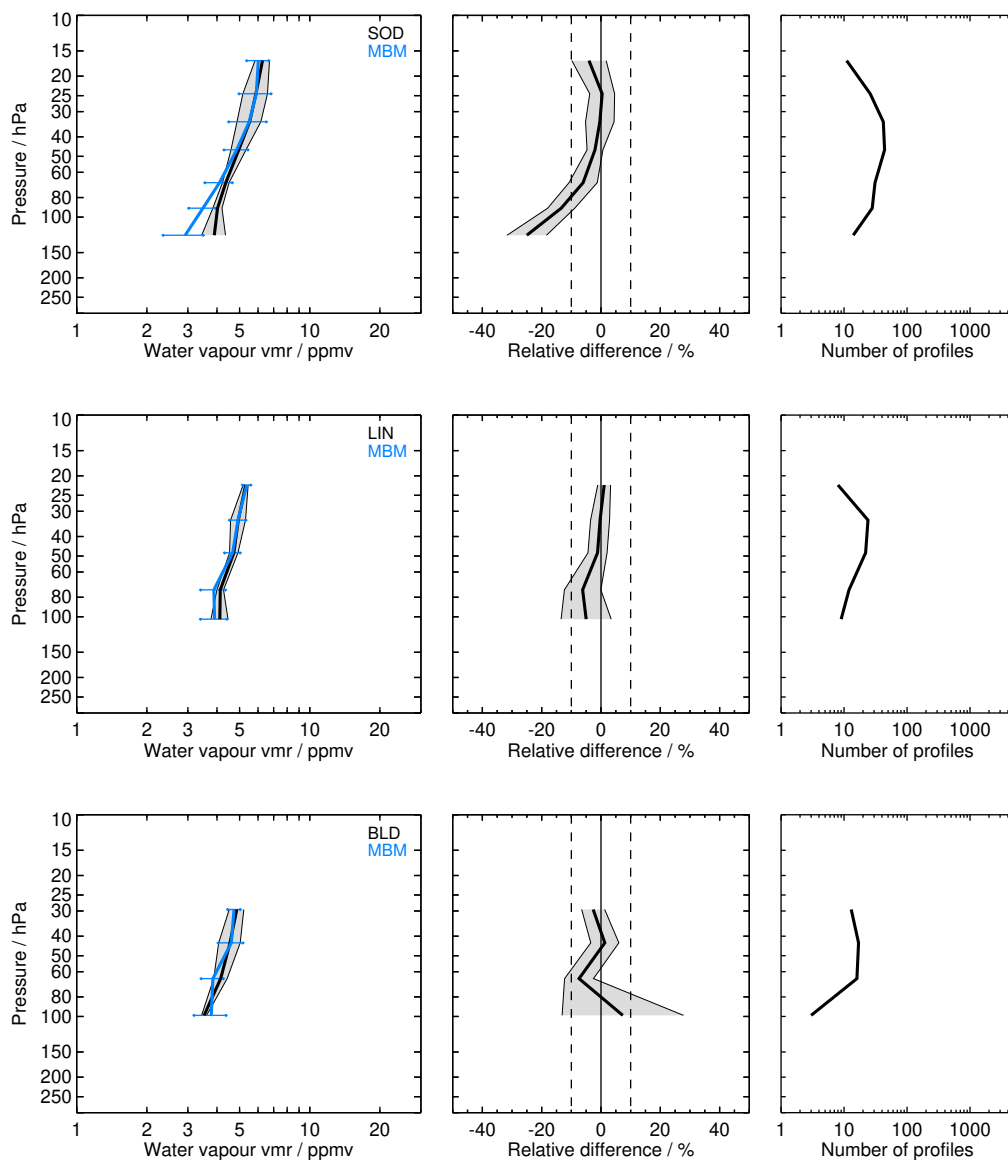


Figure S8: Same as Fig. S1 but for MBM and the SOD, LIN, BLD, BEL, TMF, TNG, KMG, HAN, HIL, SJC, BIK, RVM, LRN, LDR, and LDR balloon sites.

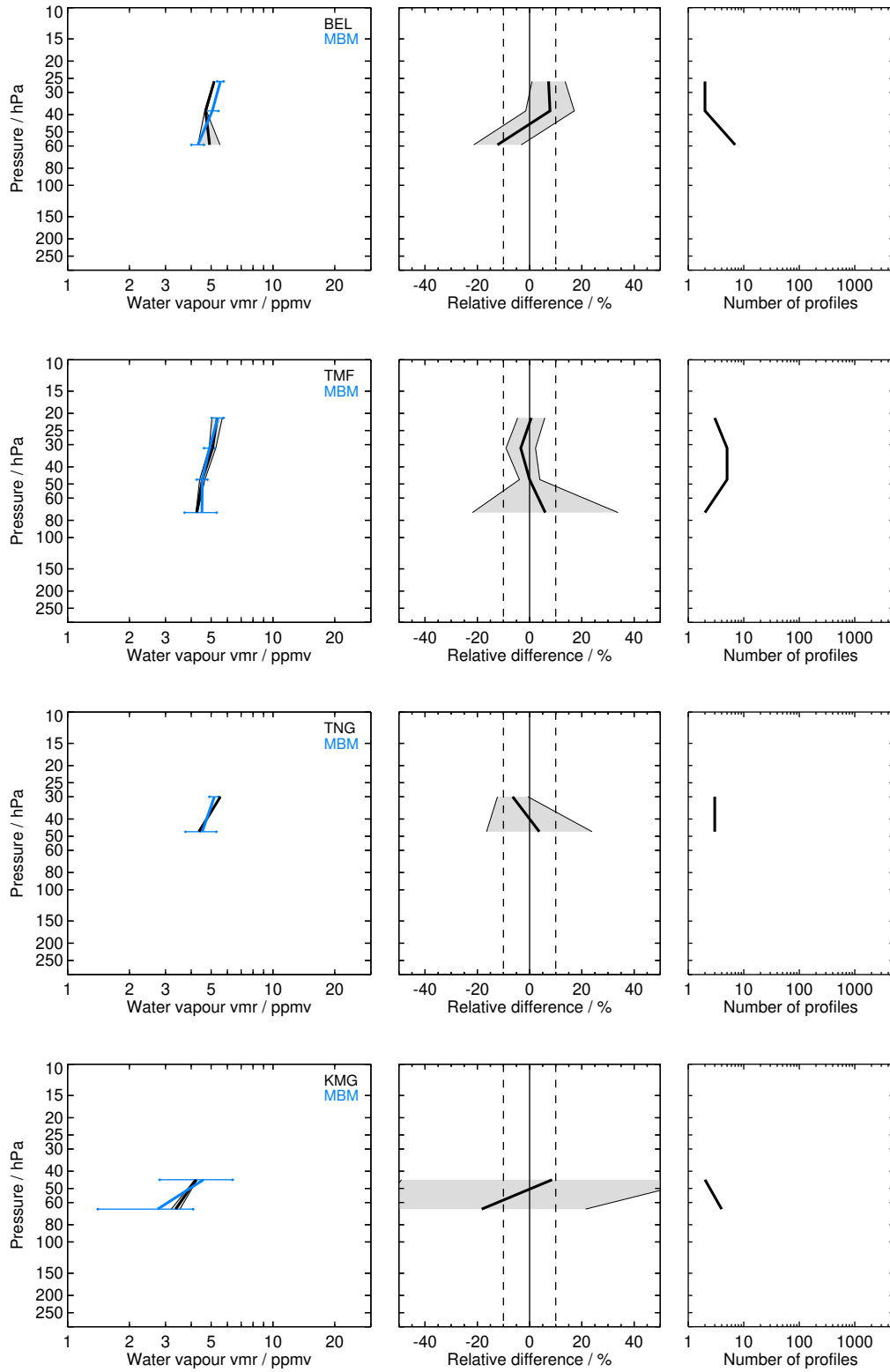


Figure S8: Continued.

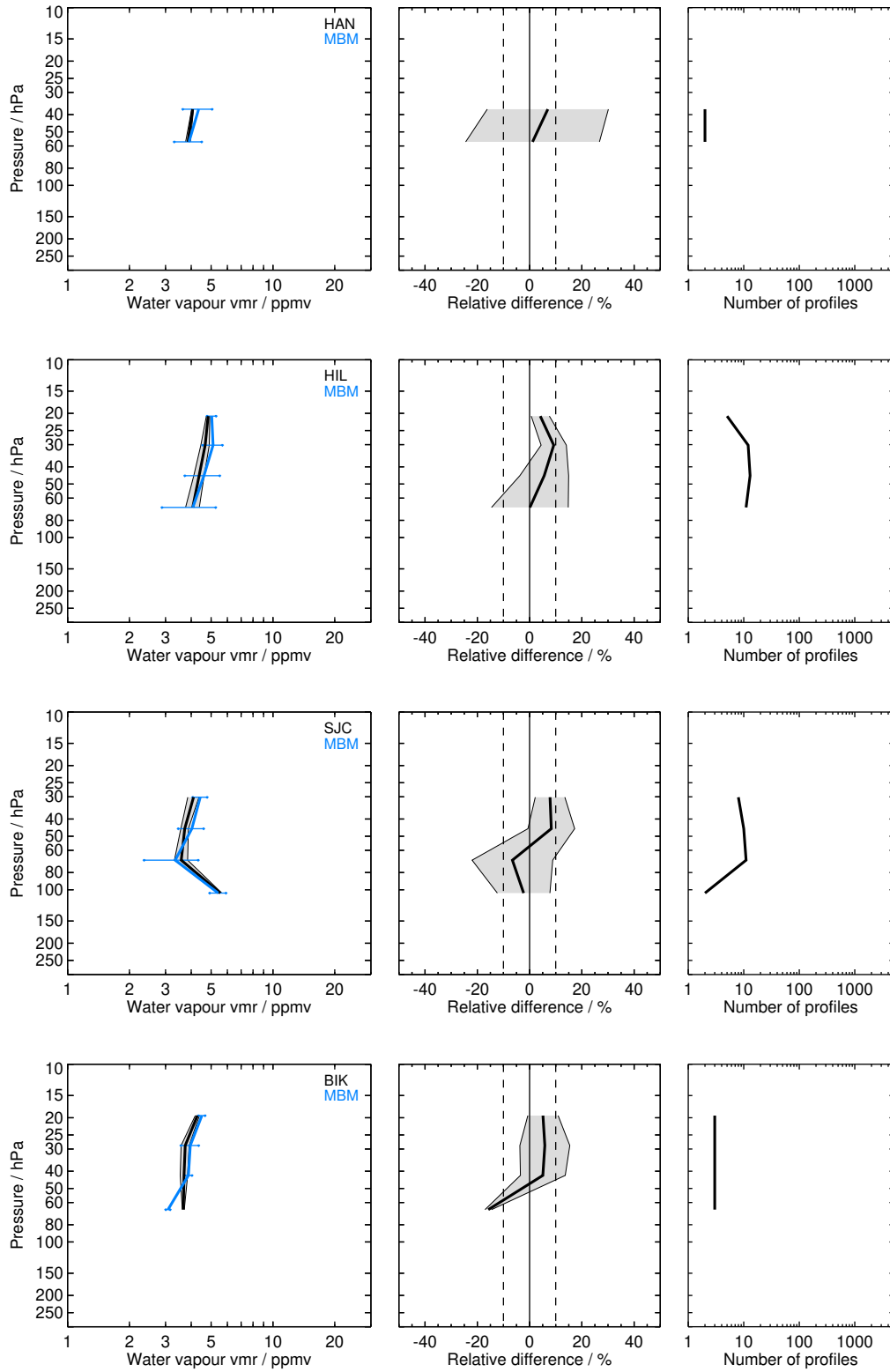


Figure S8: Continued.

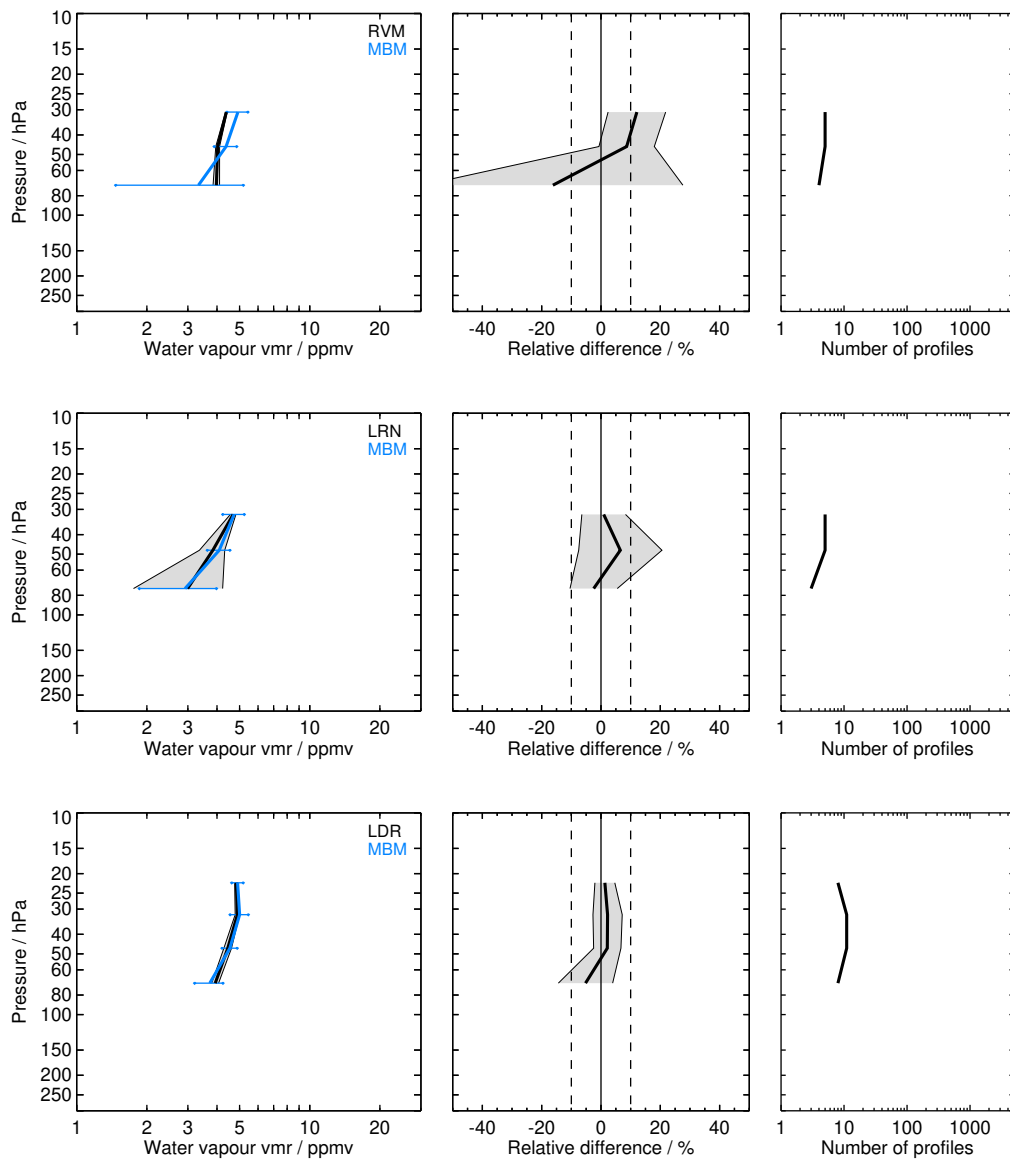


Figure S8: Continued.

2.9 MIPAS-BOL H2O_RR2.3 (MBR)

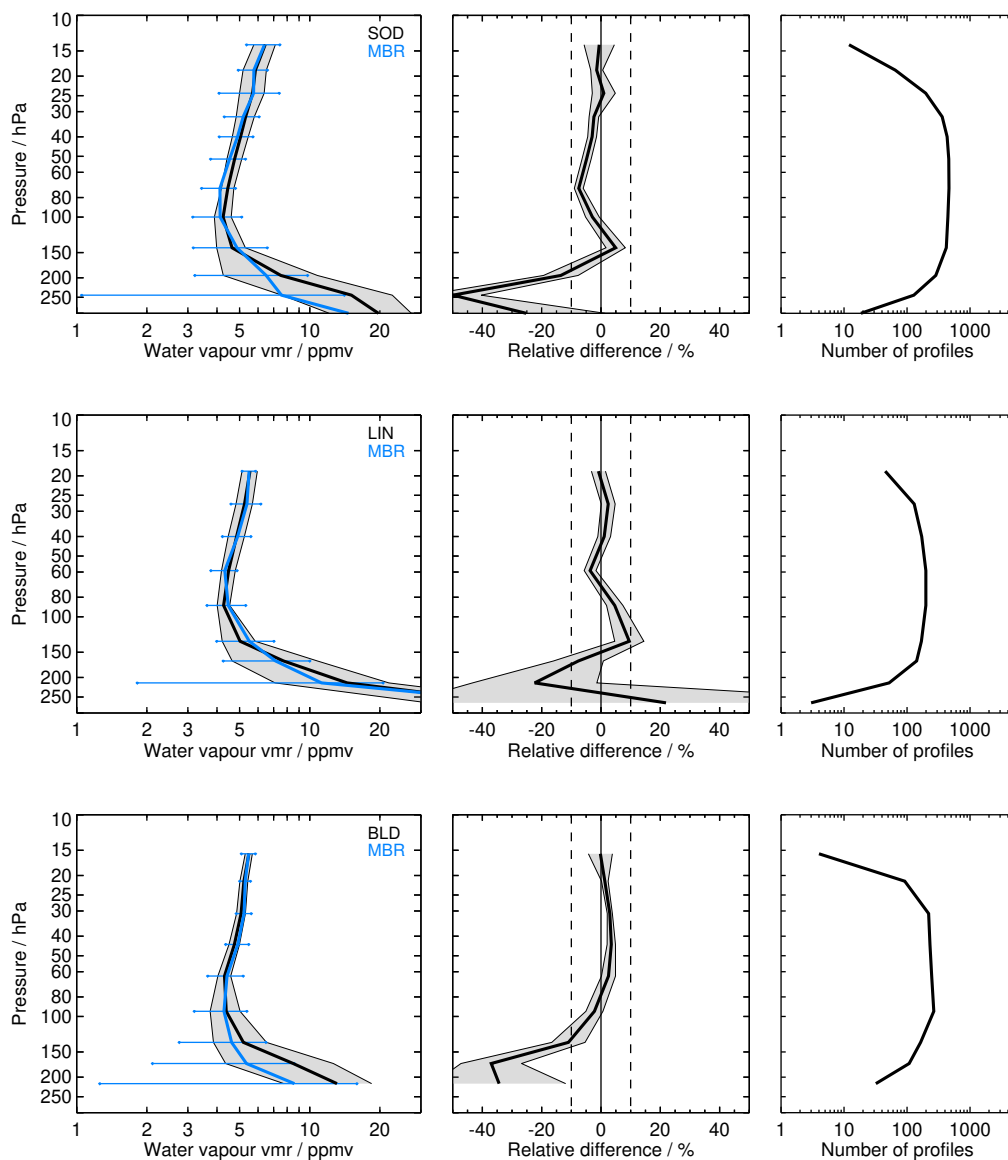


Figure S9: Same as Fig. S1 but for MBR and the SOD, LIN, BLD, BEL, TMF, LSA, HOU, TNG, KMG, YAN, HAN, HIL, SJC, TRW, KTB, SCR, BIK, RVM, LRN, LDR, and LDR balloon sites.

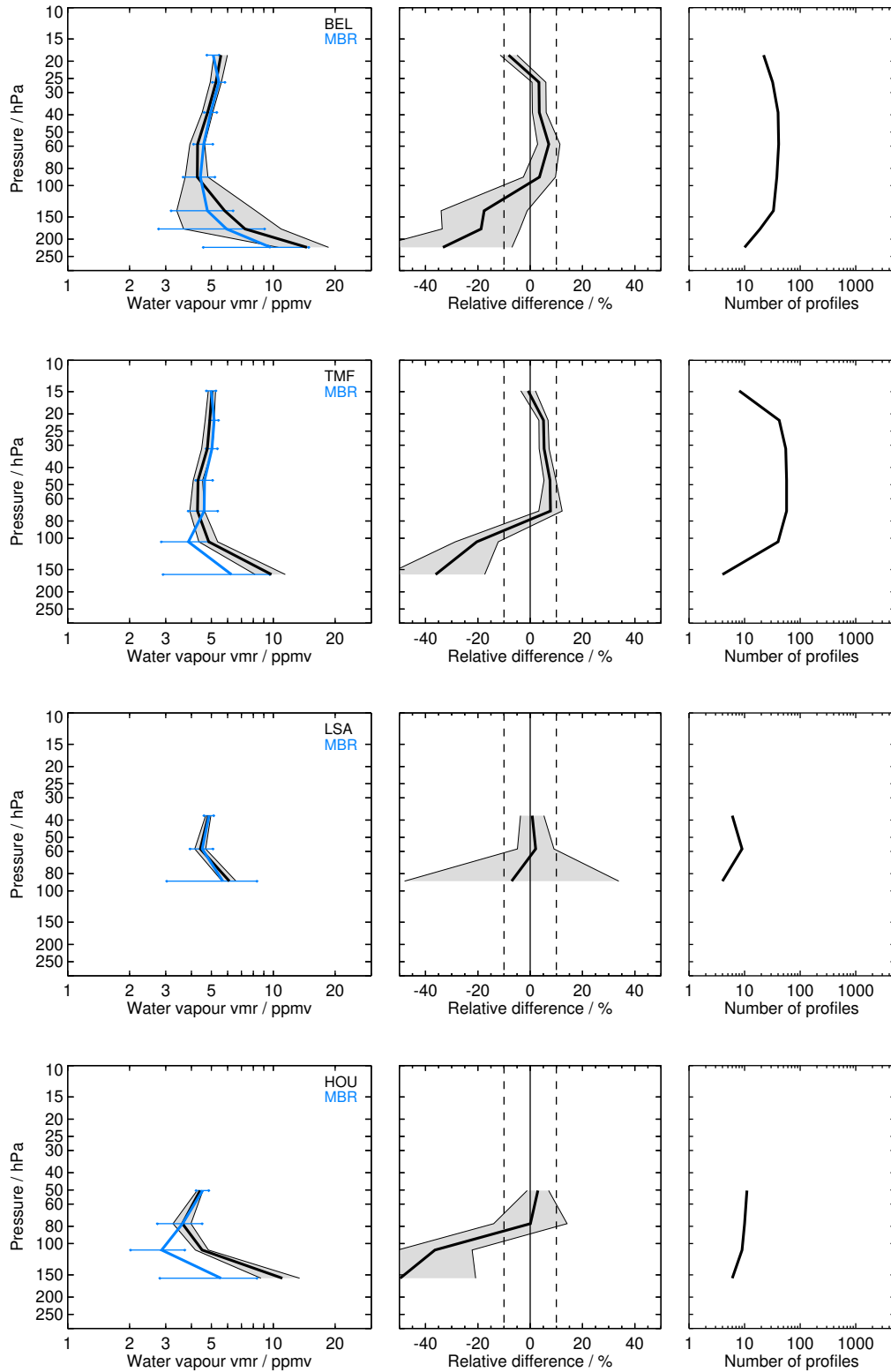


Figure S9: Continued.

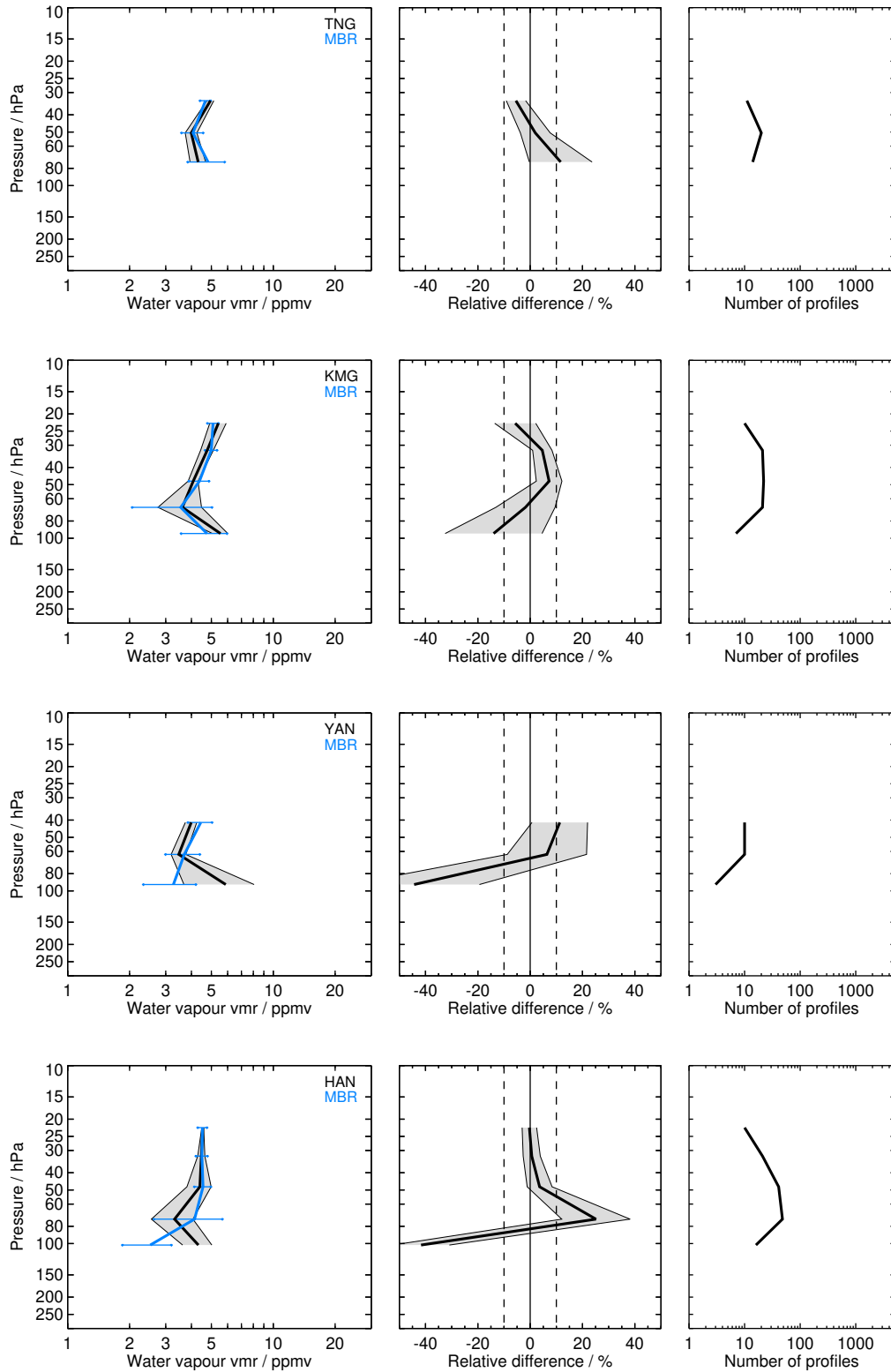


Figure S9: Continued.

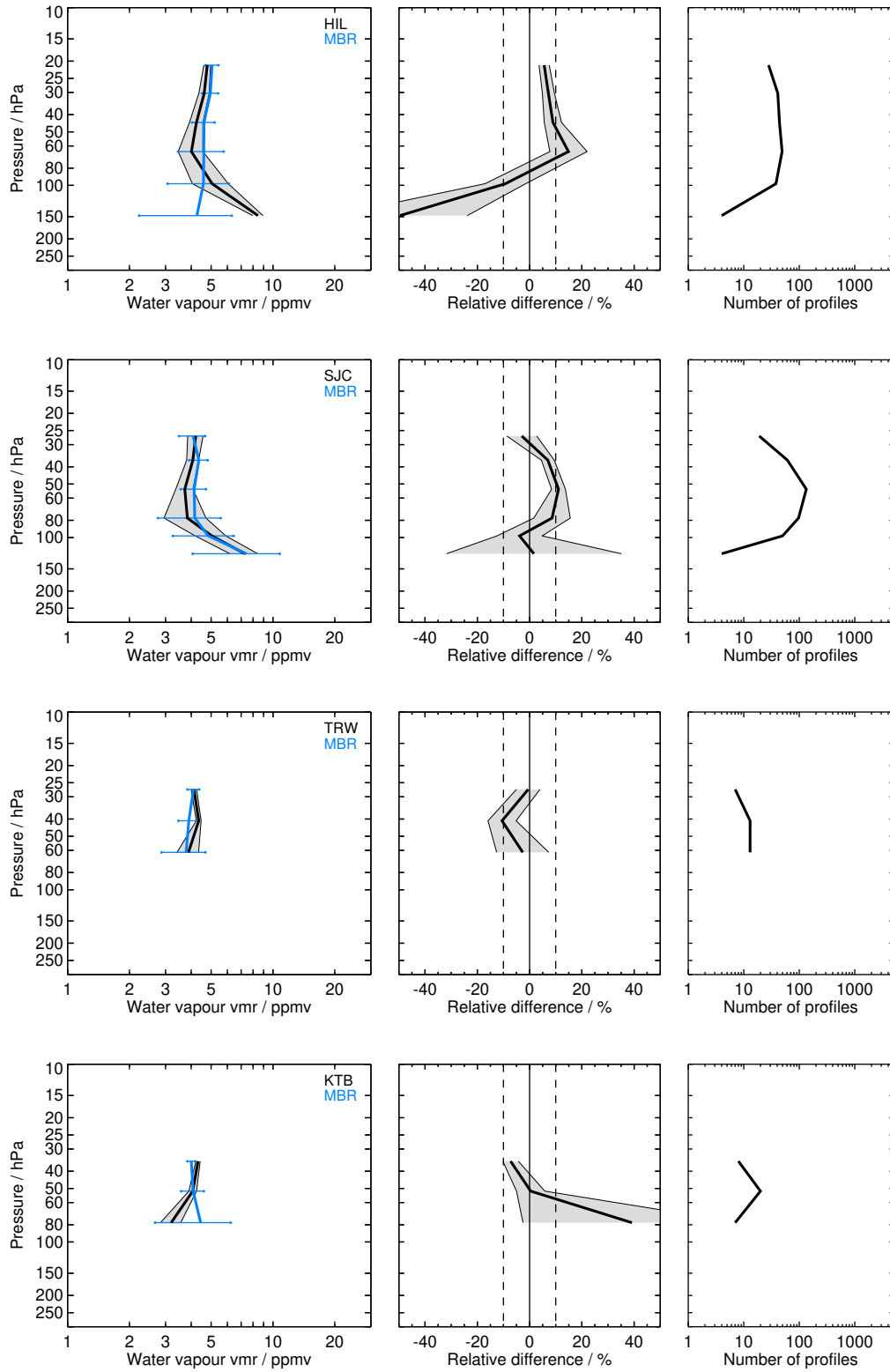


Figure S9: Continued.

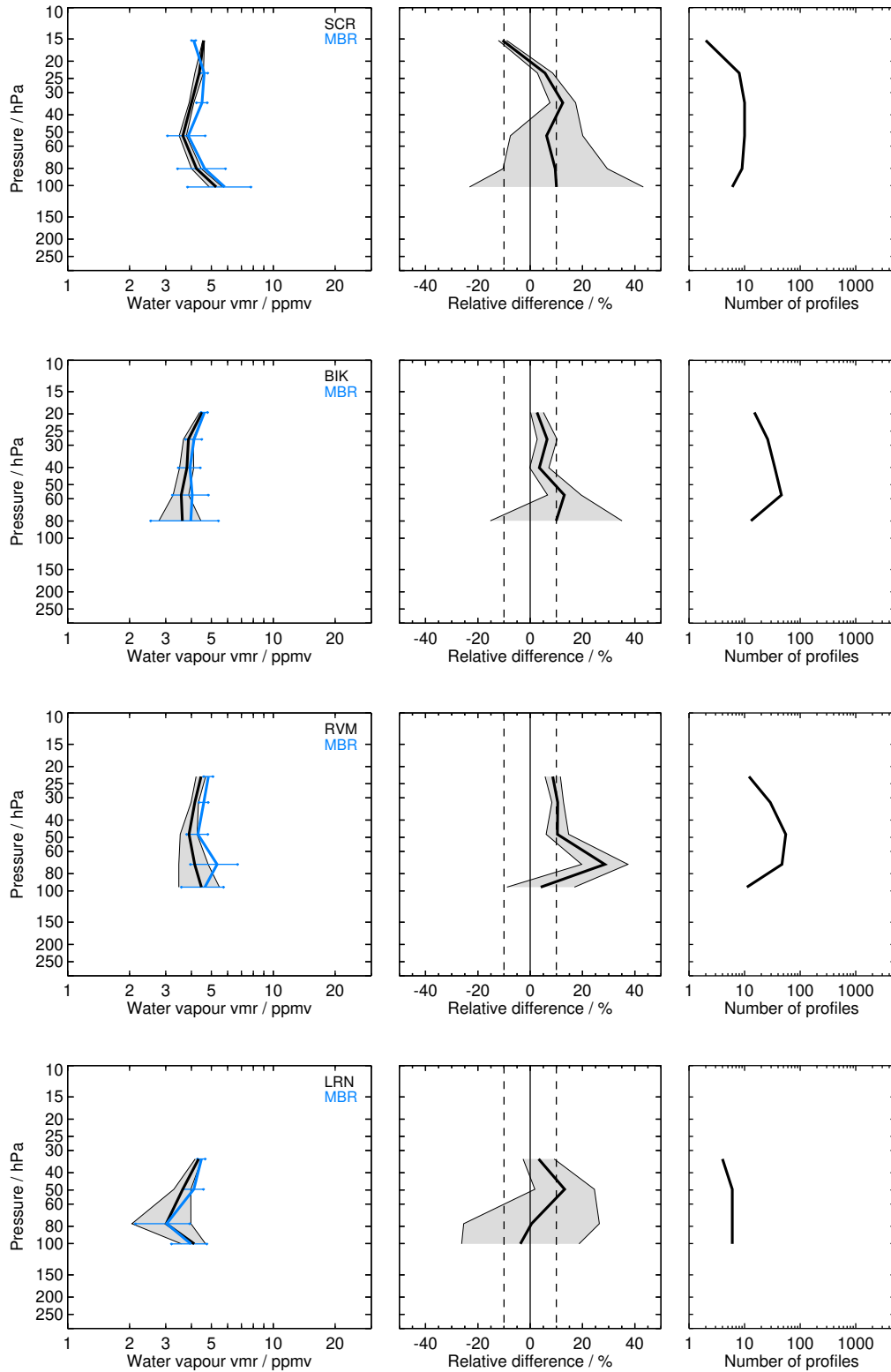


Figure S9: Continued.

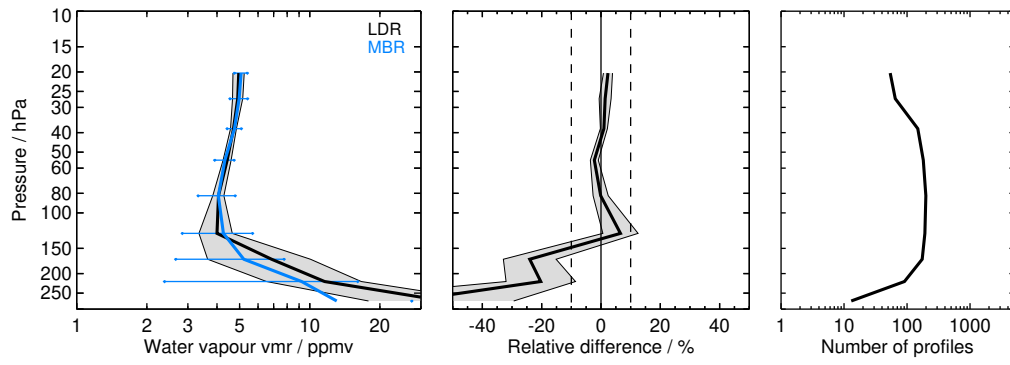


Figure S9: Continued.

2.10 MIPAS-ESA V7H_H2O_NOM (MEH)

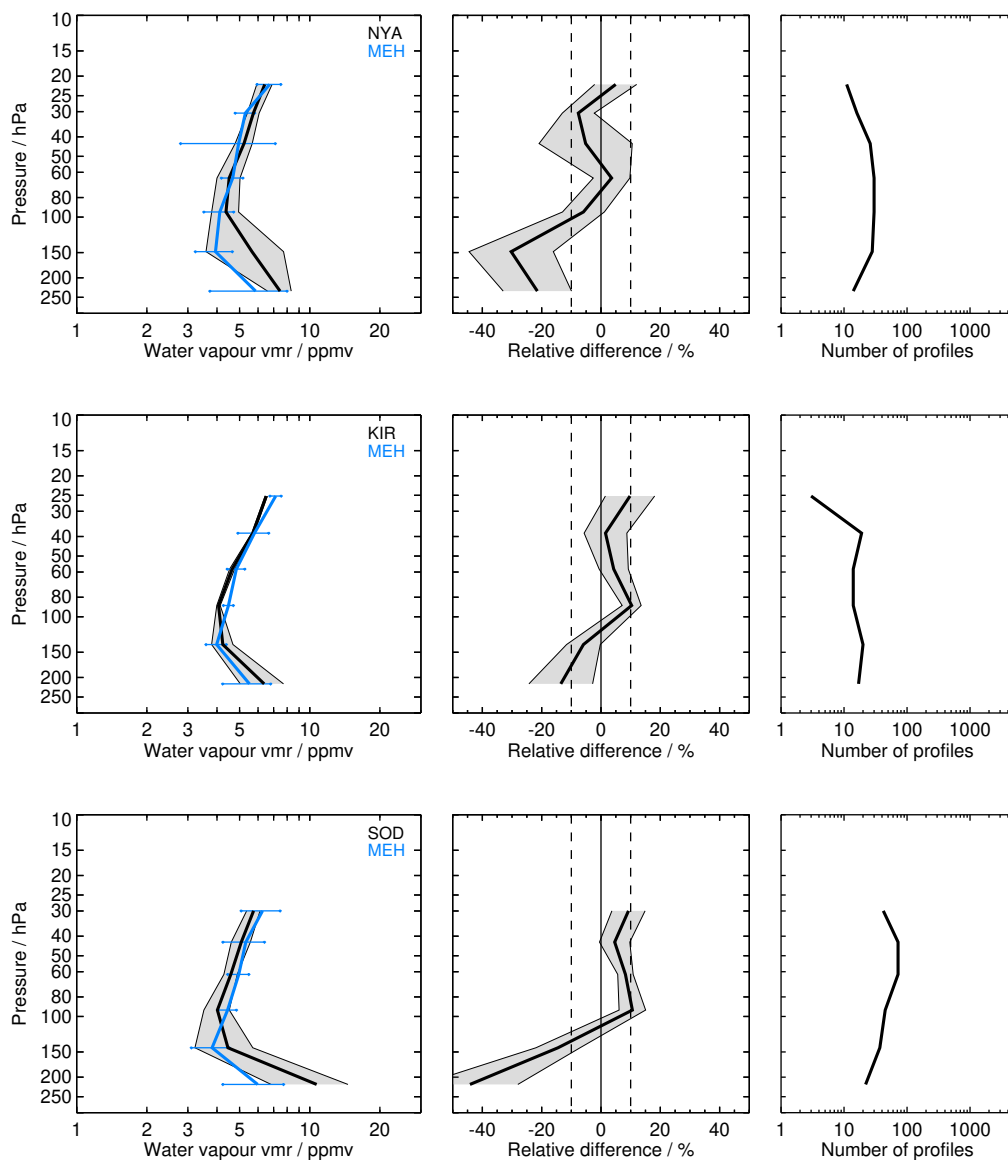


Figure S10: Same as Fig. S1 but for MEH and the NYA, KIR, SOD, BLD, SGP, FTS, HIL, SCR, WTK, and WTK balloon sites.

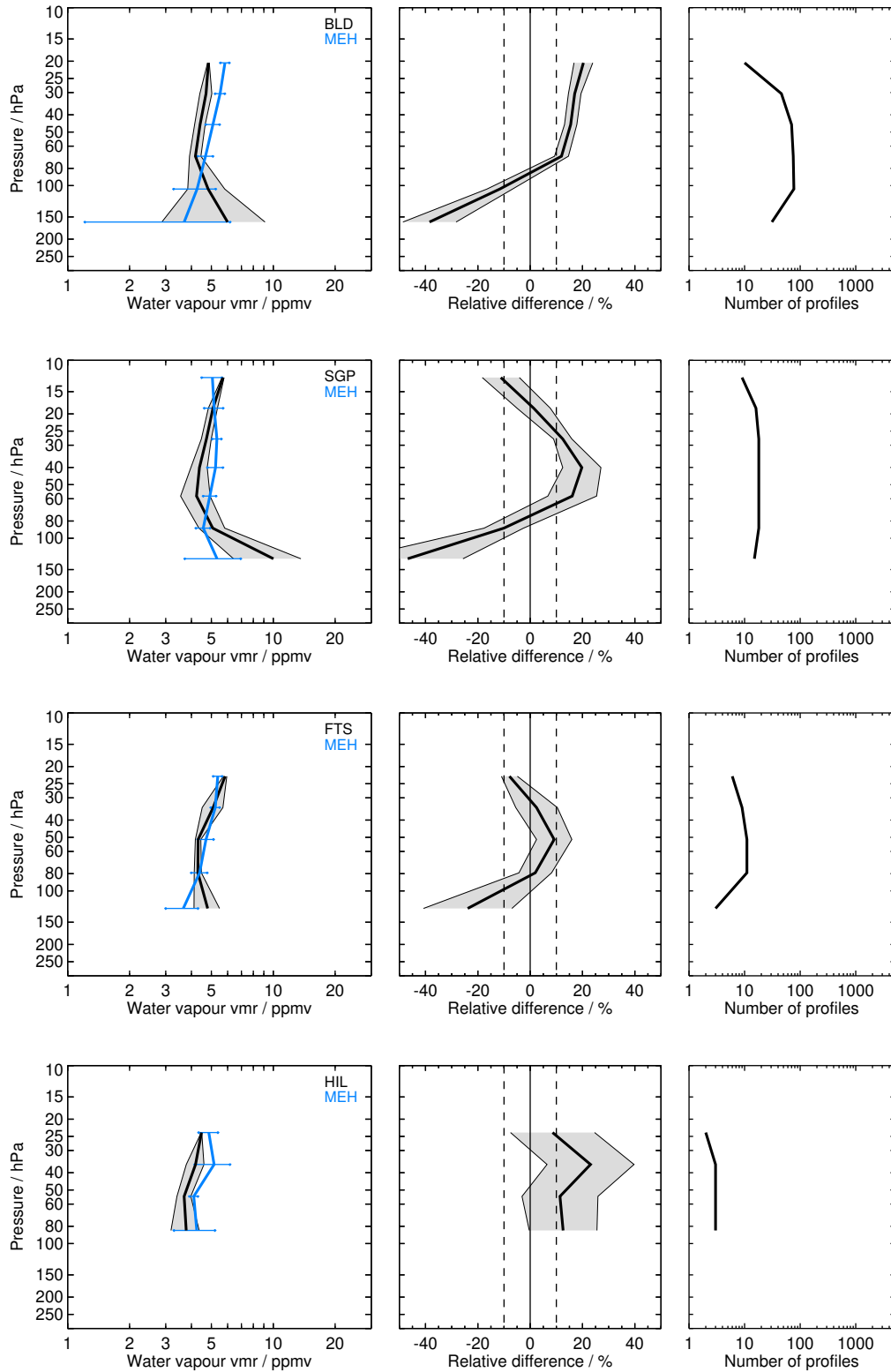


Figure S10: Continued.

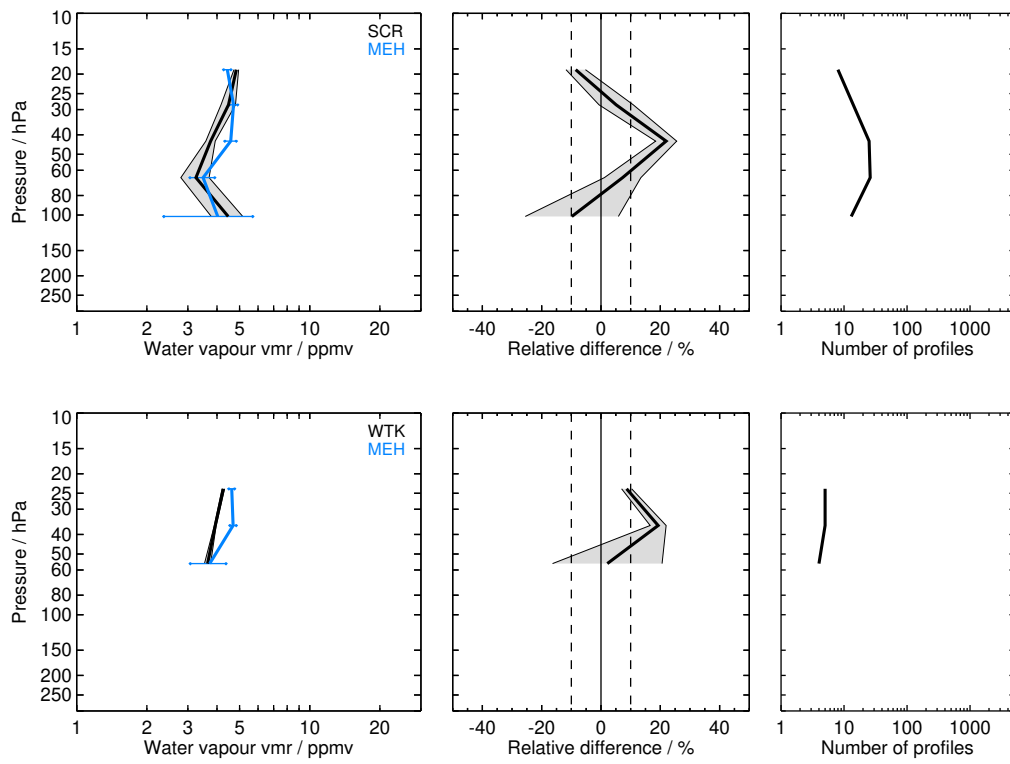


Figure S10: Continued.

2.11 MIPAS-ESA V7R_H2O_MA (MEM)

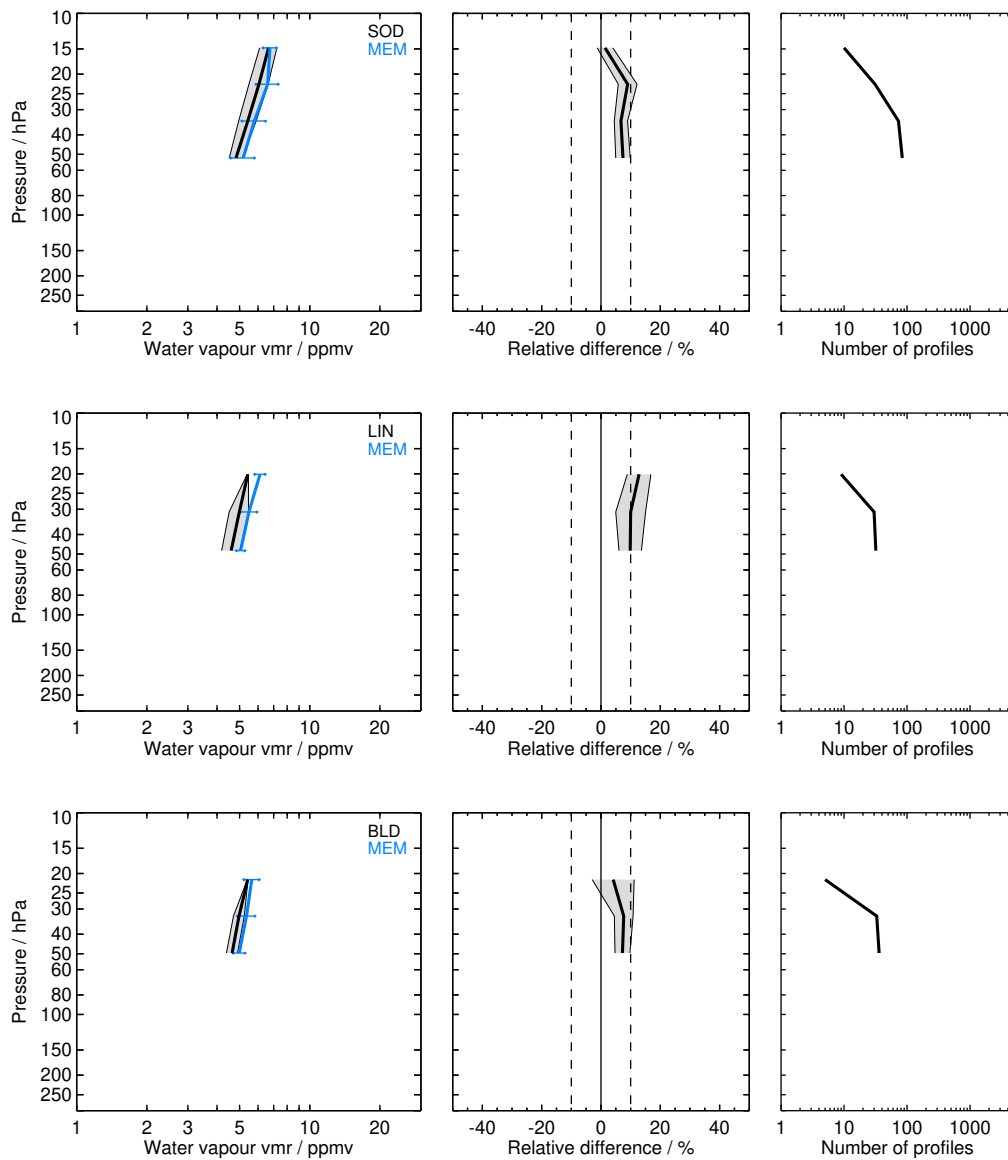


Figure S11: Same as Fig. S1 but for MEM and the SOD, LIN, BLD, BEL, TMF, TNG, KMG, YAN, HAN, HIL, SJC, BIK, RVM, LRN, LDR, and LDR balloon sites.

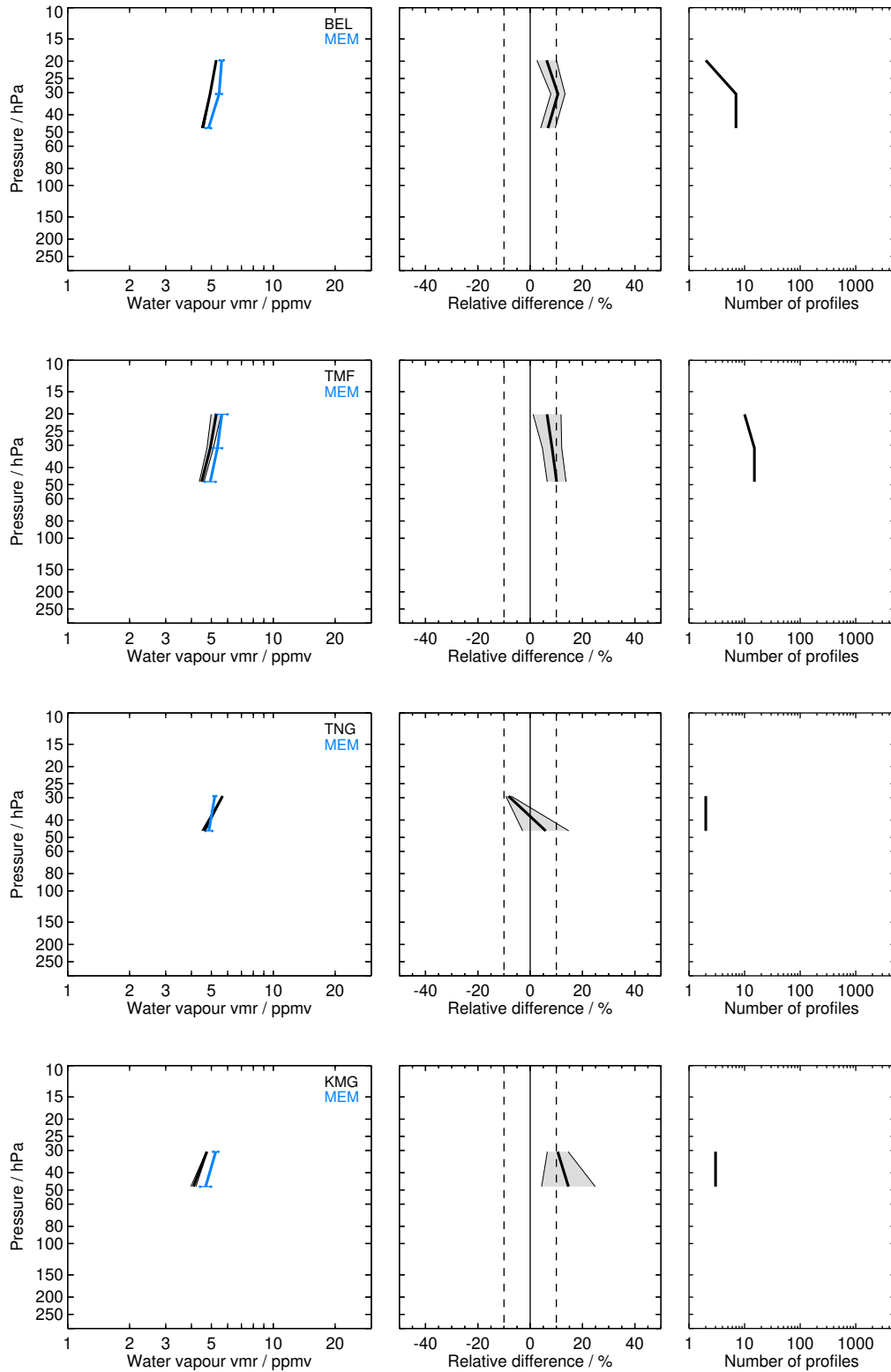


Figure S11: Continued.

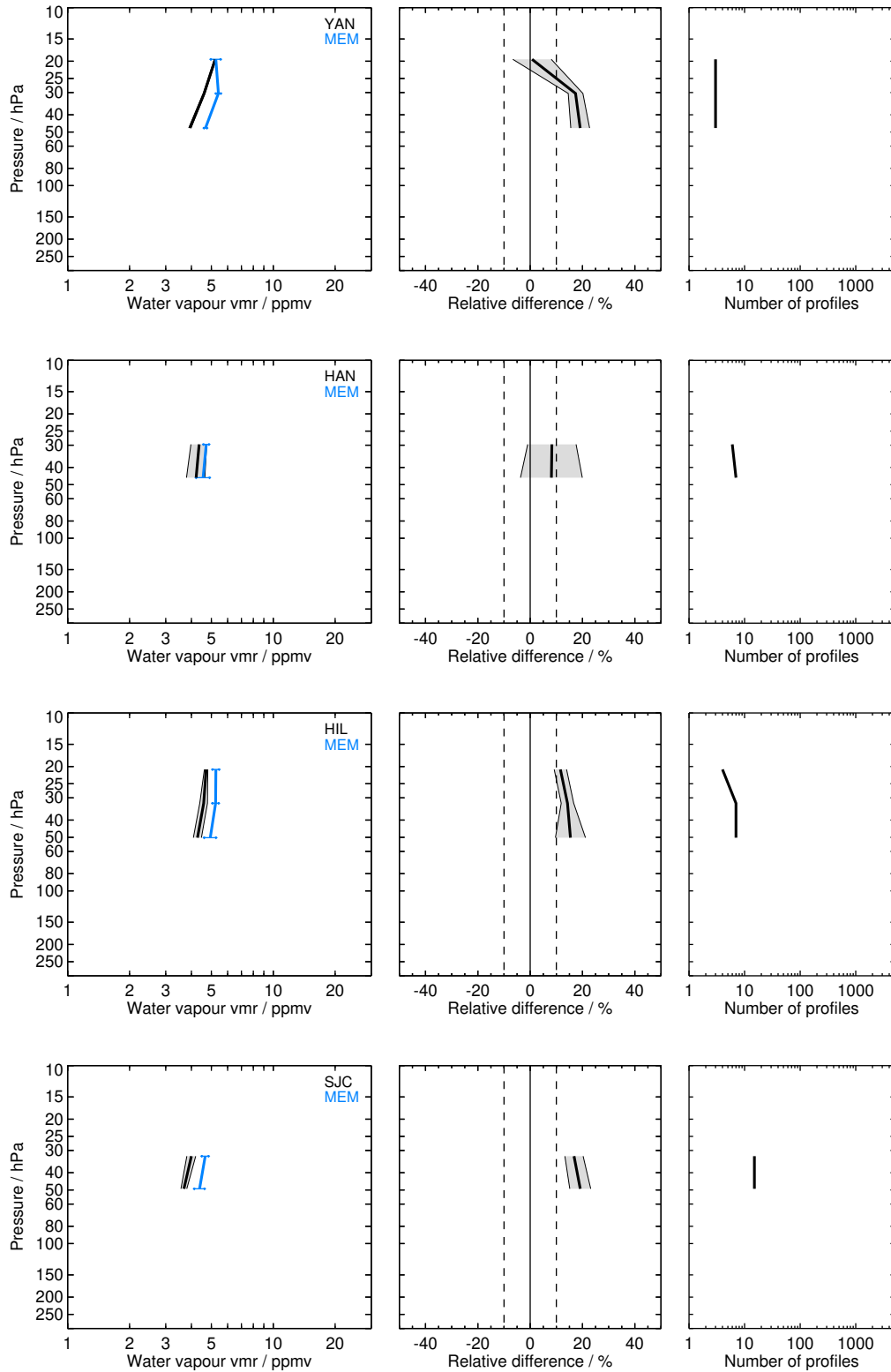


Figure S11: Continued.

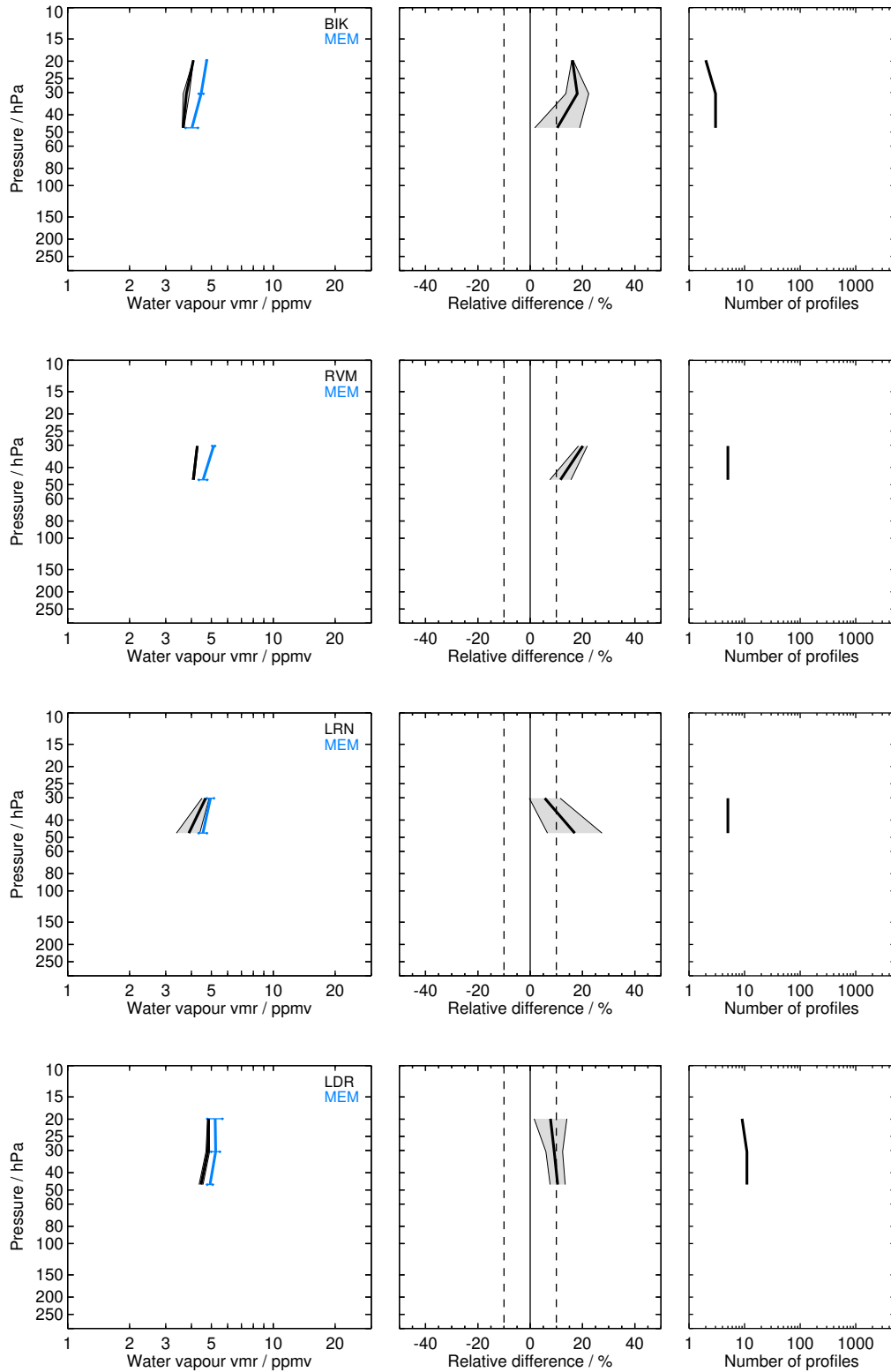


Figure S11: Continued.

2.12 MIPAS-ESA V7R_H2O_NOM (MER)

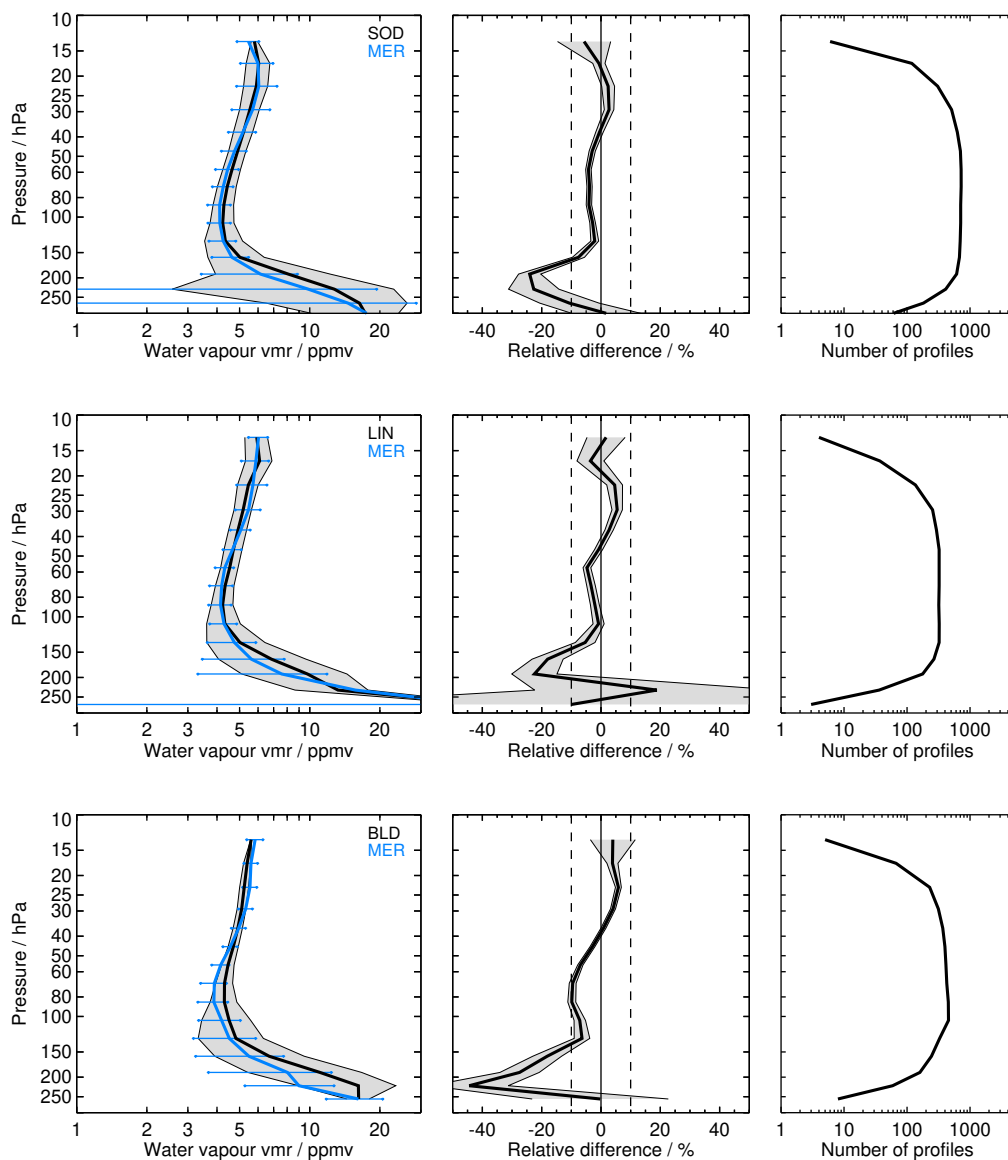


Figure S12: Same as Fig. S1 but for MER and the SOD, LIN, BLD, BEL, TMF, LSA, HOU, TNG, KMG, YAN, HAN, HIL, SJC, TRW, KTB, SCR, BIK, RVM, LRN, LDR, and LDR balloon sites.

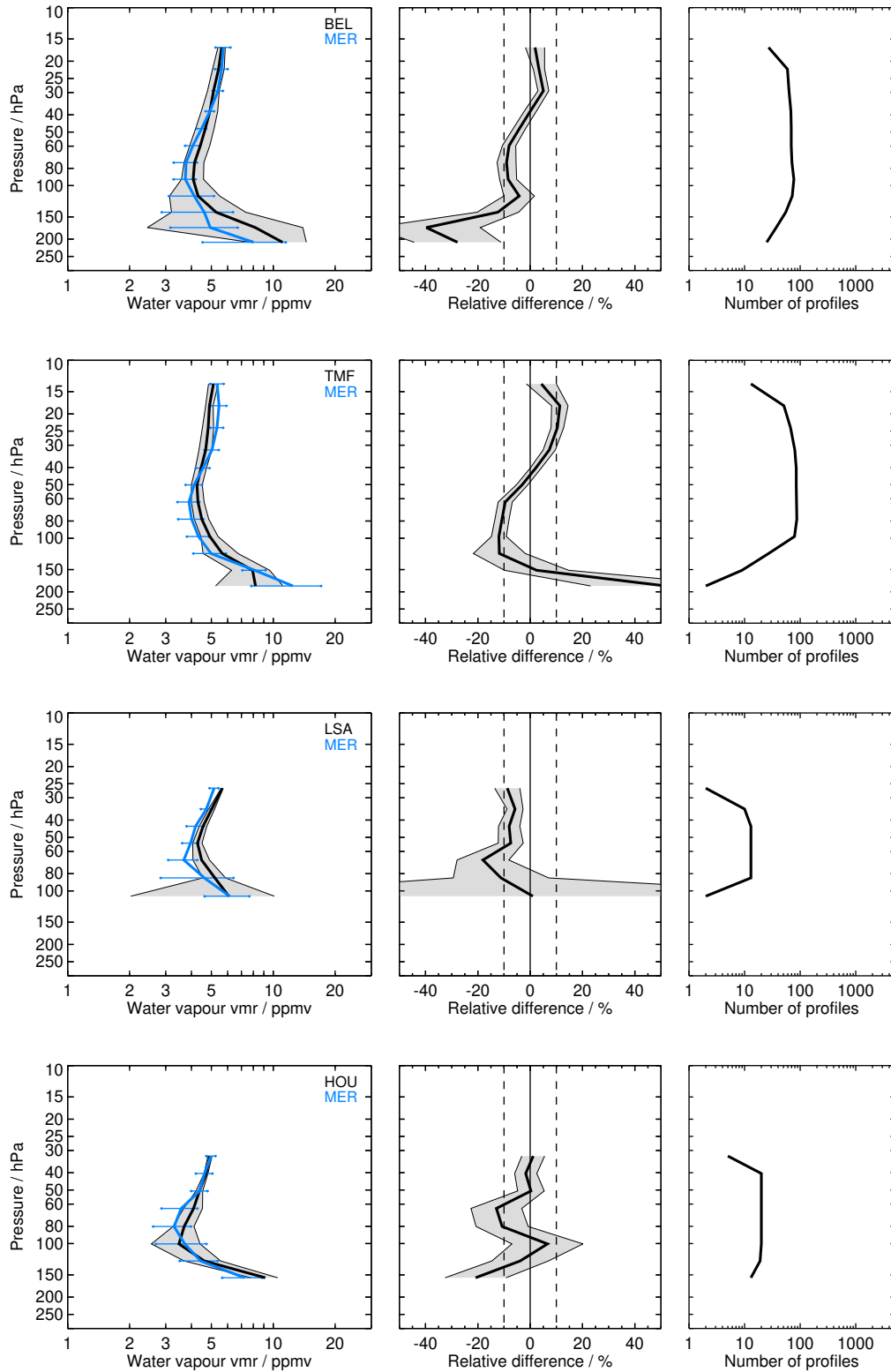


Figure S12: Continued.

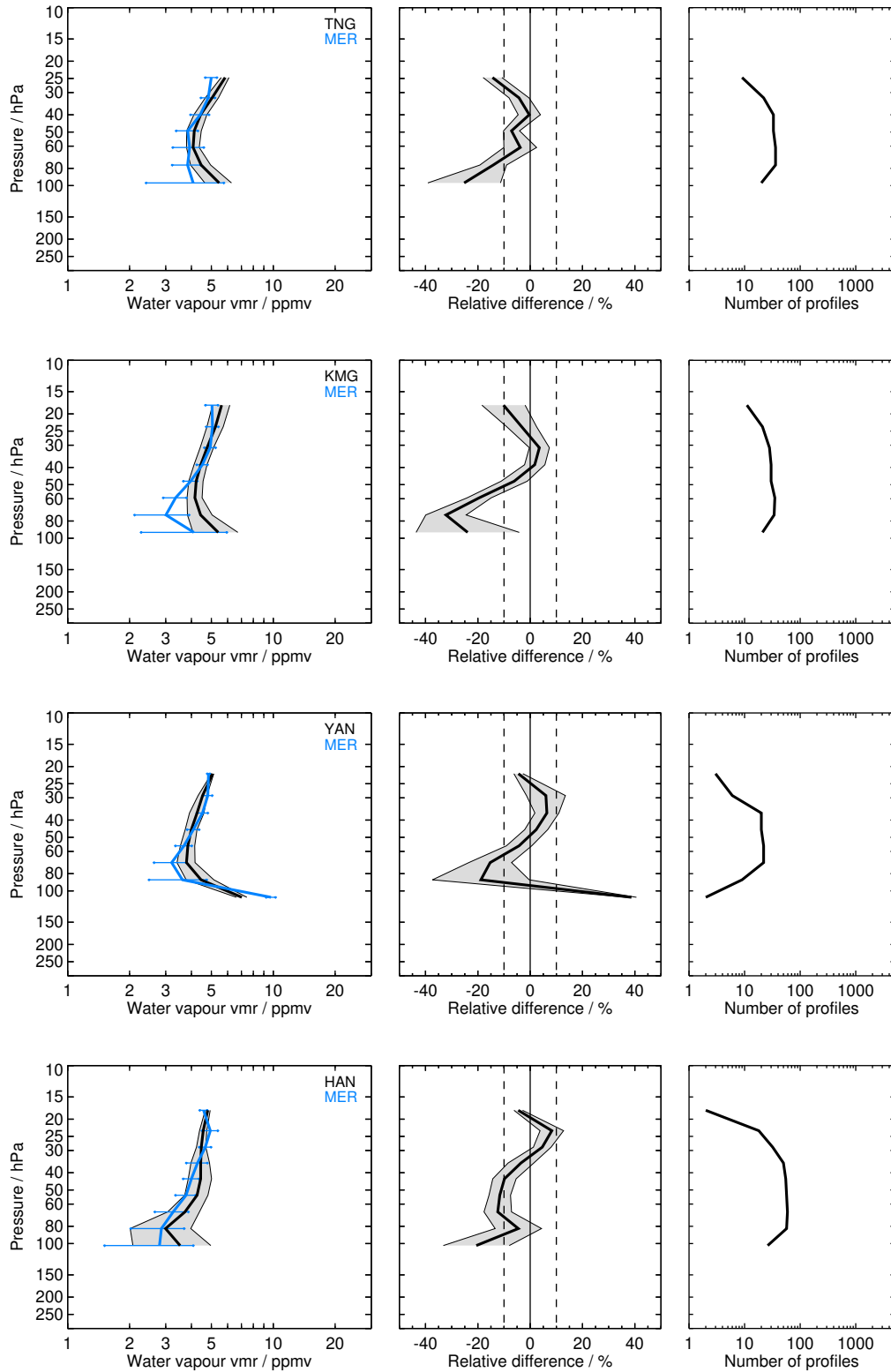


Figure S12: Continued.

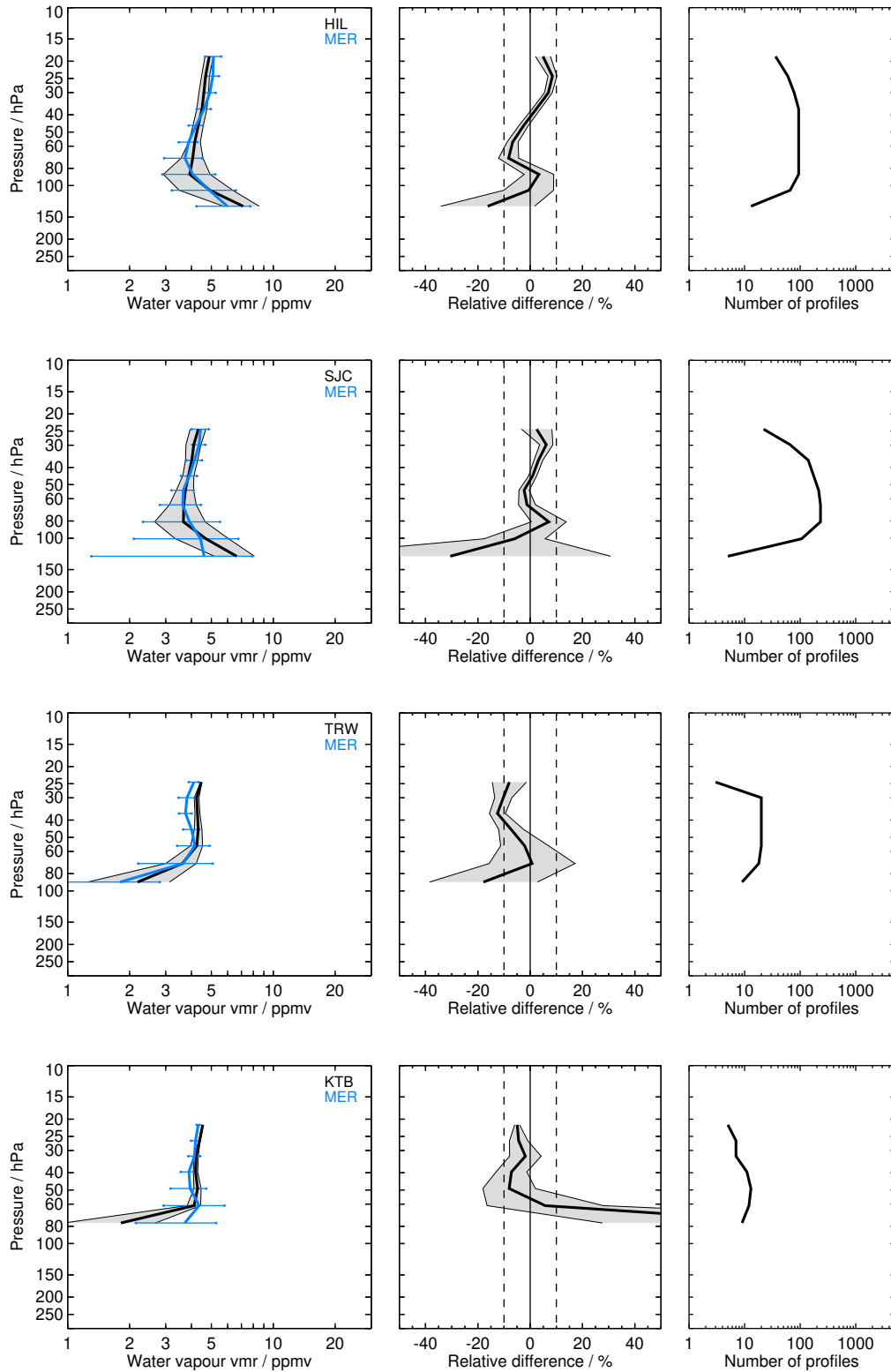


Figure S12: Continued.

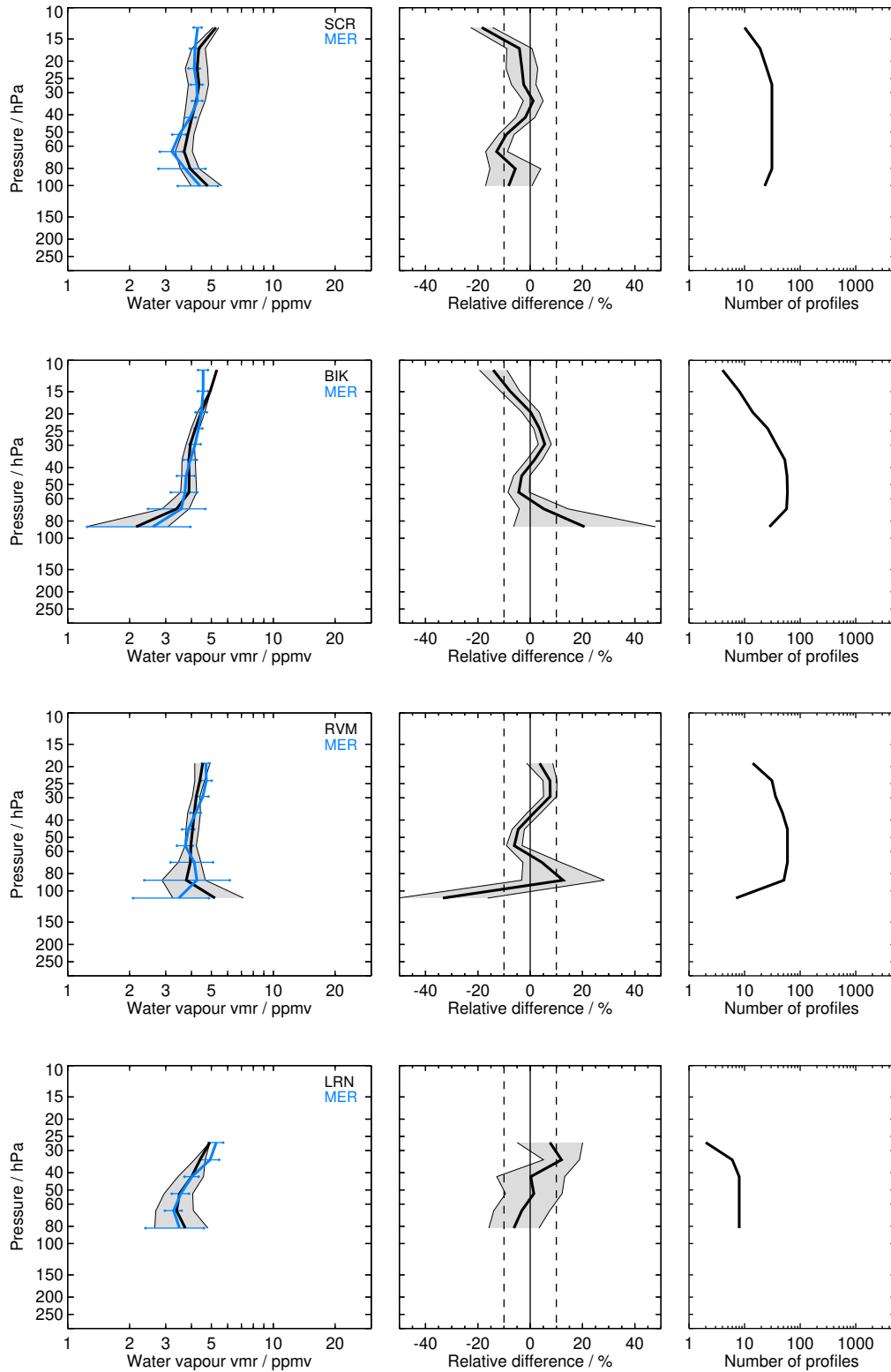


Figure S12: Continued.

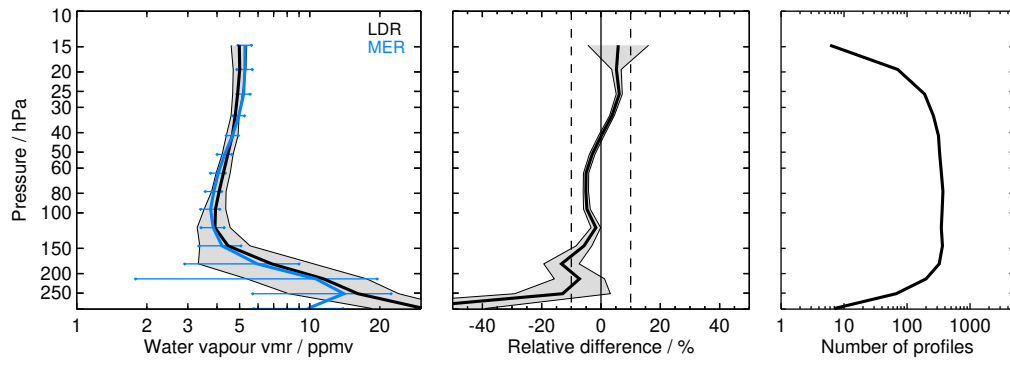


Figure S12: Continued.

2.13 MIPAS-IMK V5H_H2O_20 (MIH)

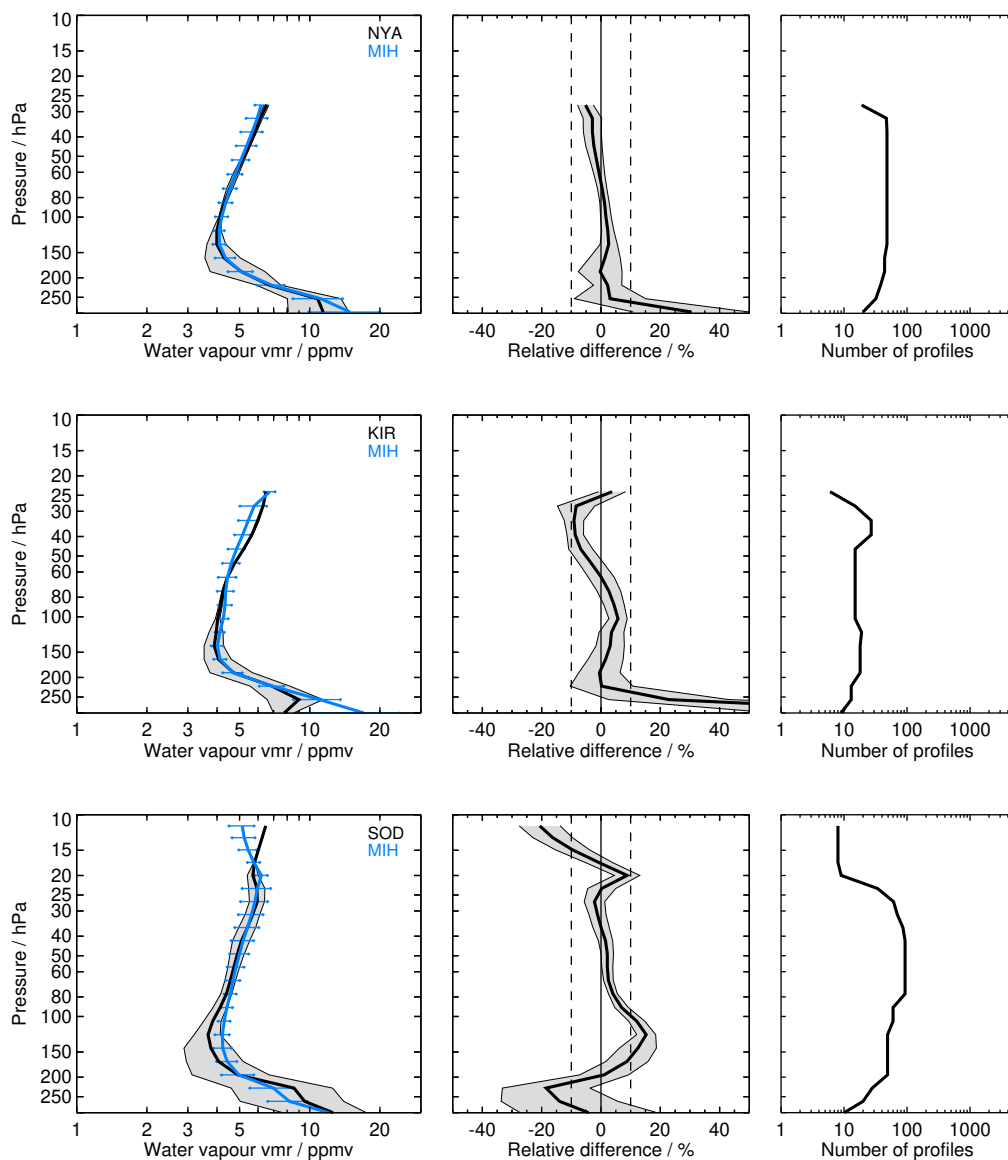


Figure S13: Same as Fig. S1 but for MIH and the NYA, KIR, SOD, BLD, SGP, HUN, FTS, HIL, SCR, WTK, LDR, and LDR balloon sites.

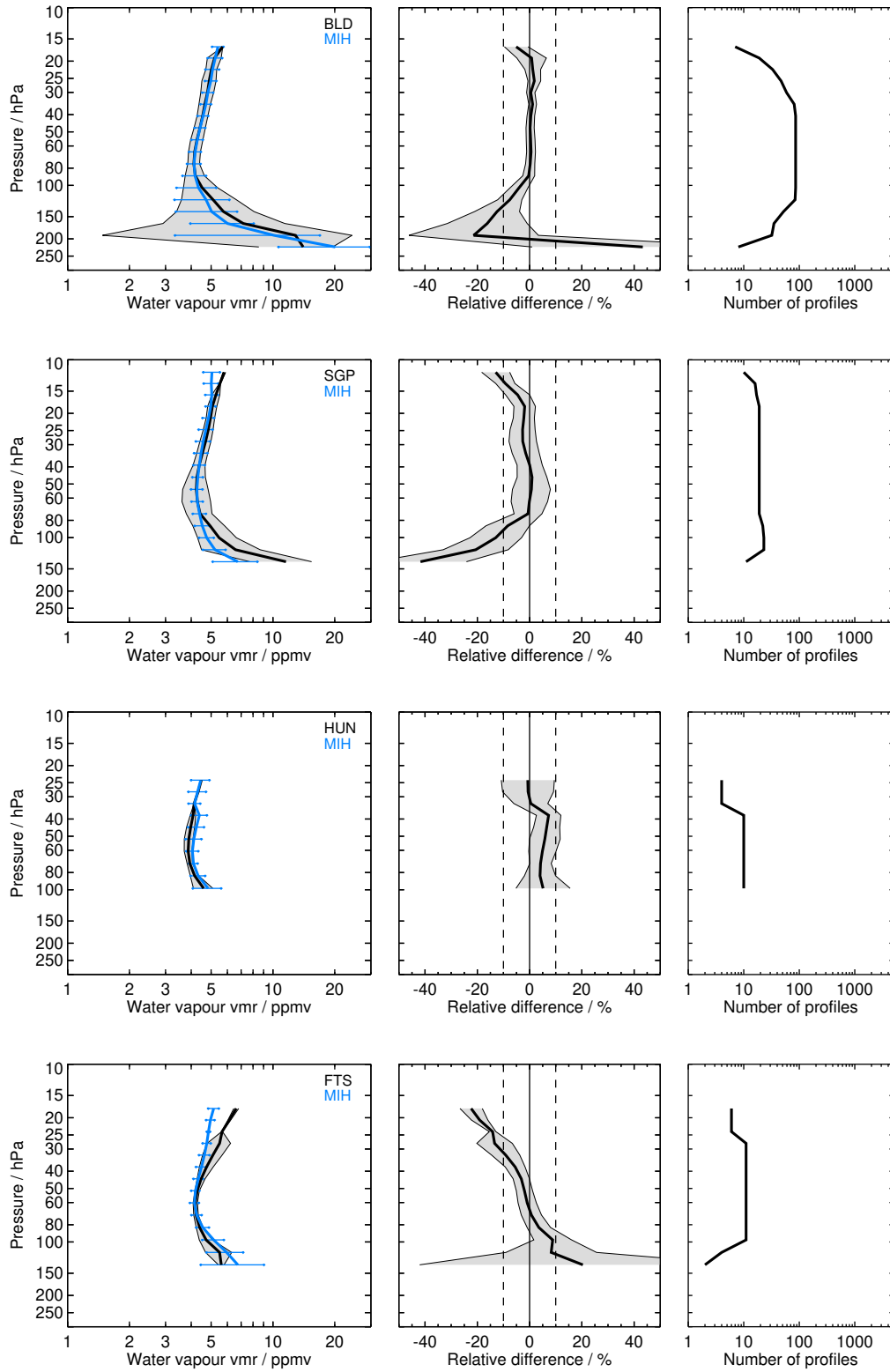


Figure S13: Continued.

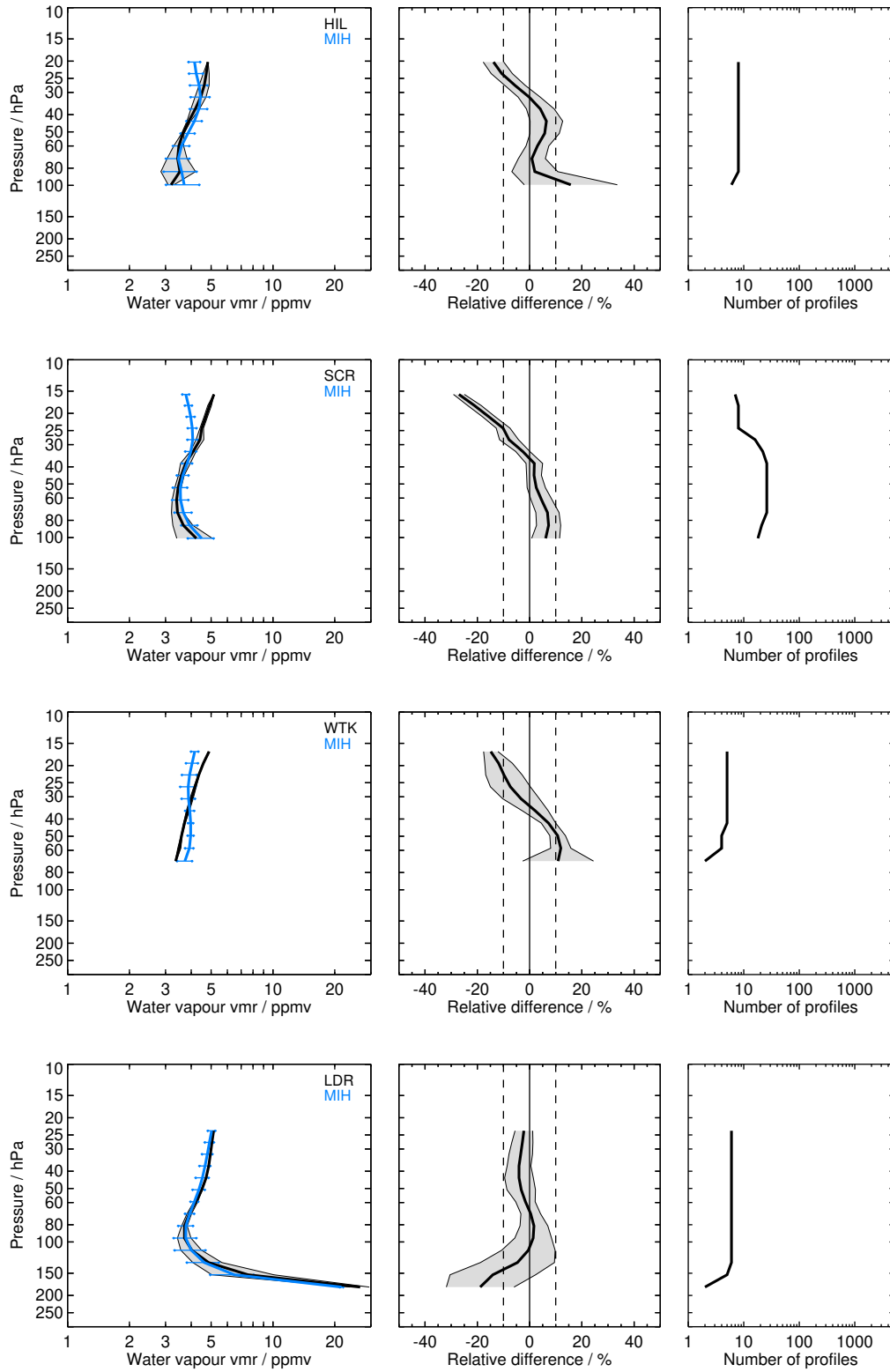


Figure S13: Continued.

2.14 MIPAS-IMK V5R_H2O_220 (MIR)

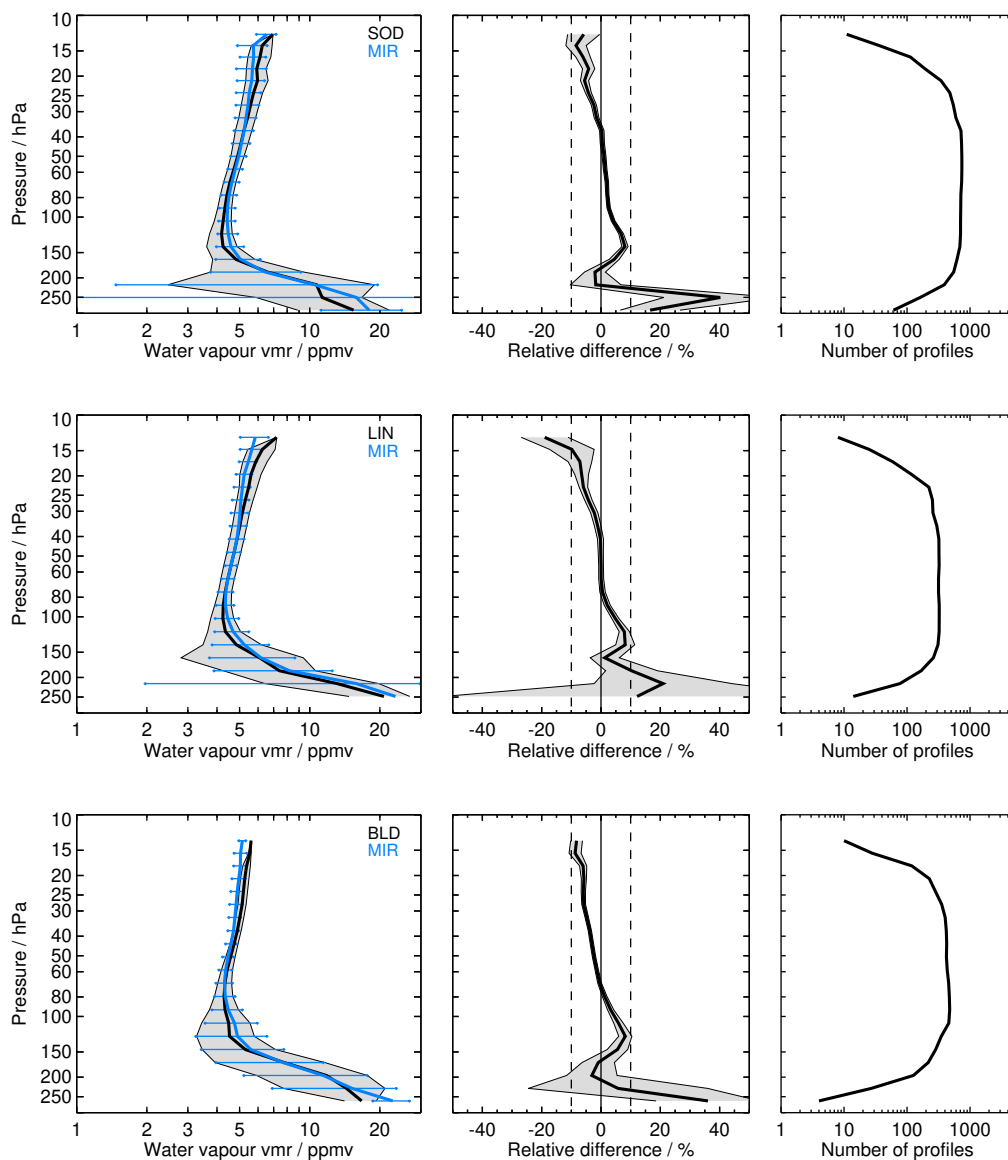


Figure S14: Same as Fig. S1 but for MIR and the SOD, LIN, BLD, BEL, TMF, LSA, HOU, TNG, KMG, YAN, HAN, HIL, SJC, TRW, KTB, SCR, BIK, RVM, LRN, LDR, and LDR balloon sites.

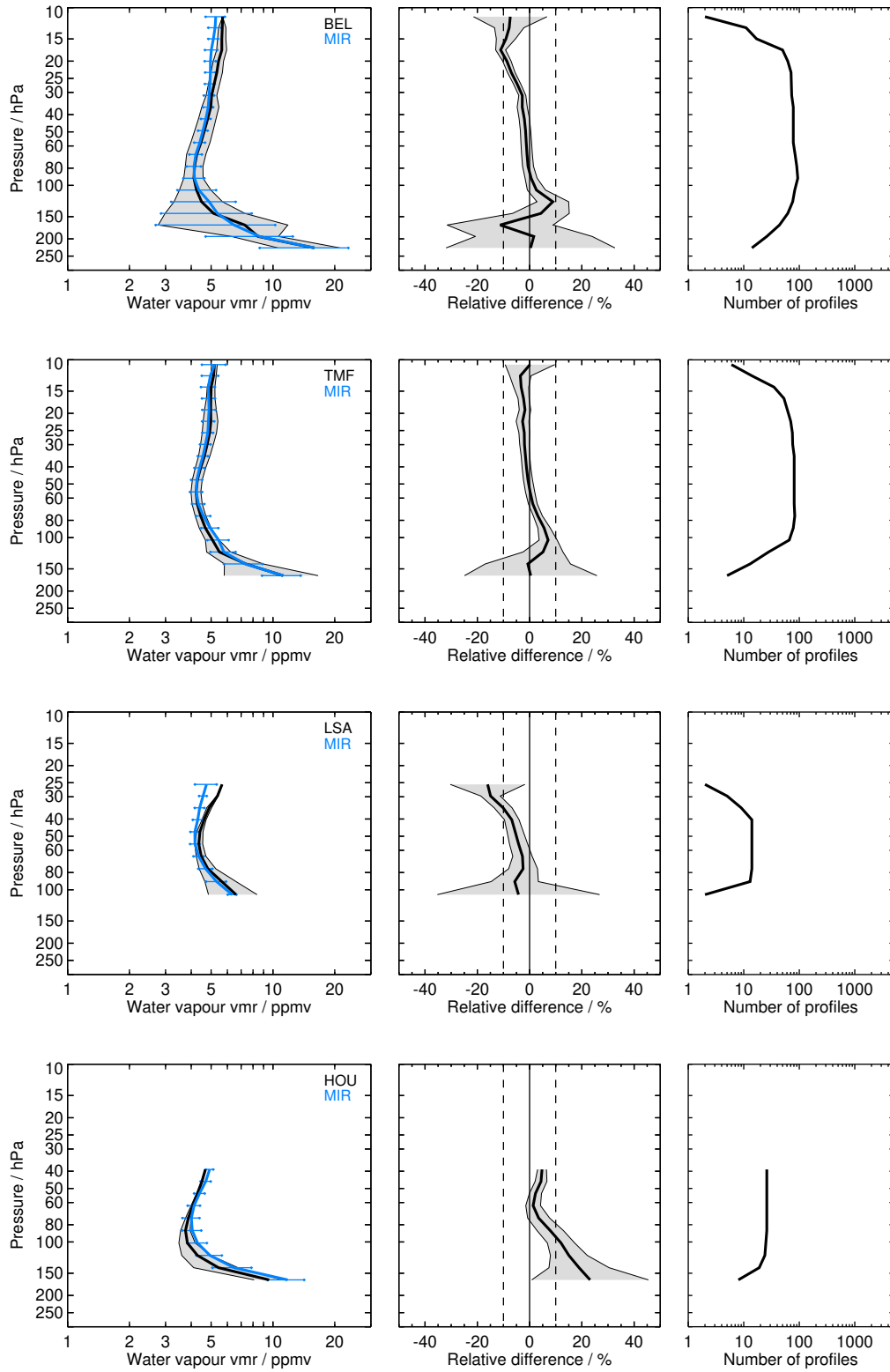


Figure S14: Continued.

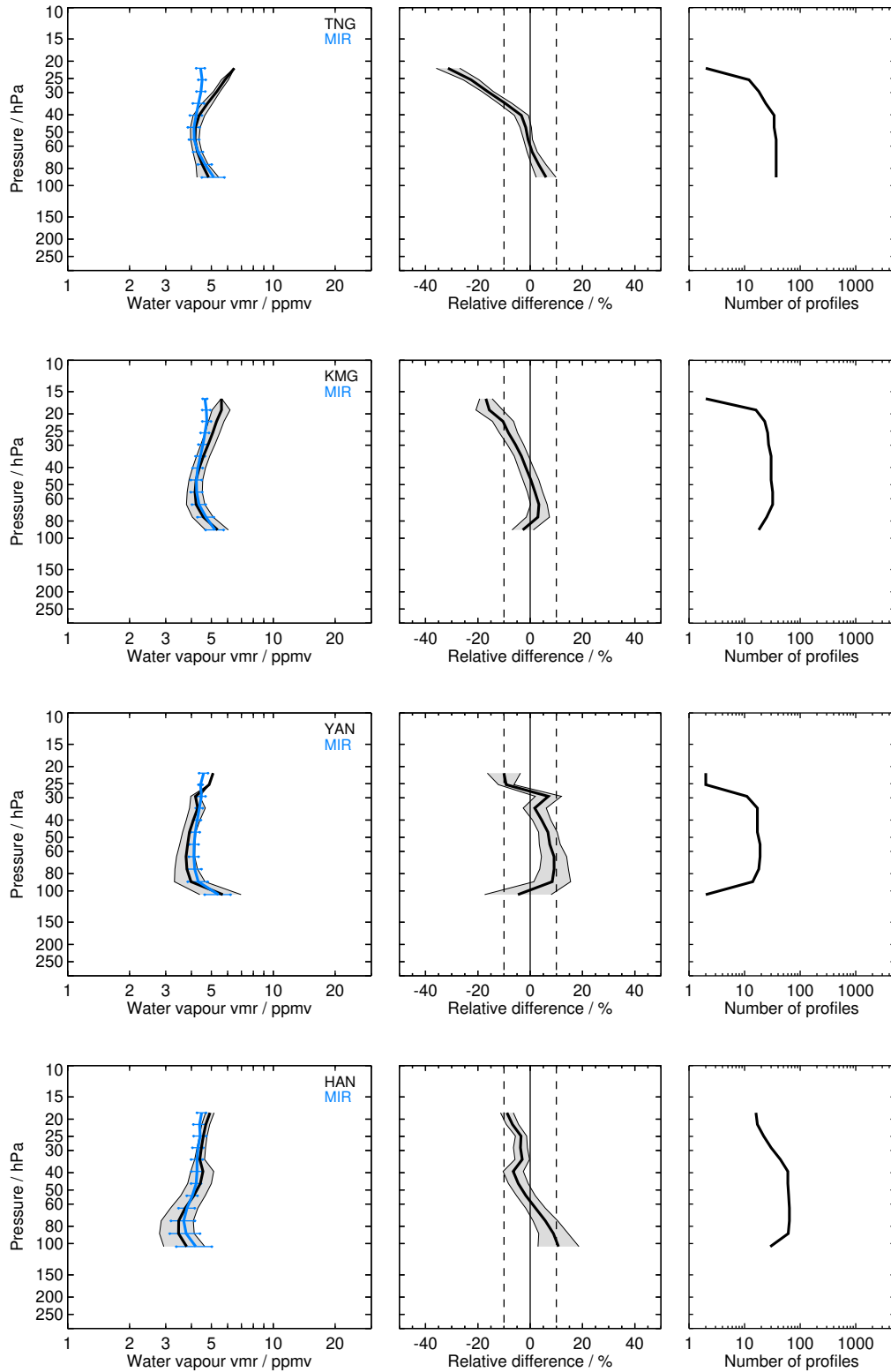


Figure S14: Continued.

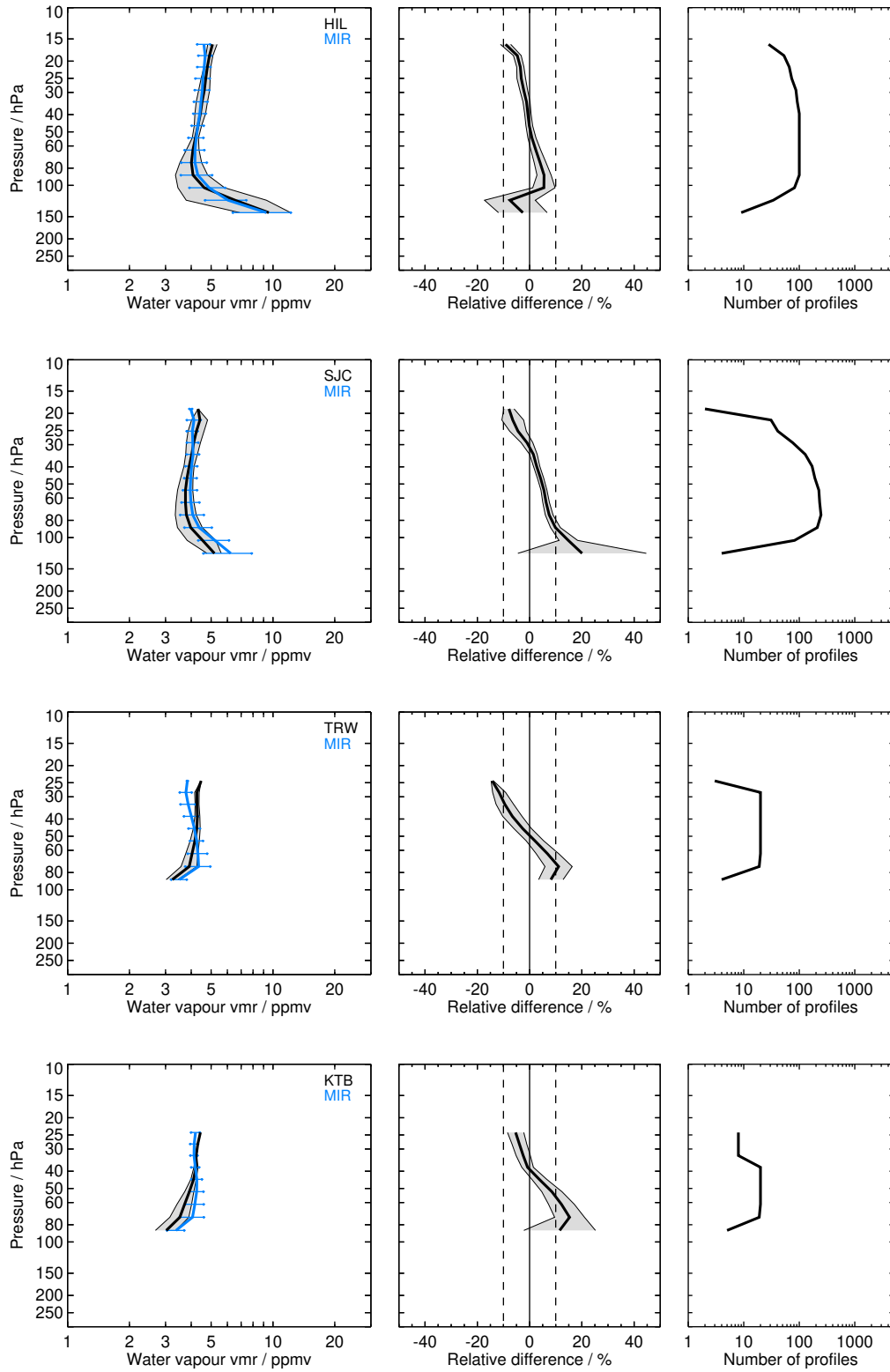


Figure S14: Continued.

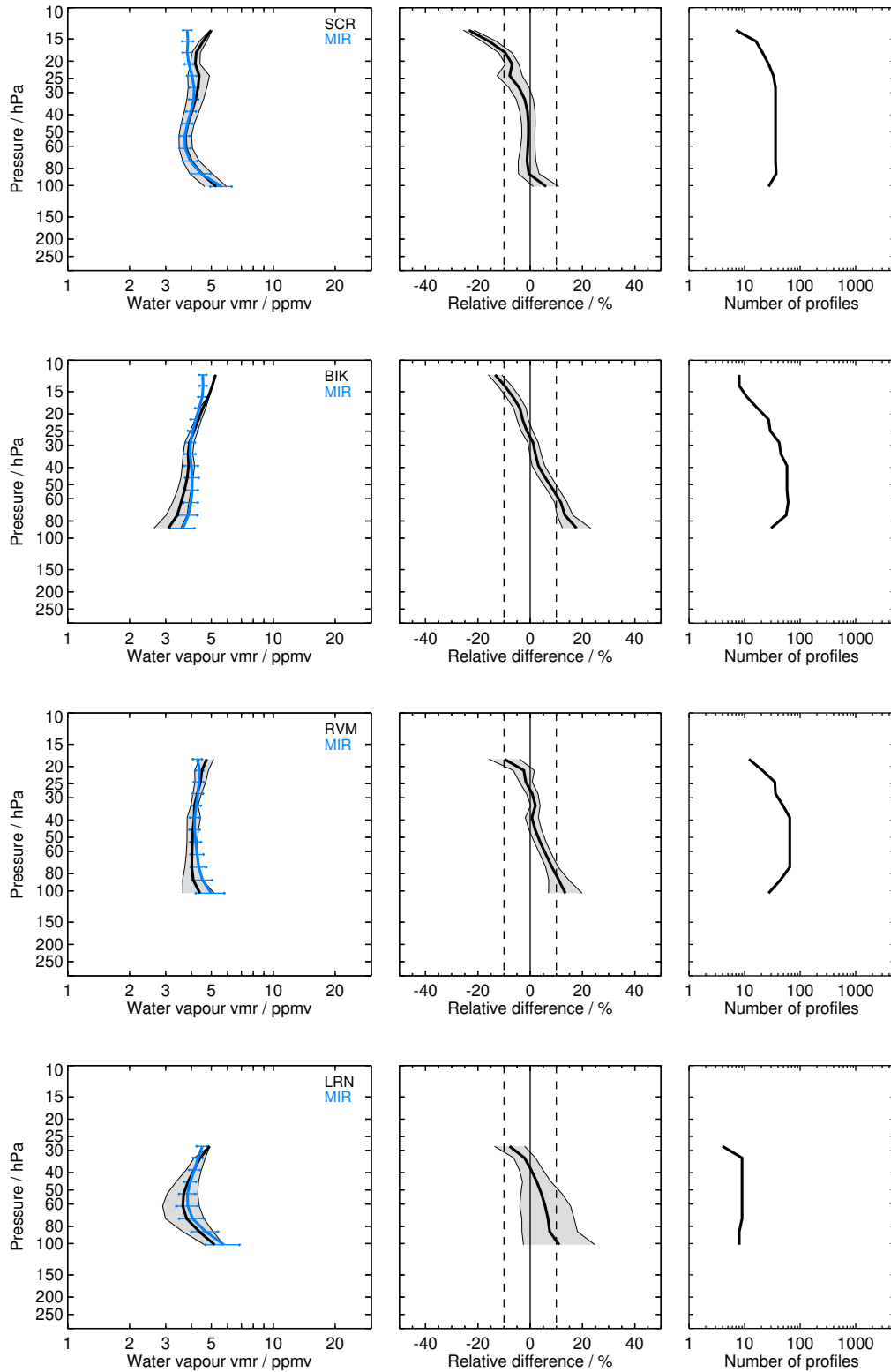


Figure S14: Continued.

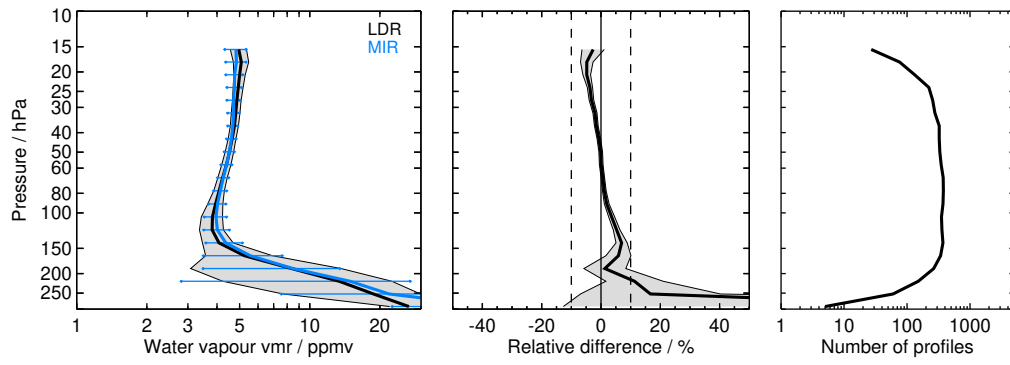


Figure S14: Continued.

2.15 MIPAS-IMK V5R_H2O_522 (MIM)

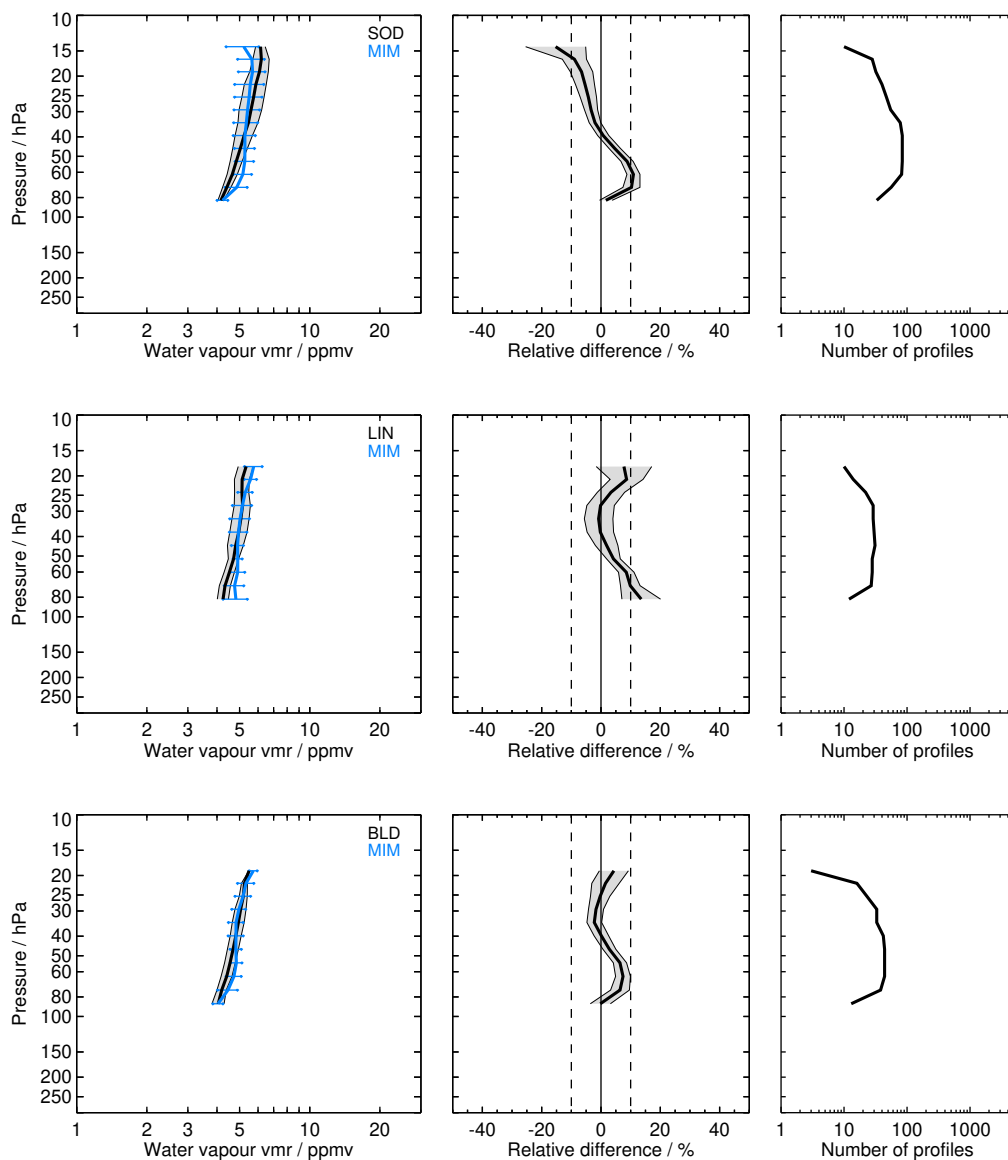


Figure S15: Same as Fig. S1 but for MIM and the SOD, LIN, BLD, BEL, TMF, TNG, KMG, YAN, HAN, HIL, SJC, BIK, RVM, LRN, LDR, and LDR balloon sites.

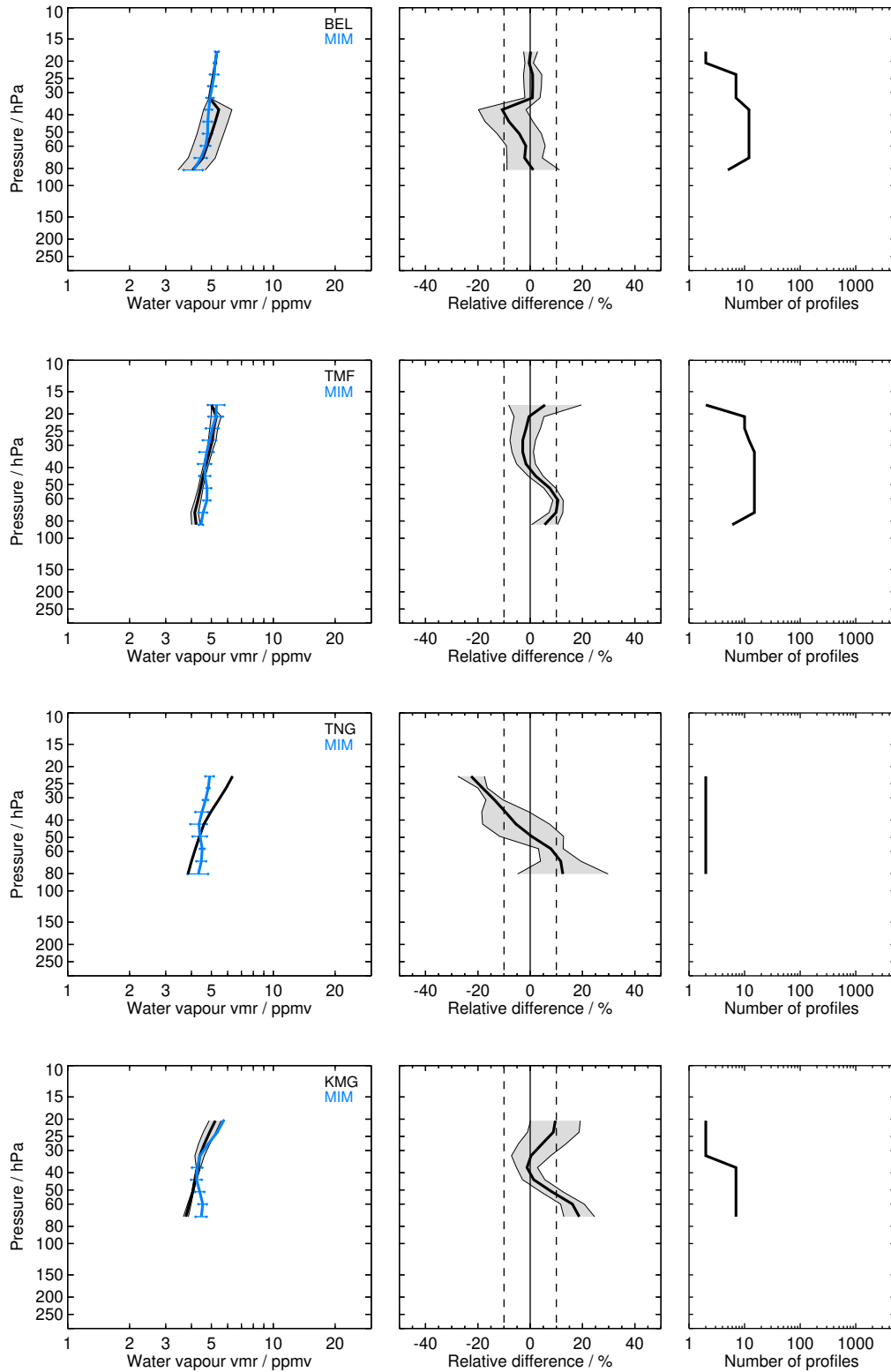


Figure S15: Continued.

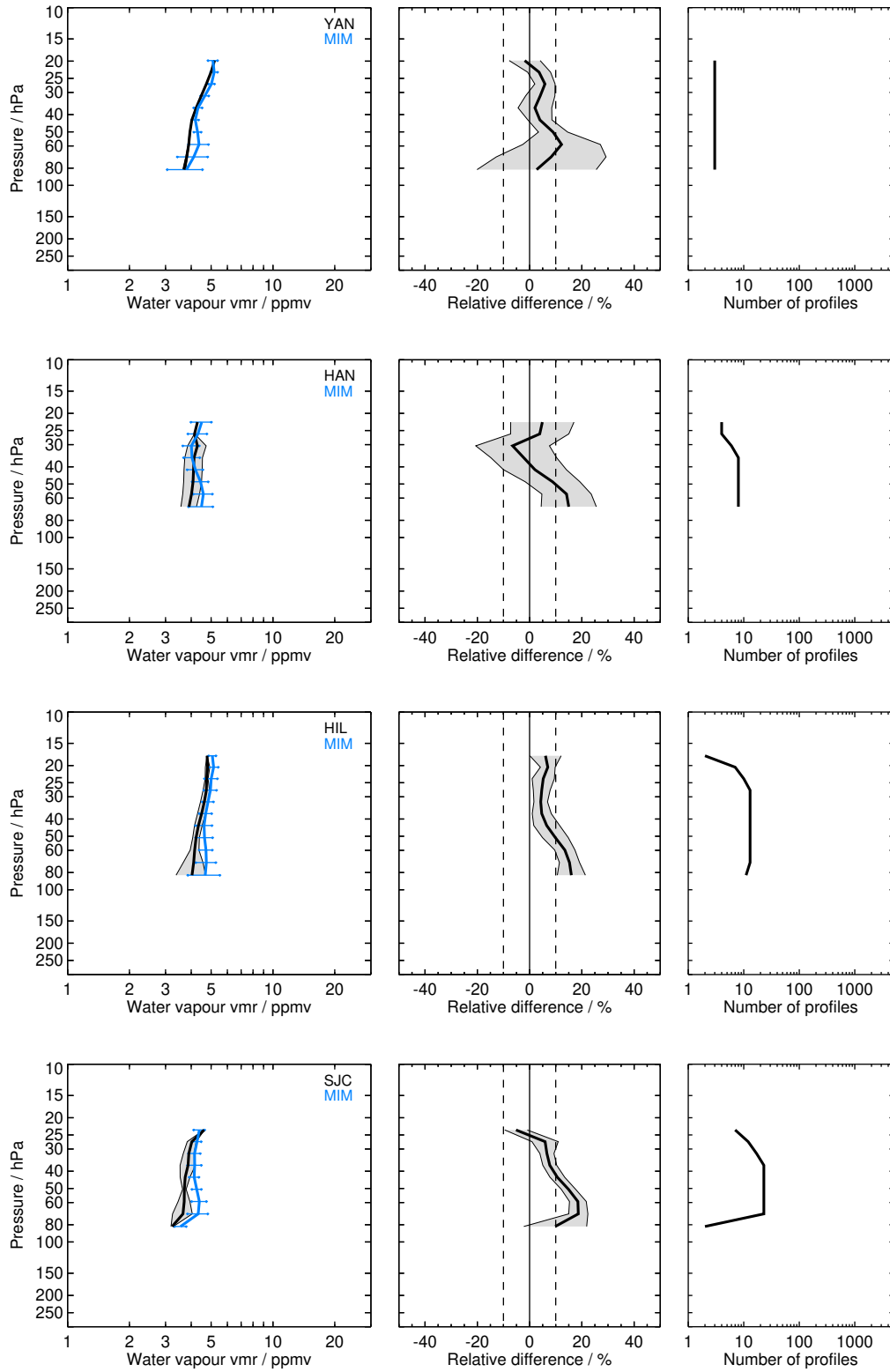


Figure S15: Continued.

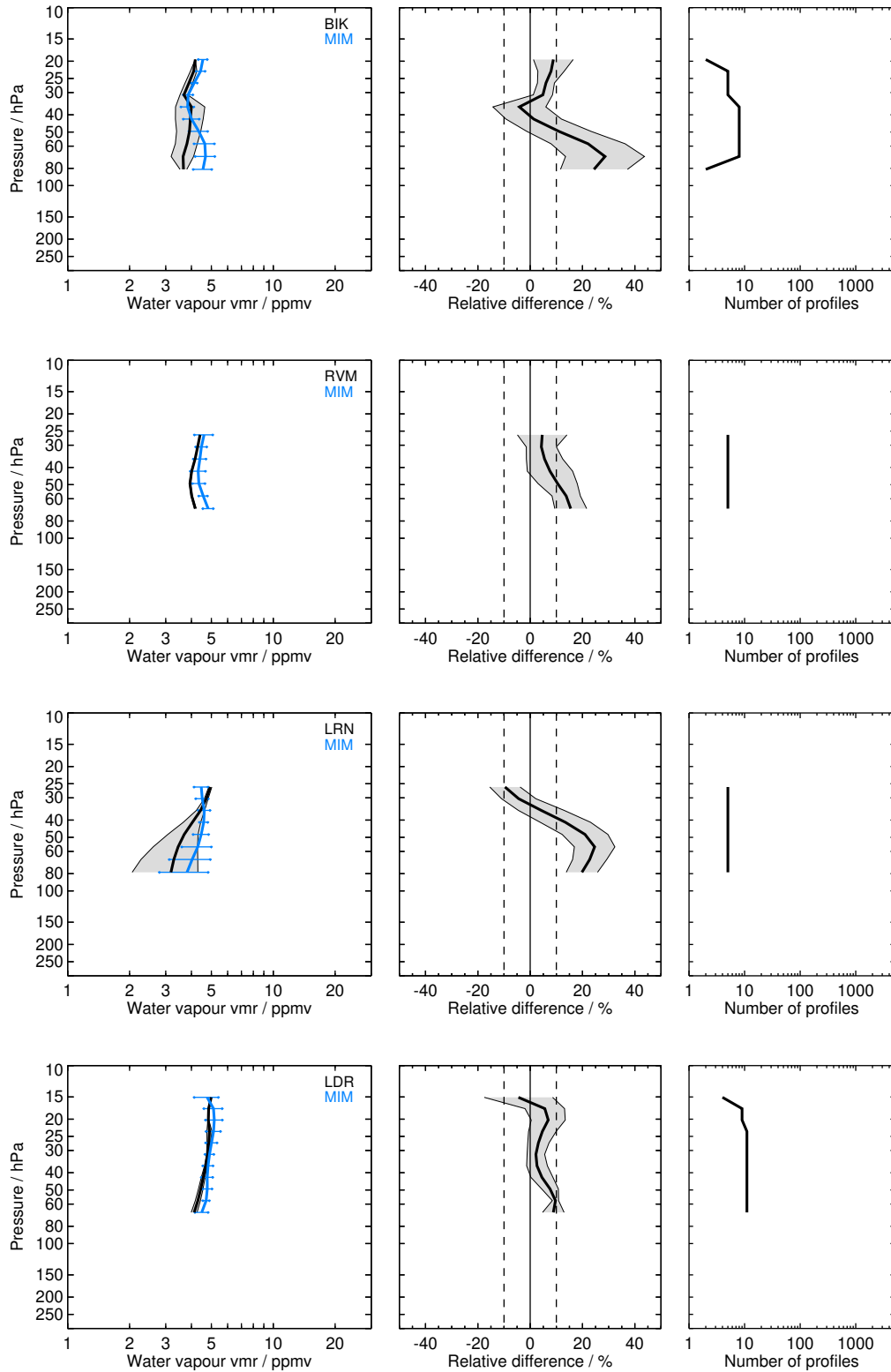


Figure S15: Continued.

2.16 MIPAS-OXF H2O_FR1.30 (MOH)

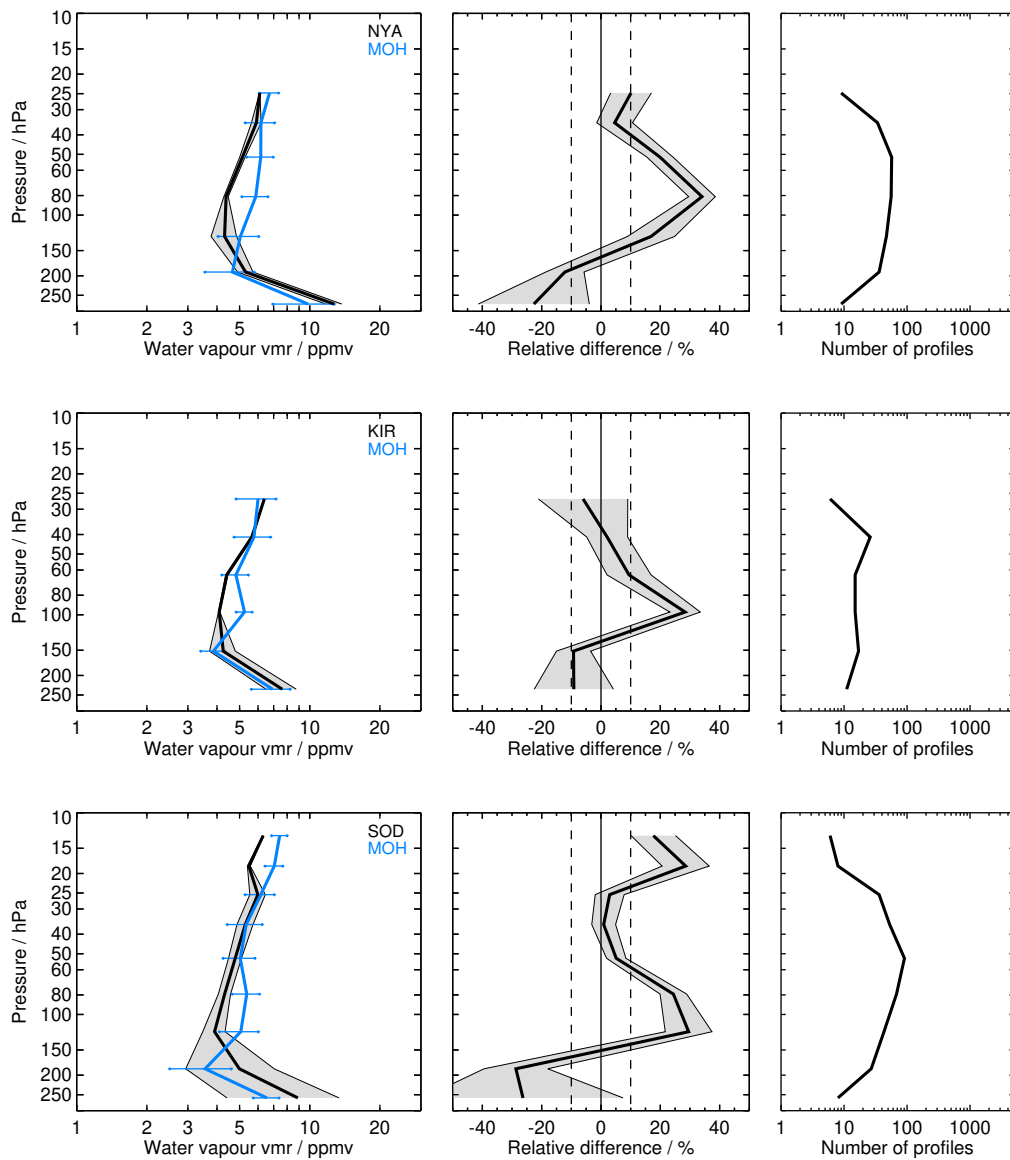


Figure S16: Same as Fig. S1 but for MOH and the NYA, KIR, SOD, BLD, SGP, HUN, FTS, HIL, SCR, WTK, LDR, and LDR balloon sites.

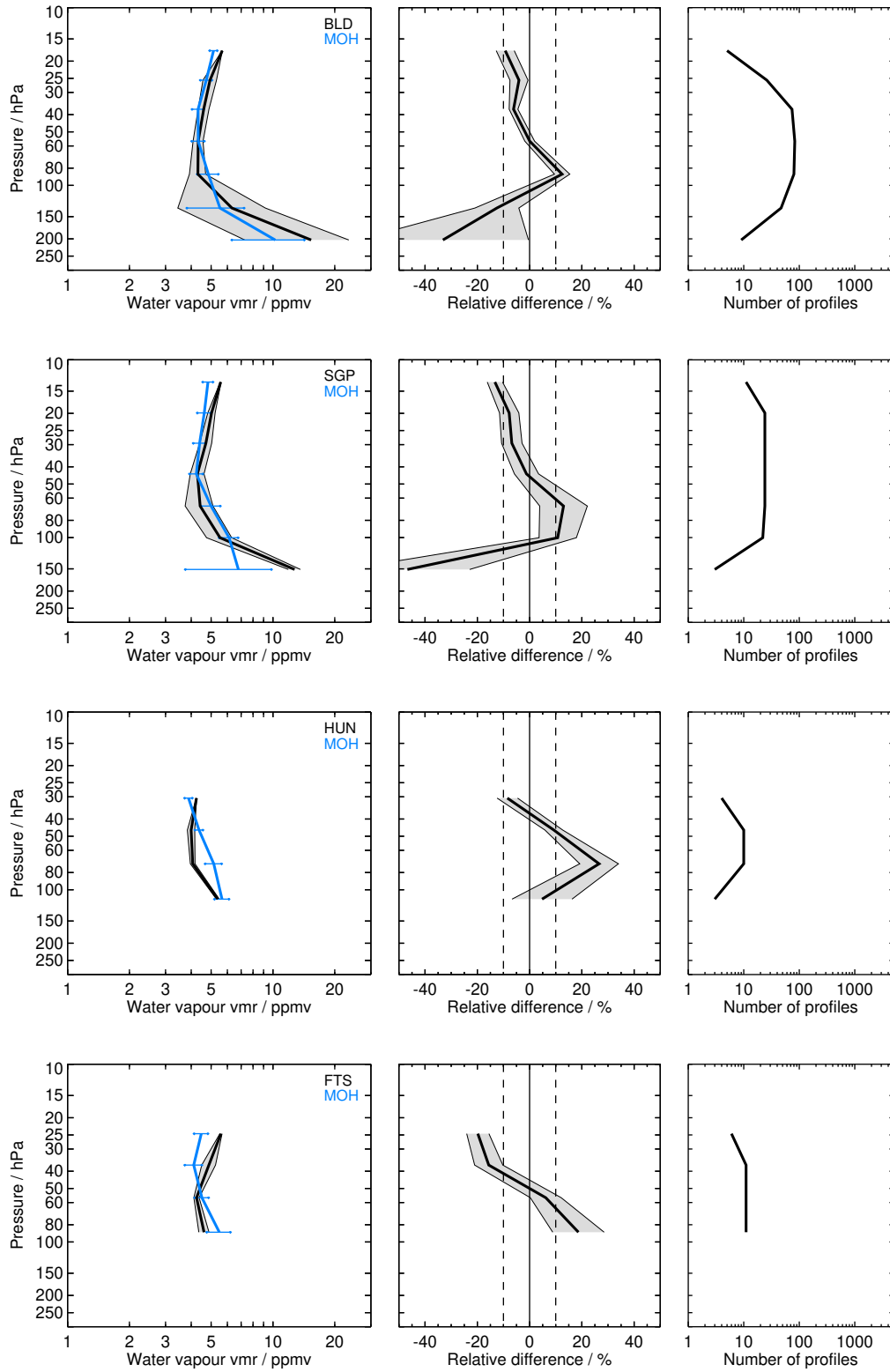


Figure S16: Continued.

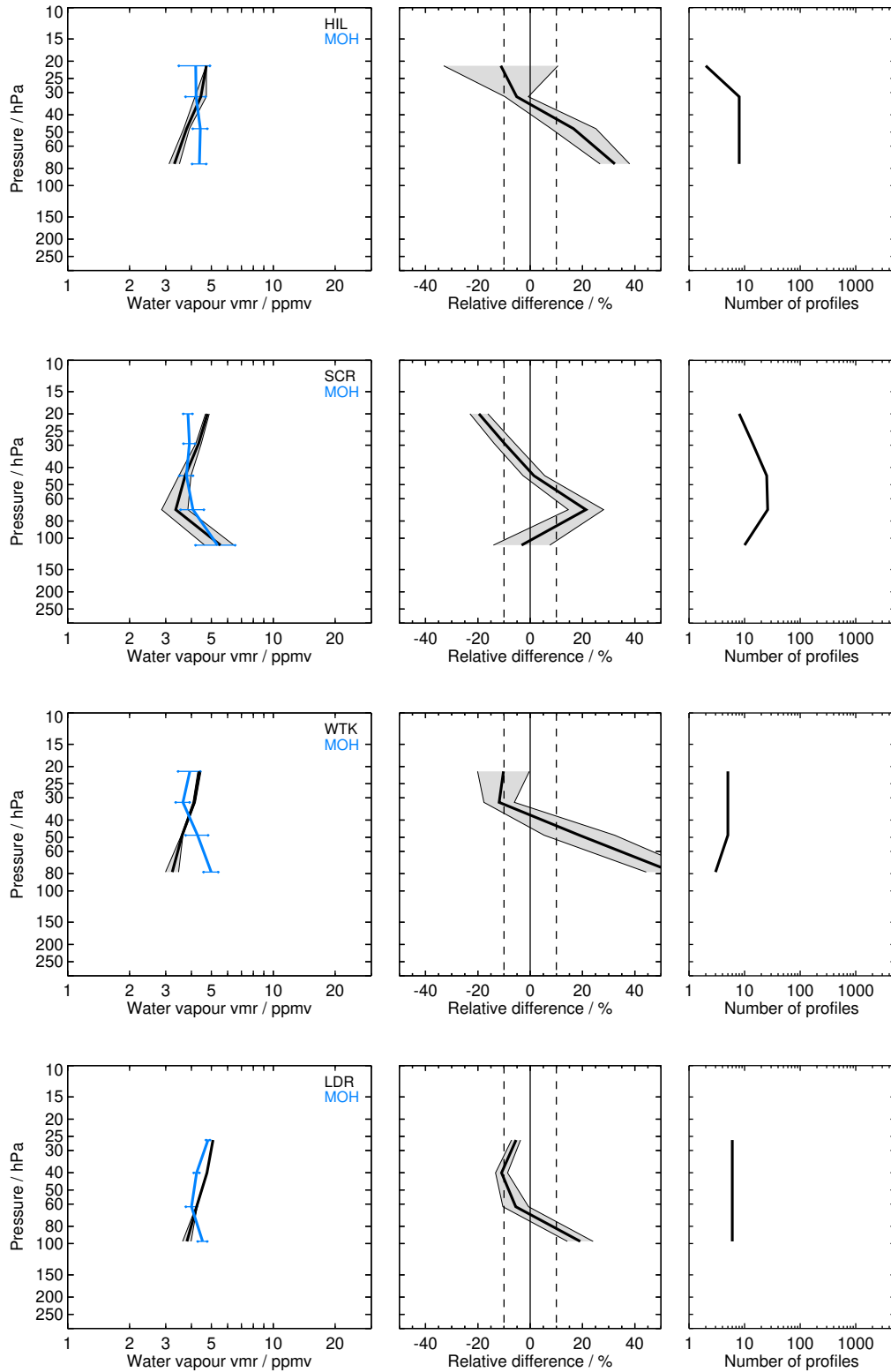


Figure S16: Continued.

2.17 MIPAS-OXF H2O_MA1.30 (MOM)

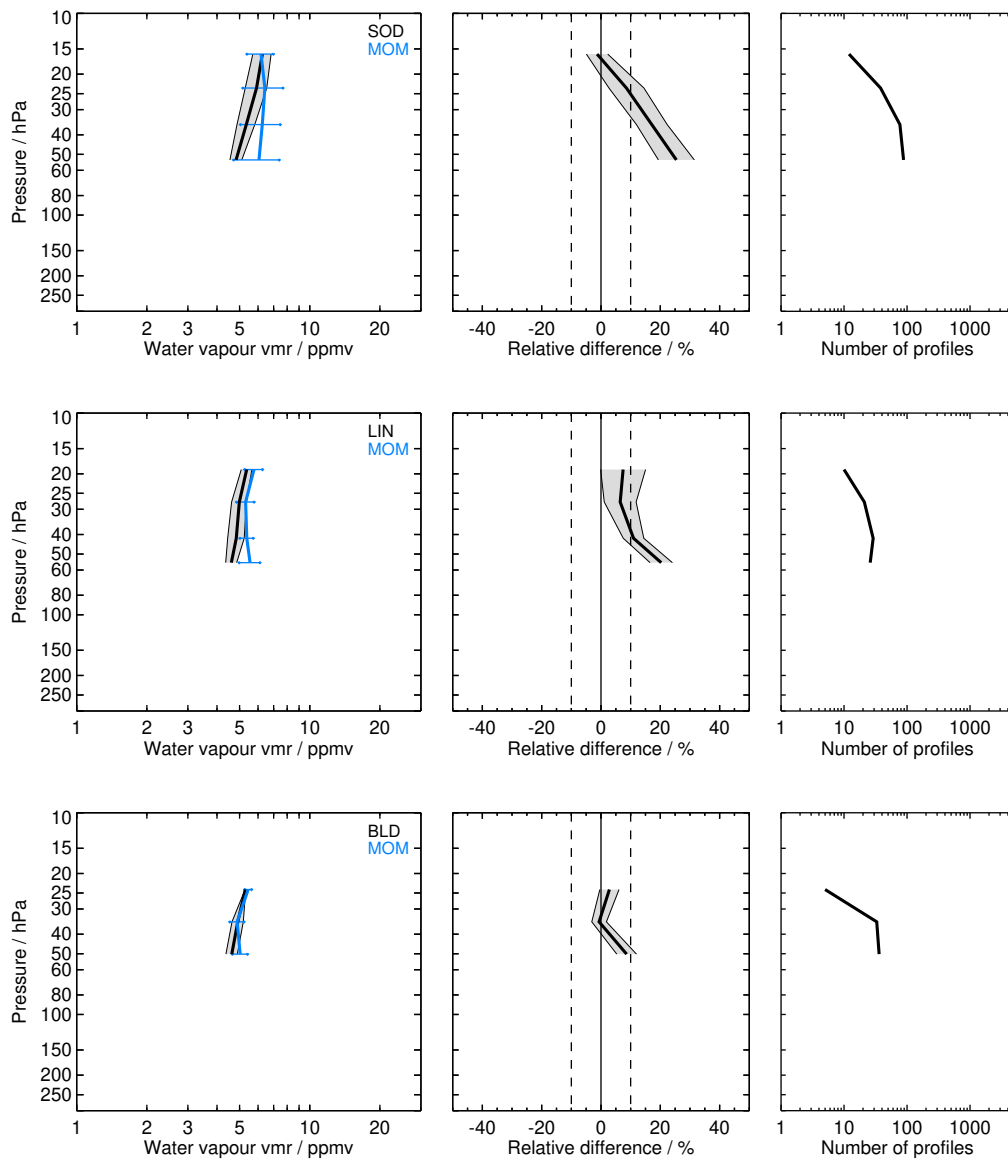


Figure S17: Same as Fig. S1 but for MOM and the SOD, LIN, BLD, BEL, TMF, TNG, KMG, YAN, HAN, HIL, SJC, BIK, RVM, LRN, LDR, and LDR balloon sites.

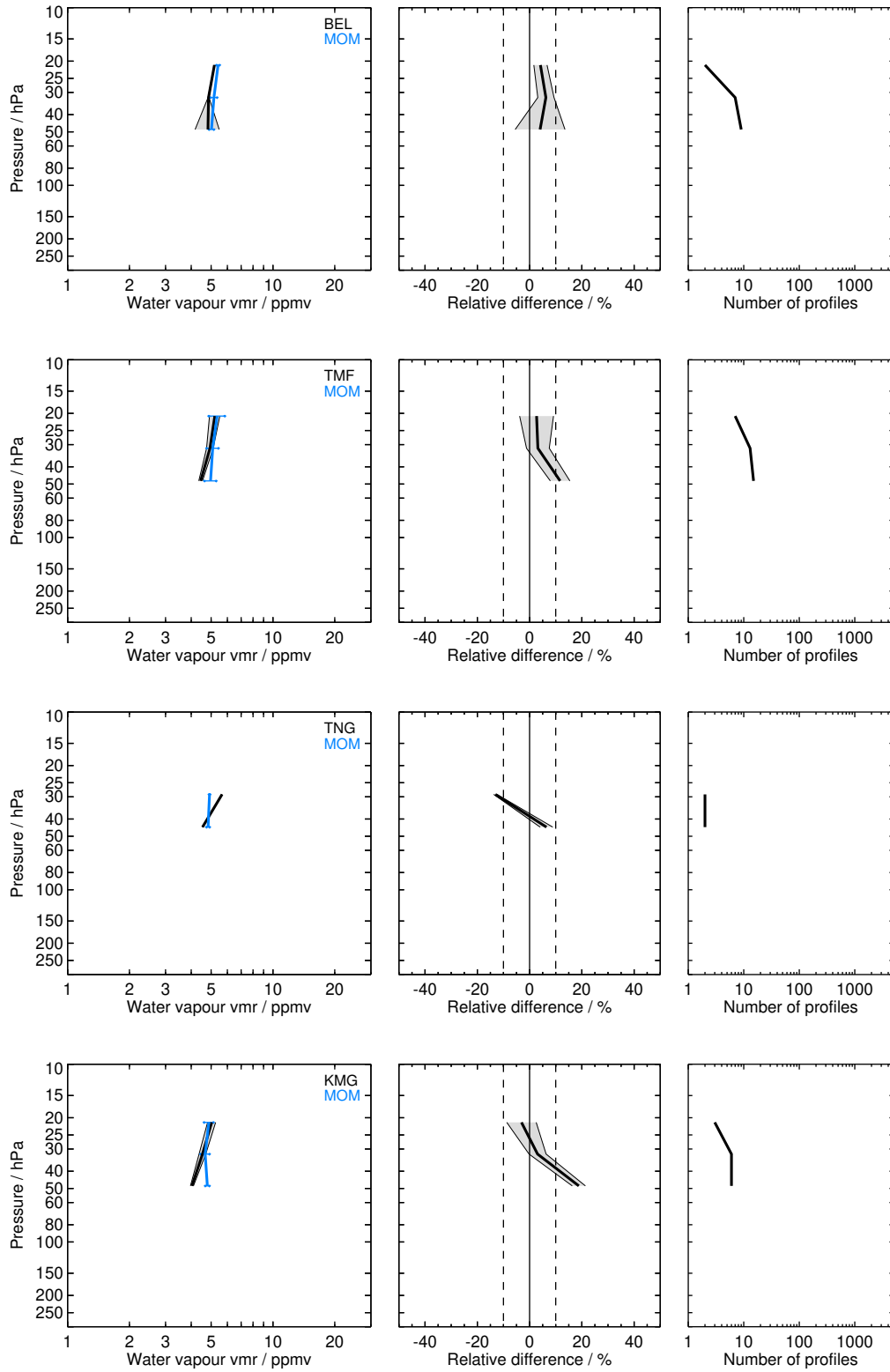


Figure S17: Continued.

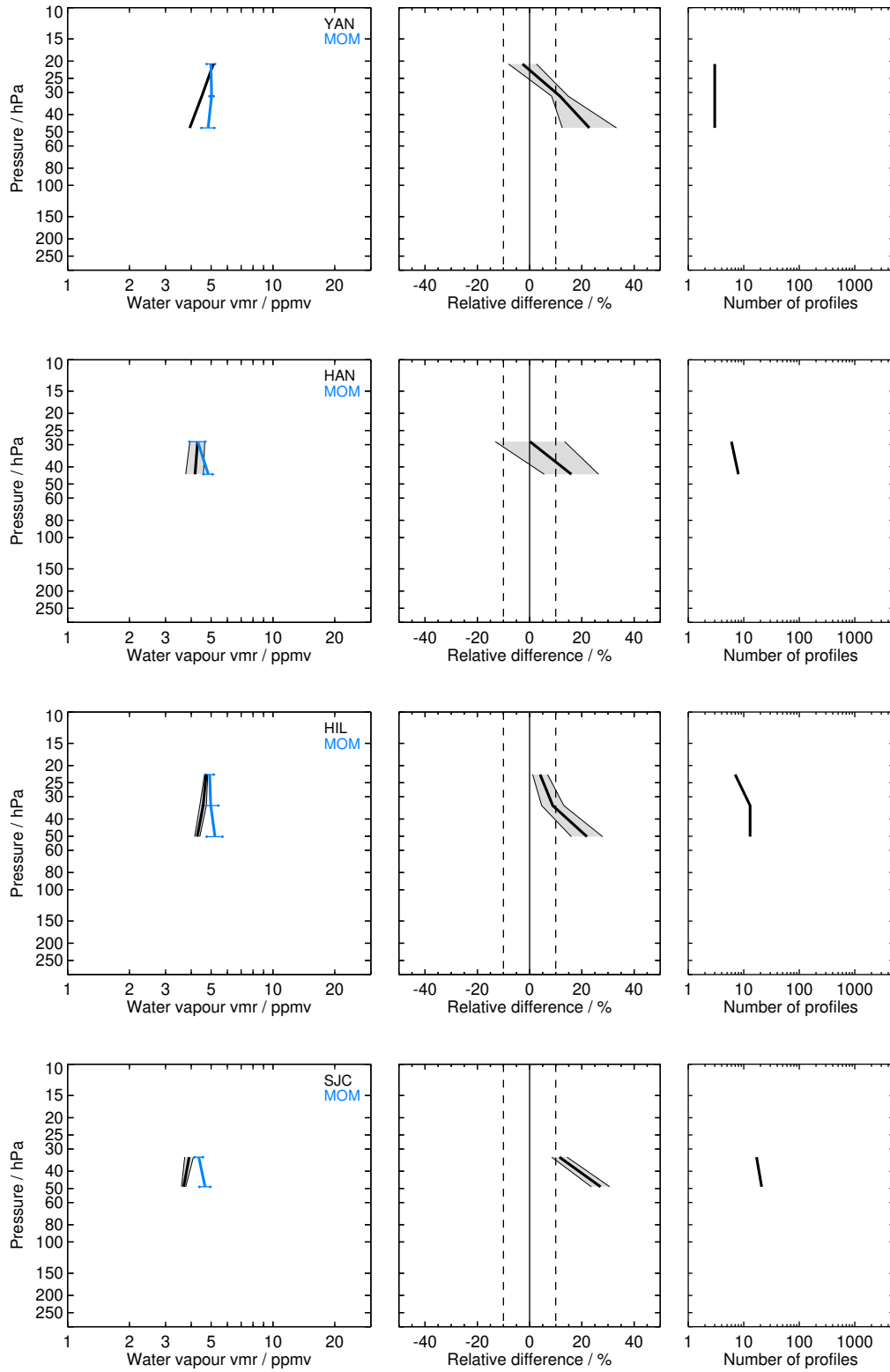


Figure S17: Continued.

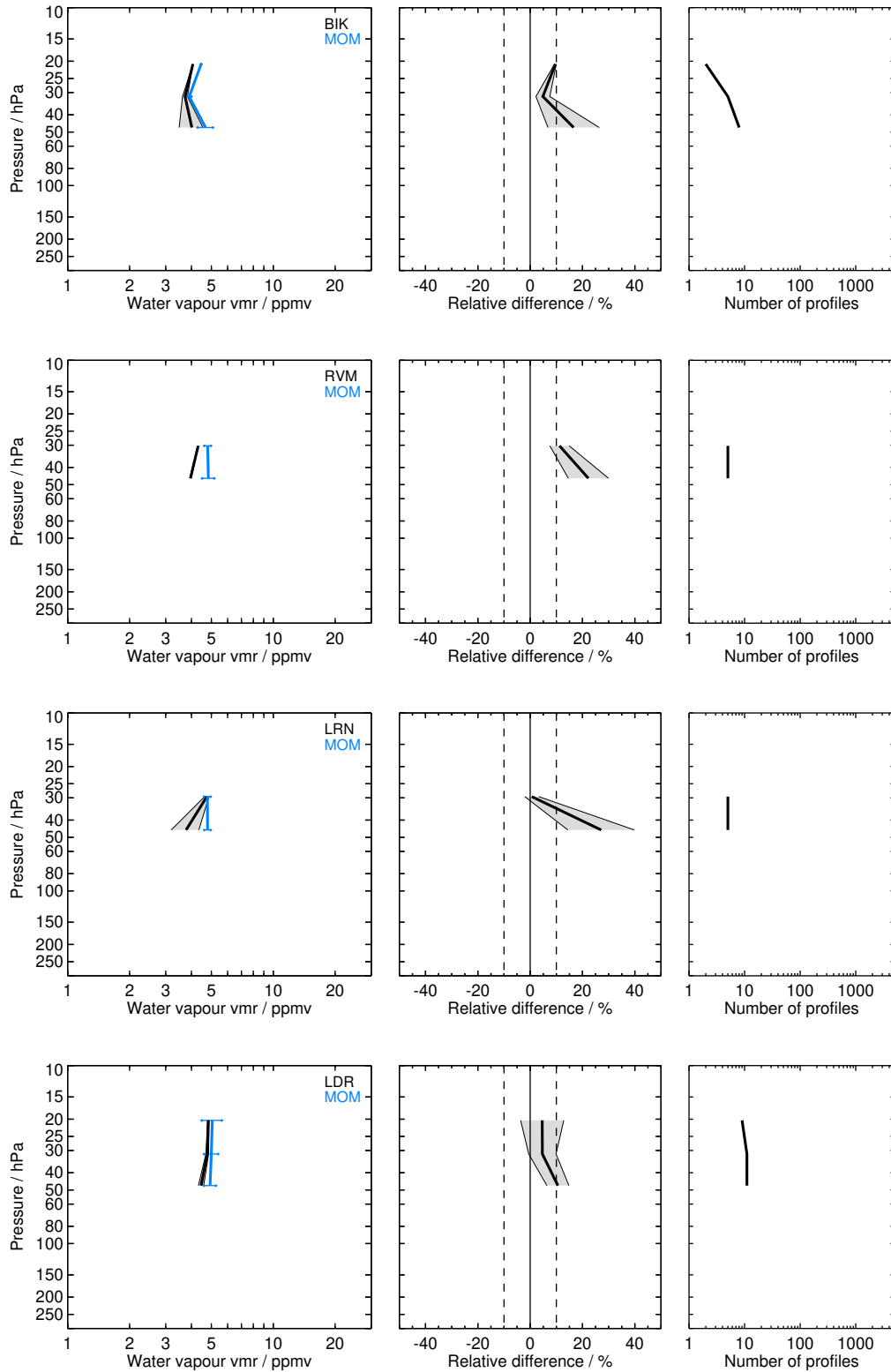


Figure S17: Continued.

2.18 MIPAS-OXF H2O_RR1.30 (MOR)

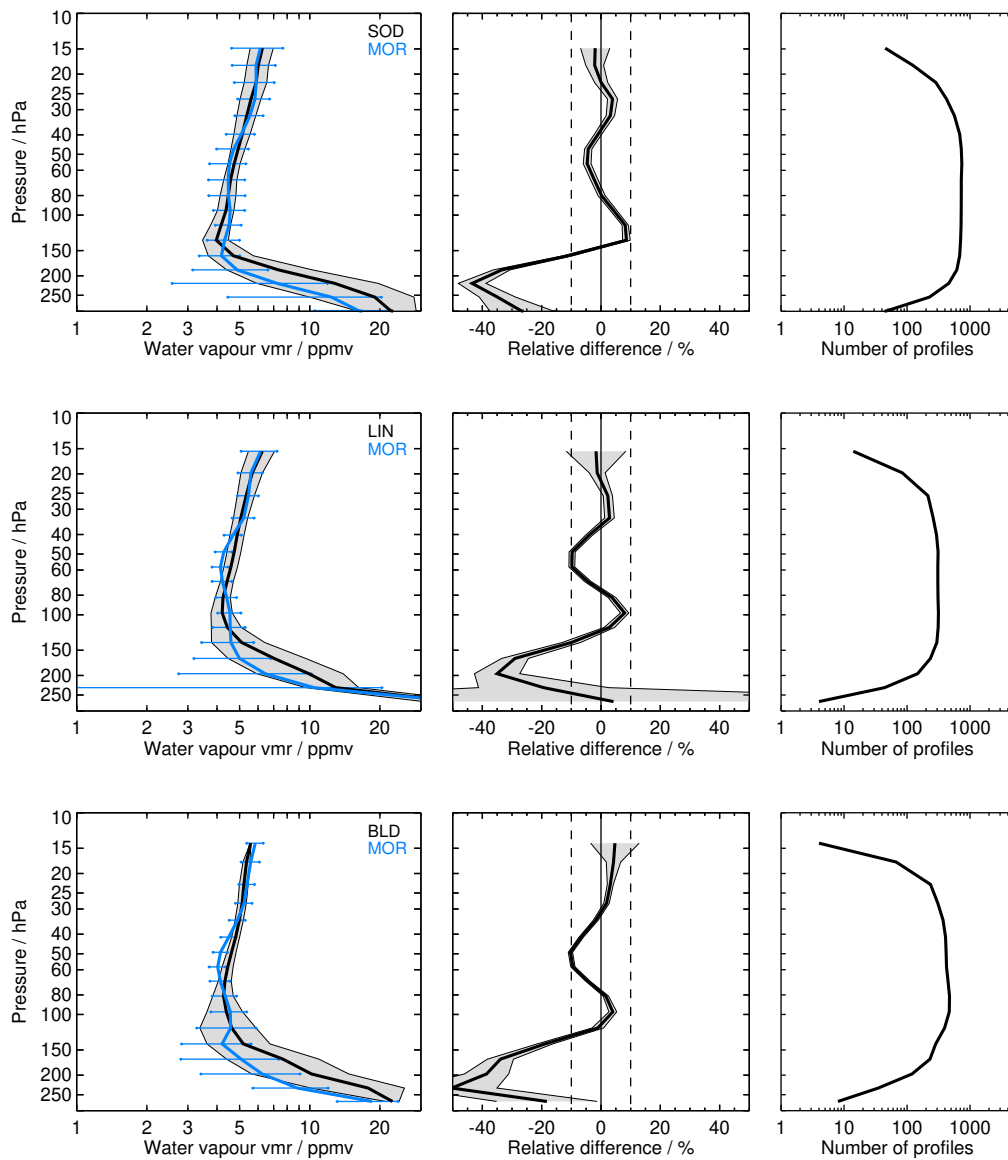


Figure S18: Same as Fig. S1 but for MOR and the SOD, LIN, BLD, BEL, TMF, LSA, HOU, TNG, KMG, YAN, HAN, HIL, SJC, TRW, KTB, SCR, BIK, RVM, LRN, LDR, and LDR balloon sites.

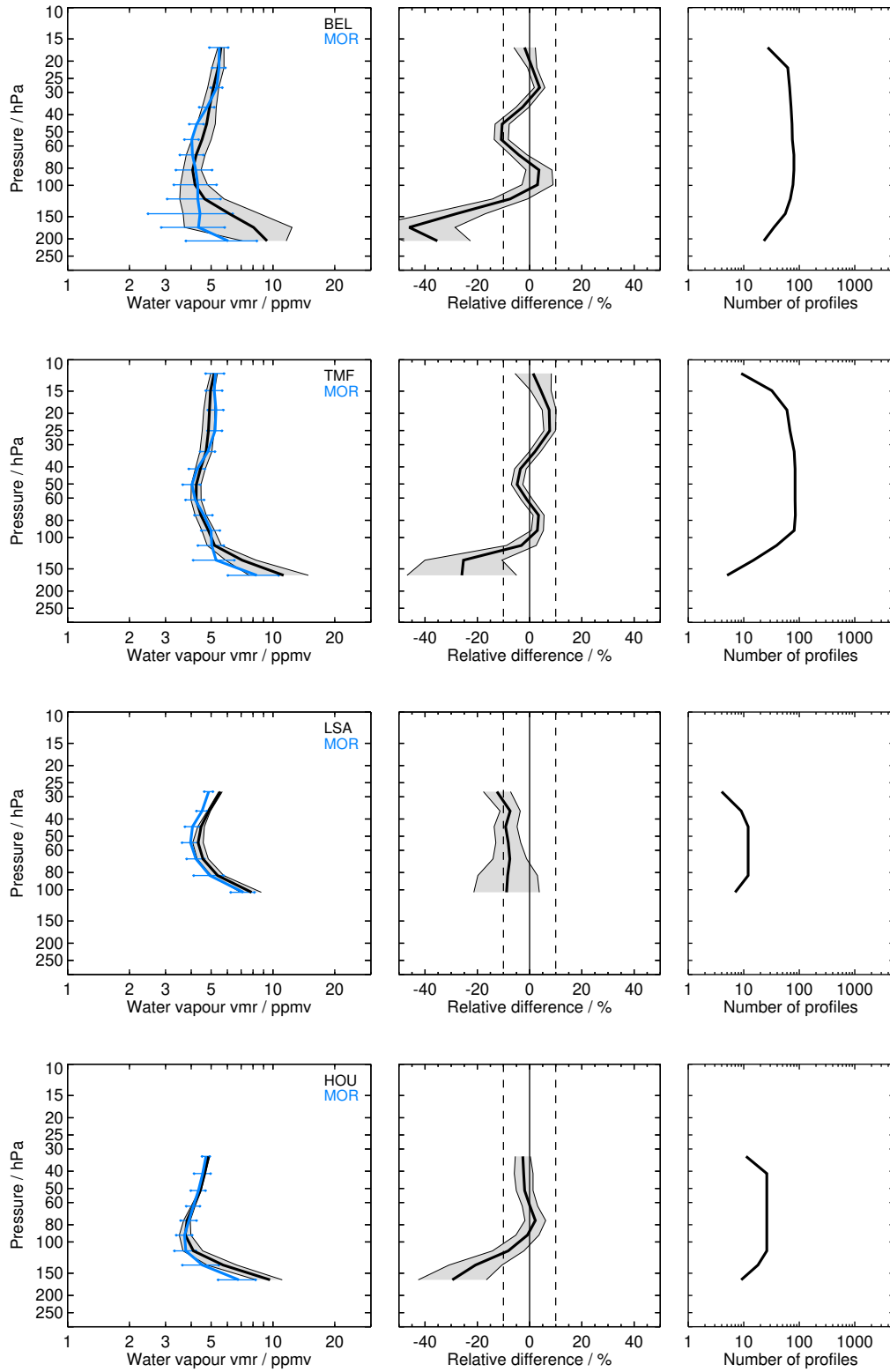


Figure S18: Continued.

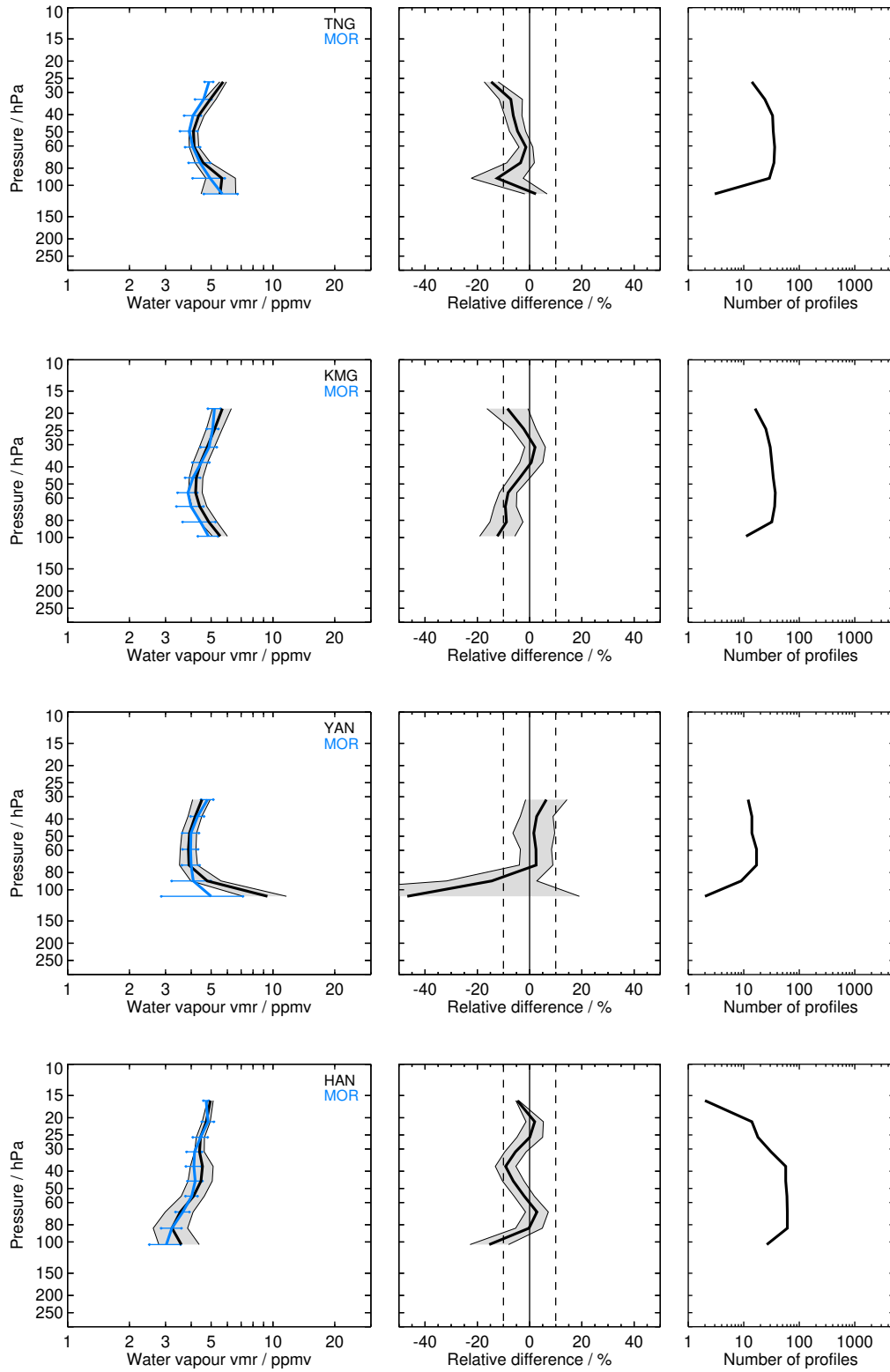


Figure S18: Continued.

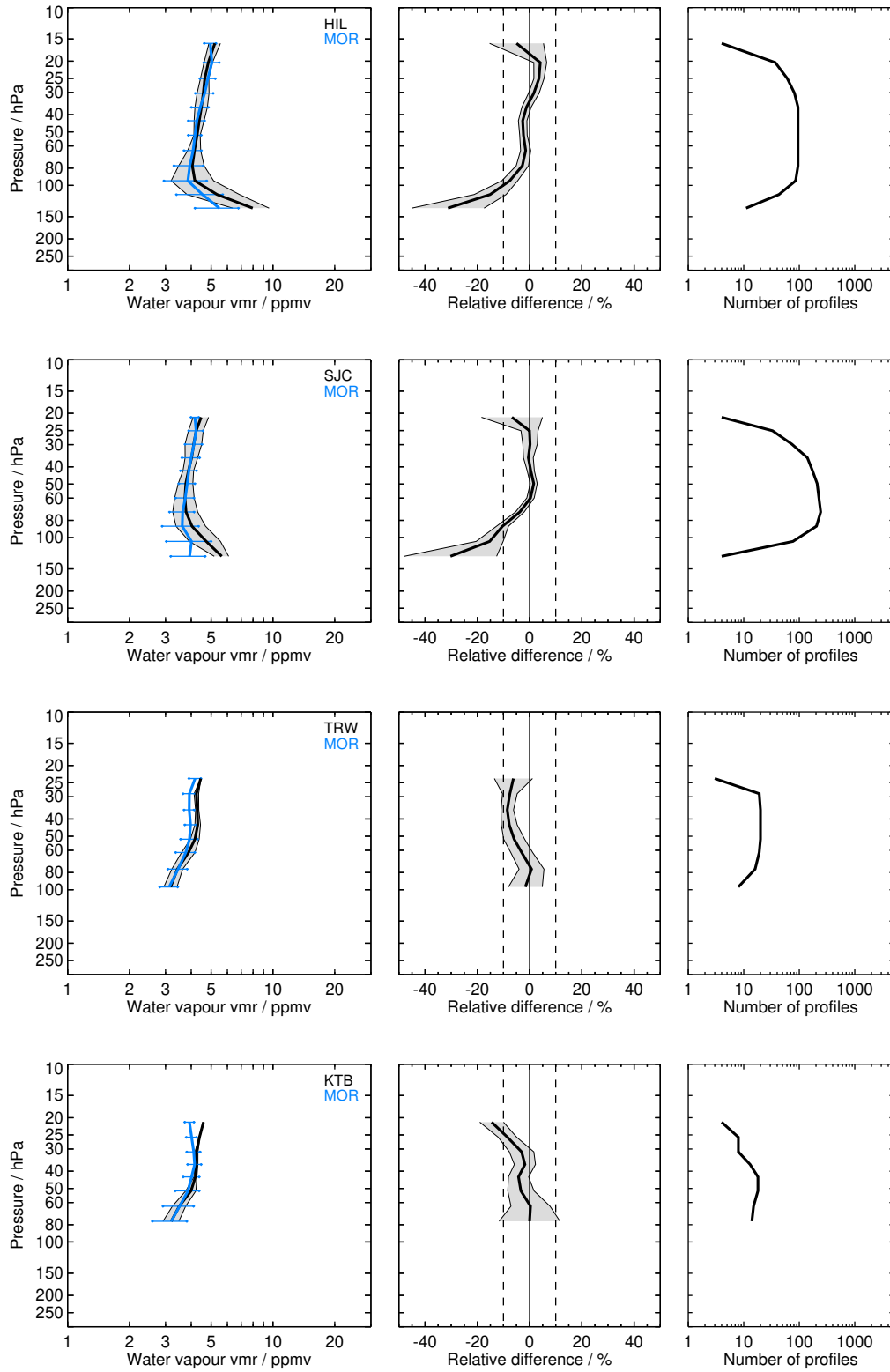


Figure S18: Continued.

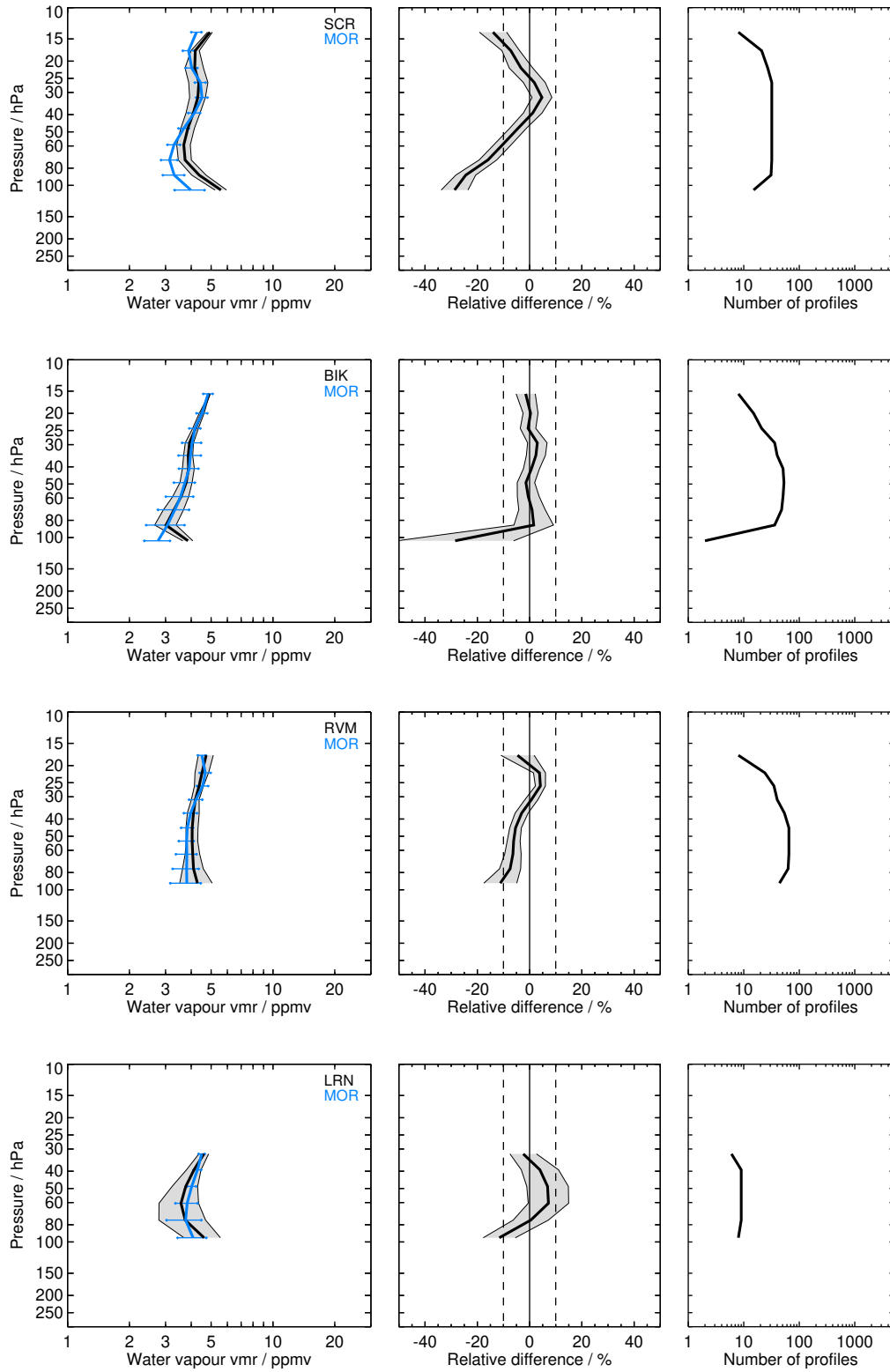


Figure S18: Continued.

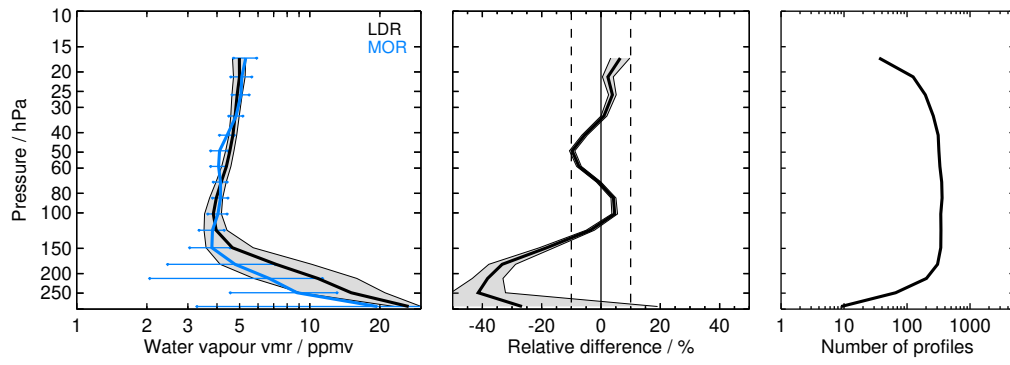


Figure S18: Continued.

2.19 MLS-Aura H2O_V4.2 (MLS)

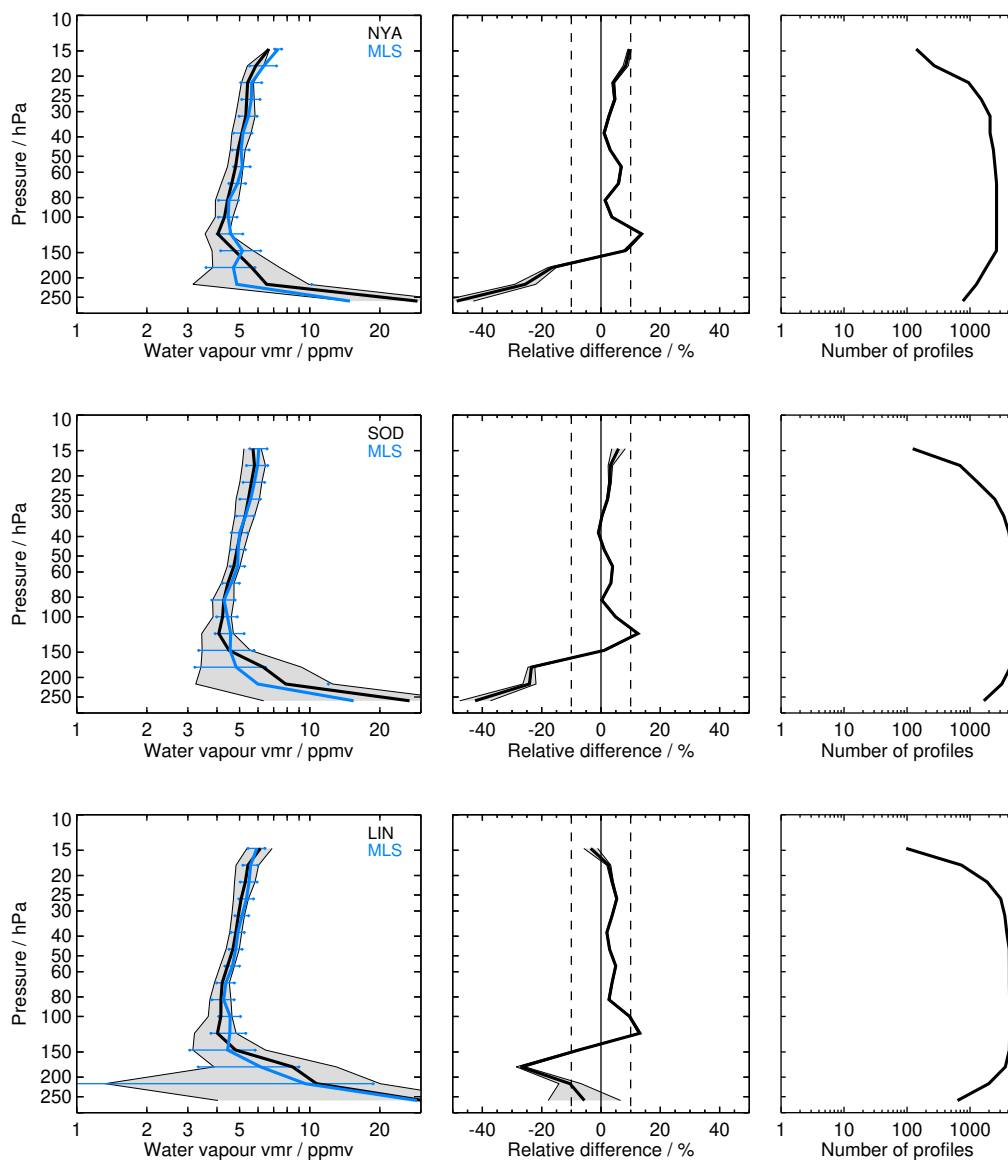


Figure S19: Same as Fig. S1 but for MLS and the NYA, SOD, LIN, BLD, BEL, FTS, TMF, LSA, HOU, TNG, KMG, YAN, HAN, HIL, SJC, TRW, KTB, SCR, BIK, BND, RVM, LRN, LDR, and LDR balloon sites.

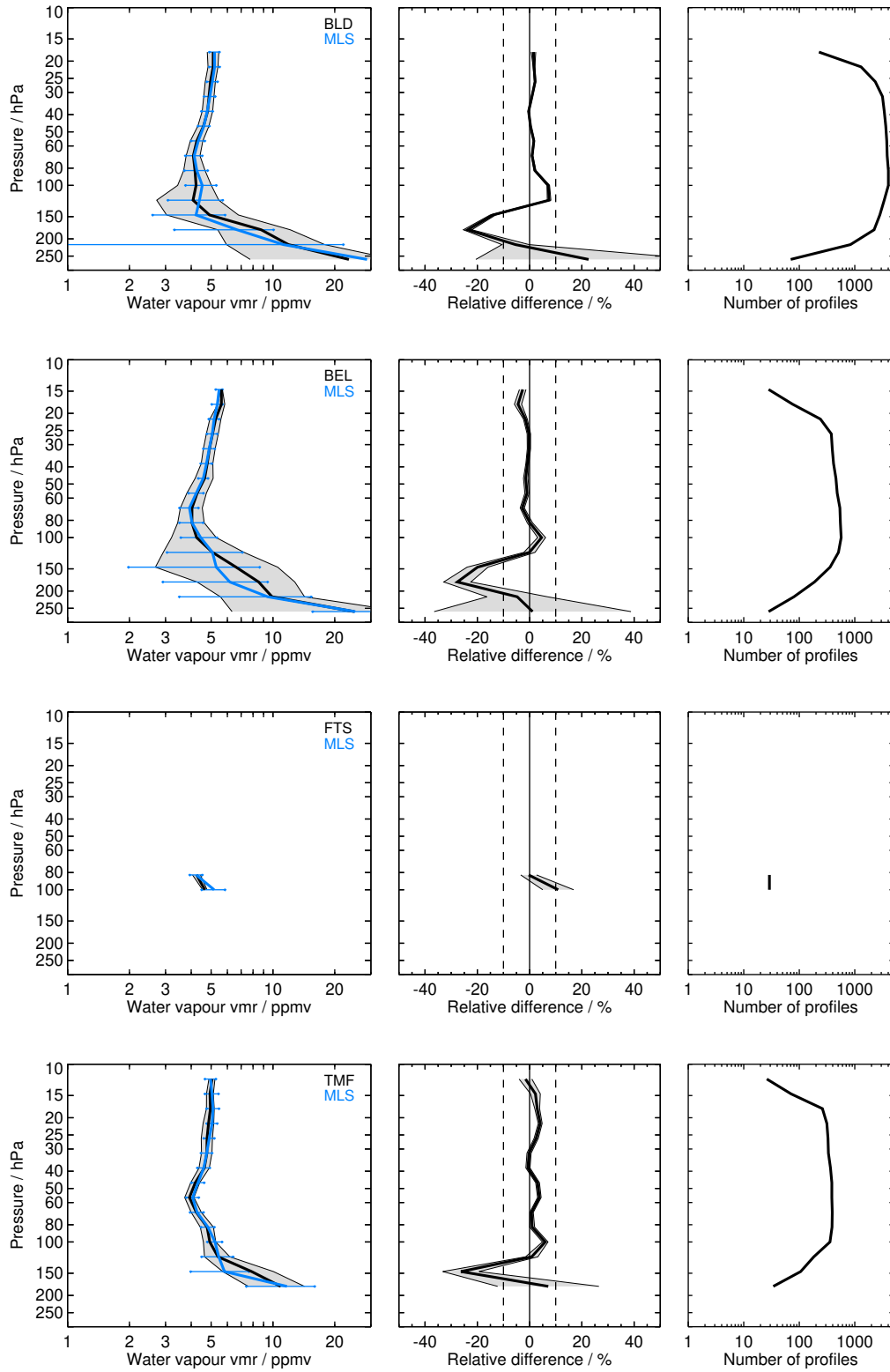


Figure S19: Continued.

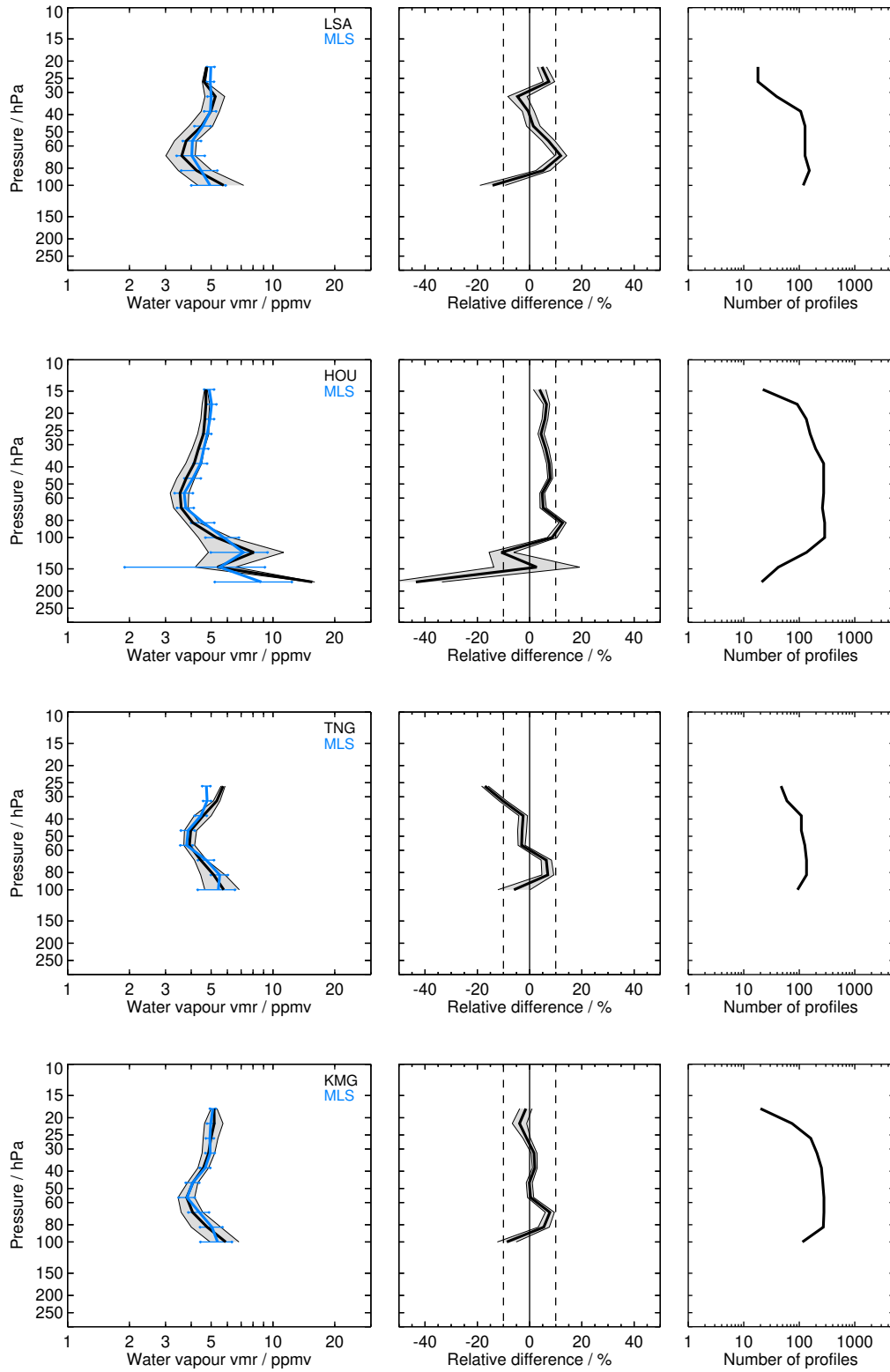


Figure S19: Continued.

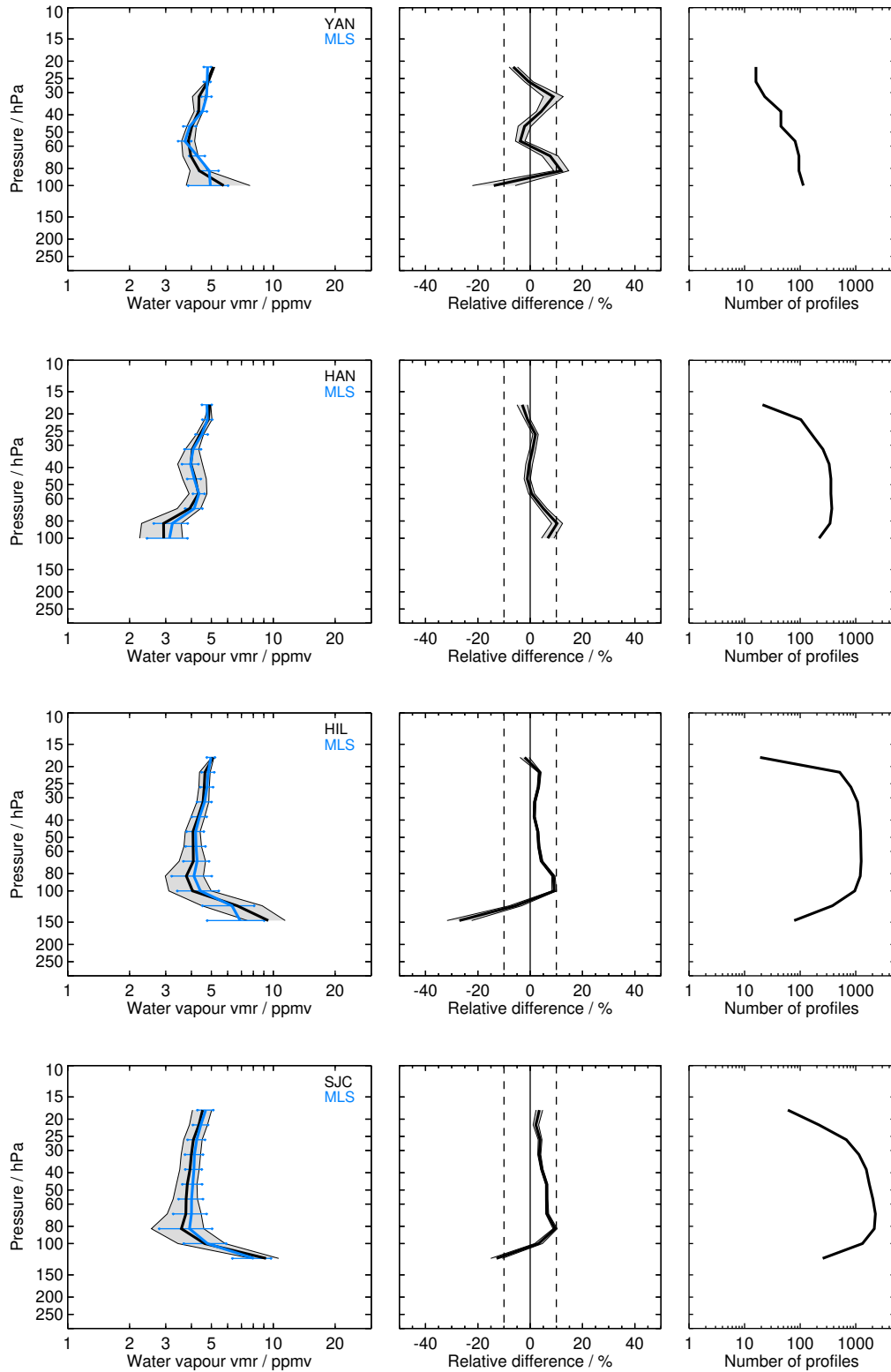


Figure S19: Continued.

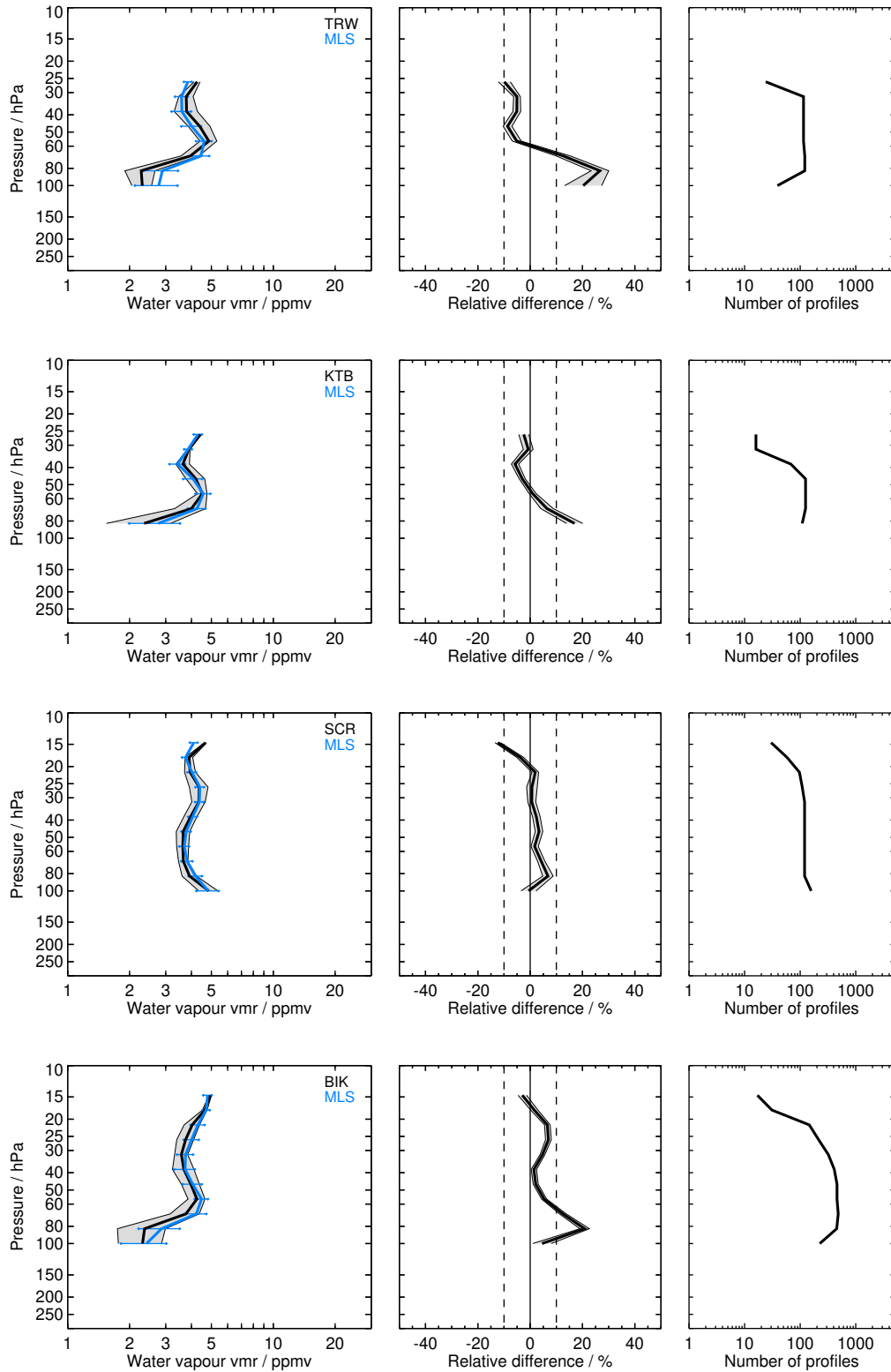


Figure S19: Continued.

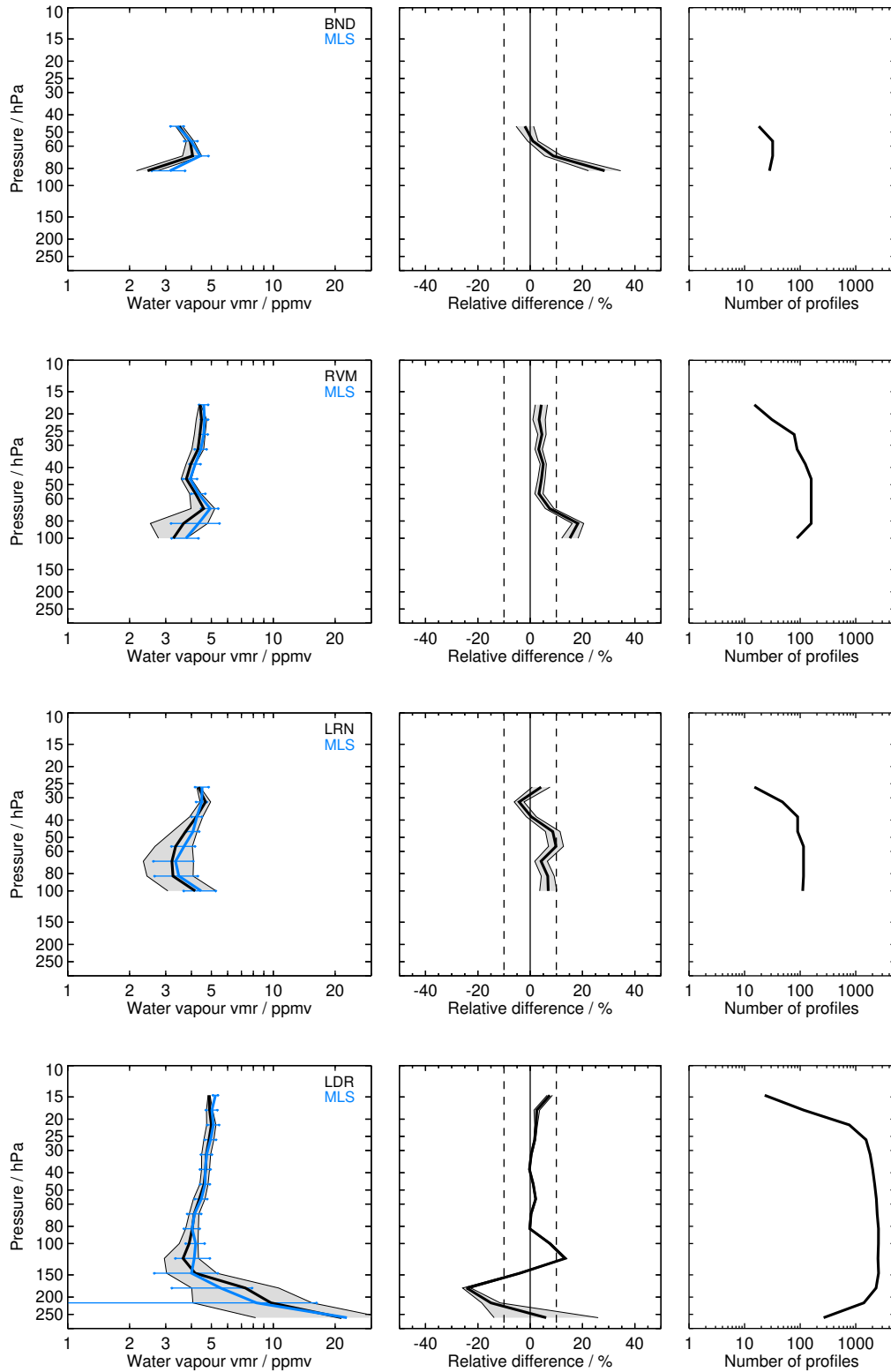


Figure S19: Continued.

2.20 POAM_III H2O_v4 (POM)

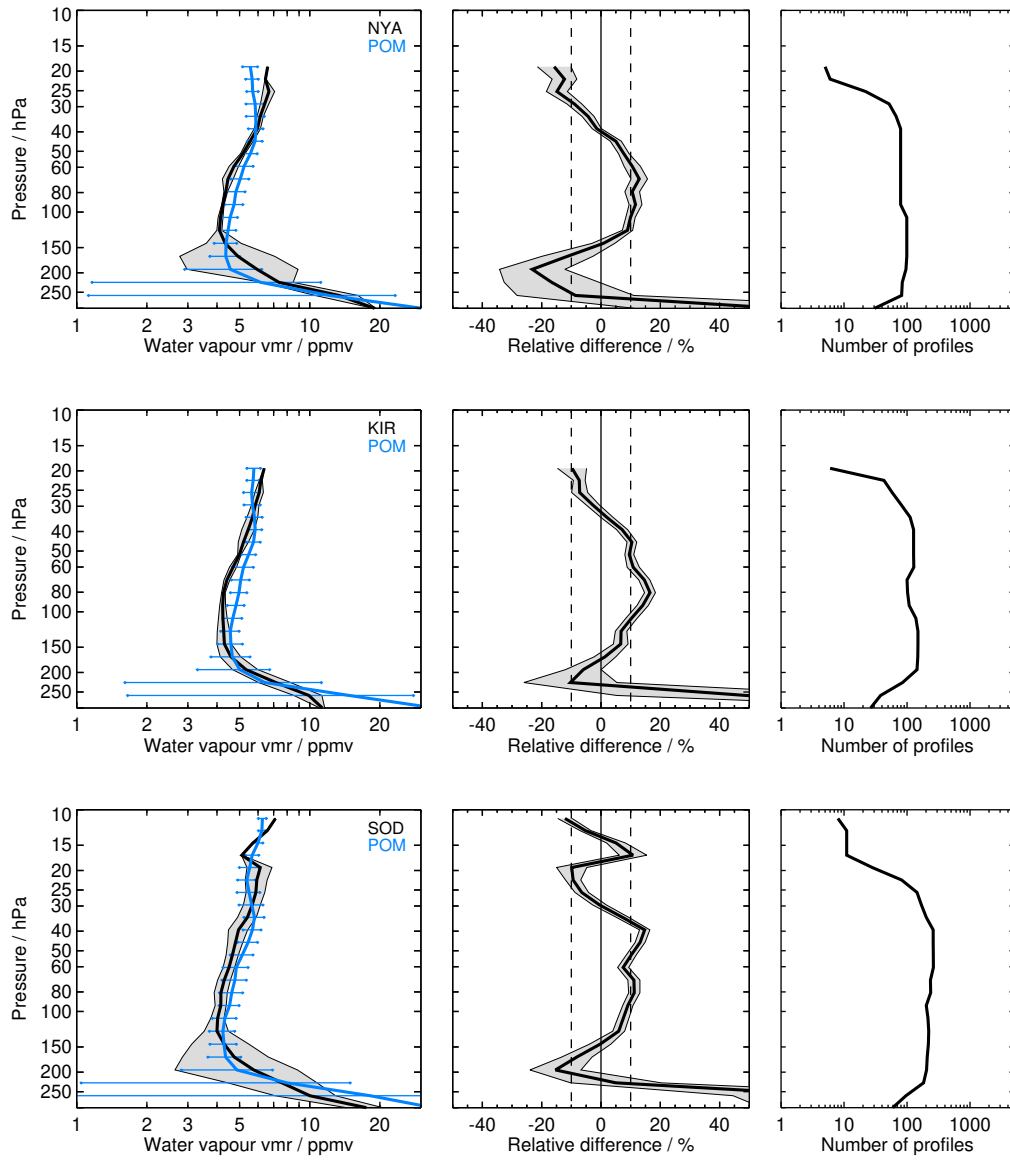


Figure S20: Same as Fig. S1 but for POM and the NYA, KIR, SOD, BLD, and BLD balloon sites.

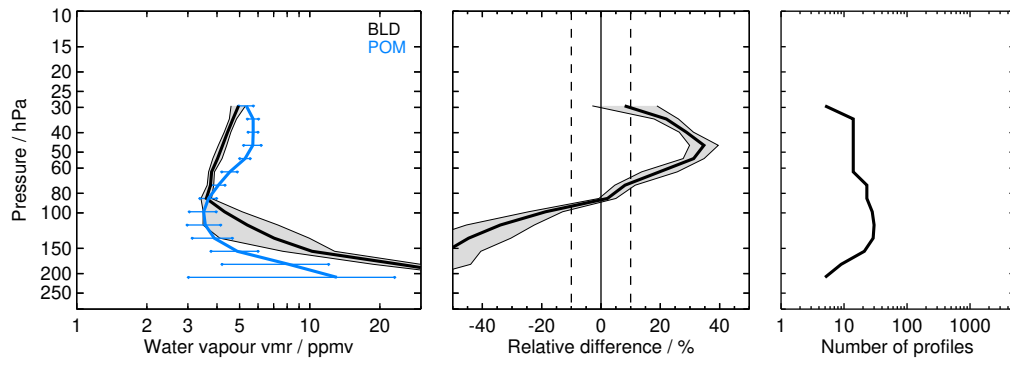


Figure S20: Continued.

2.21 SAGE_II v7.0 (SG2)

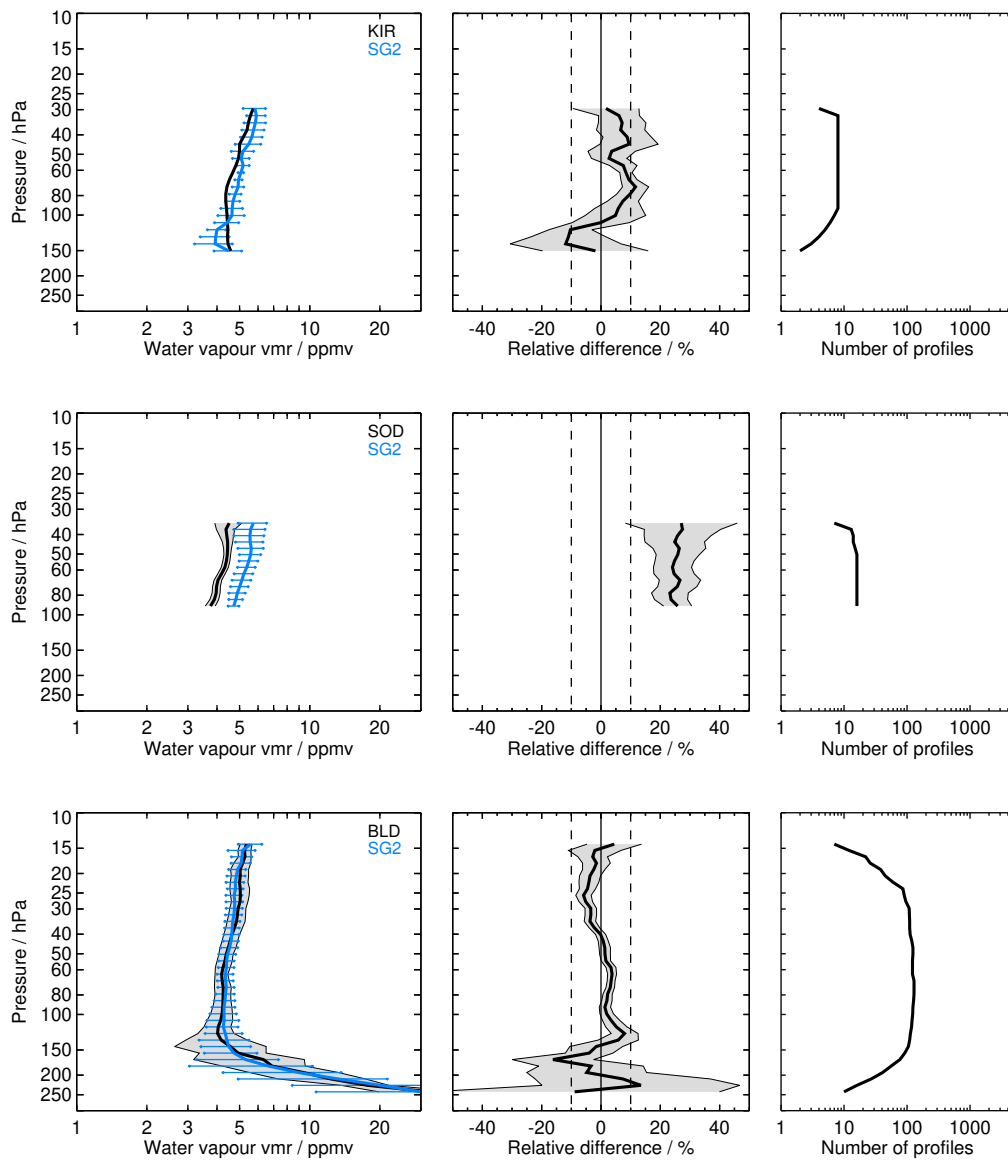


Figure S21: Same as Fig. S1 but for SG2 and the KIR, SOD, BLD, SGP, HUN, HIL, SCR, WTK, LRN, LDR, and LDR balloon sites.

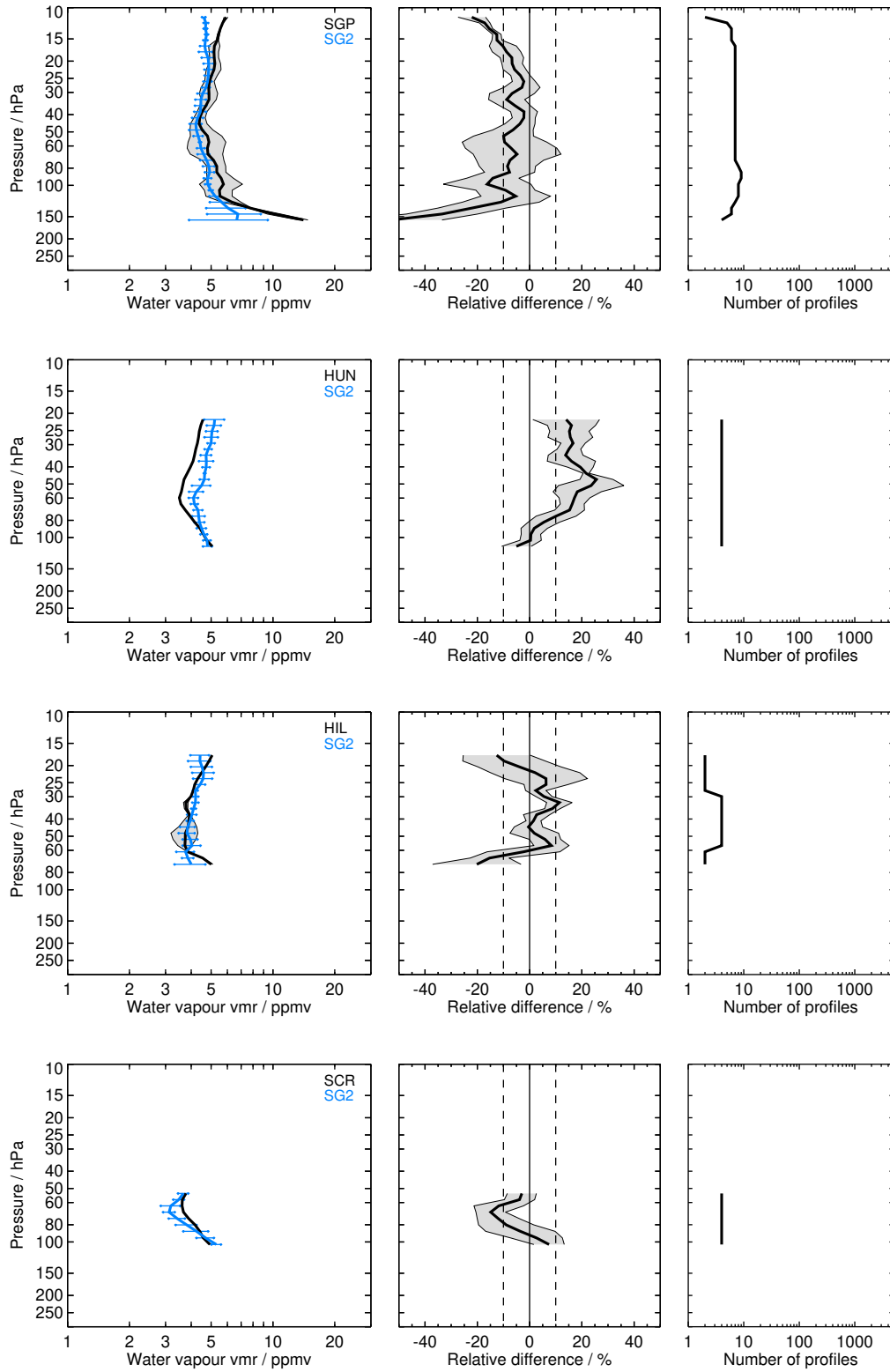


Figure S21: Continued.

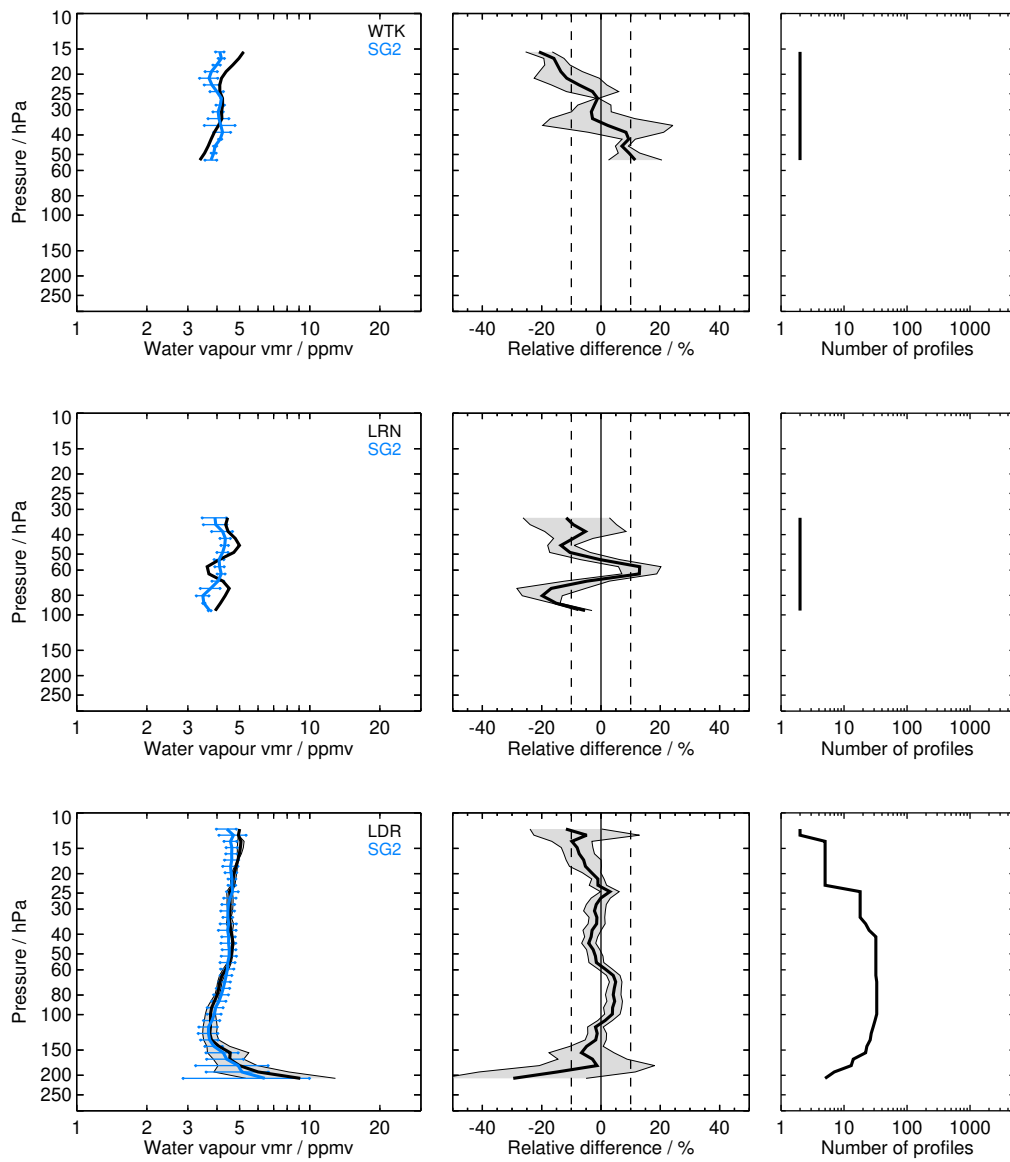


Figure S21: Continued.

2.22 SAGE_III H2O_v4 (SG3)

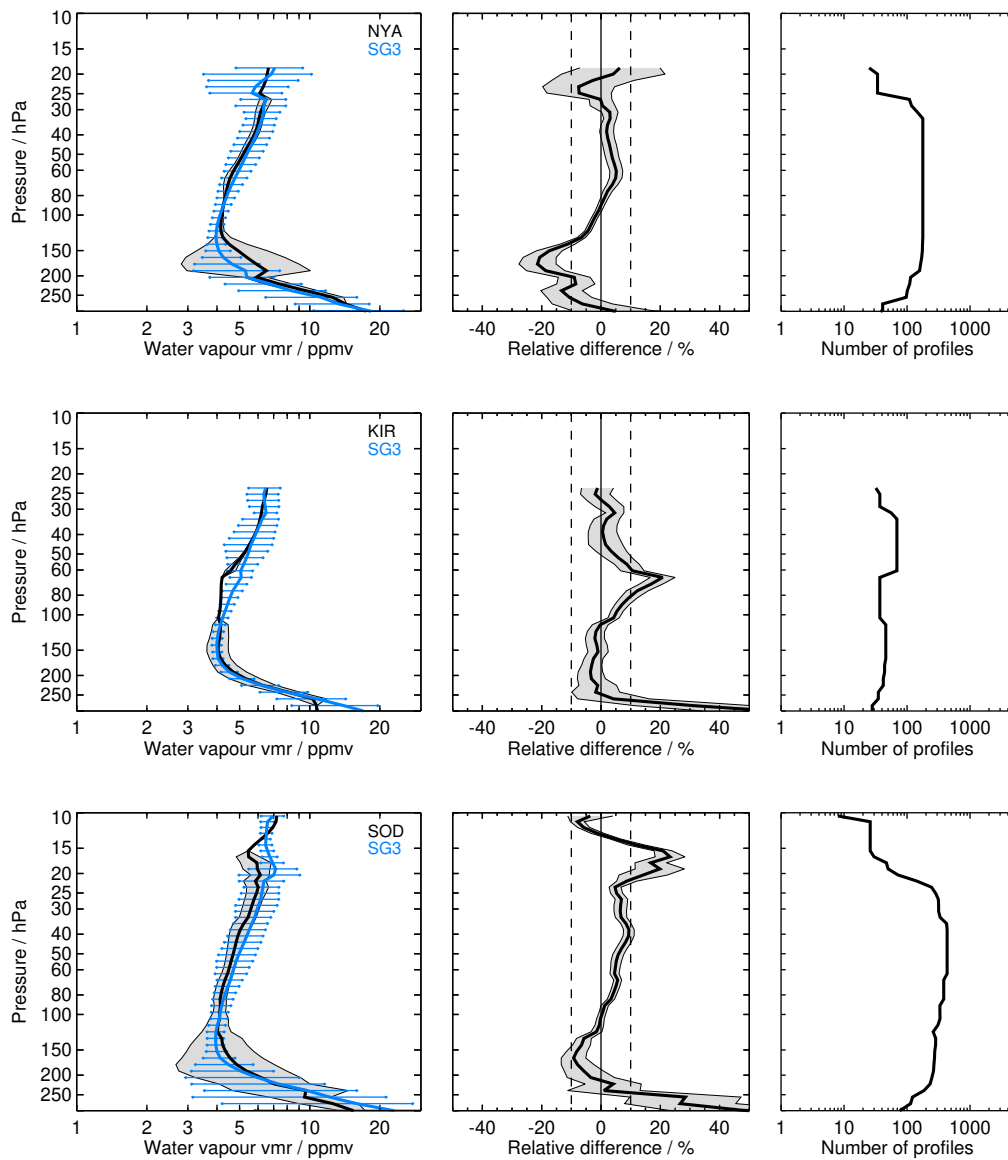


Figure S22: Same as Fig. S1 but for SG3 and the NYA, KIR, SOD, BLD, LDR, and LDR balloon sites.

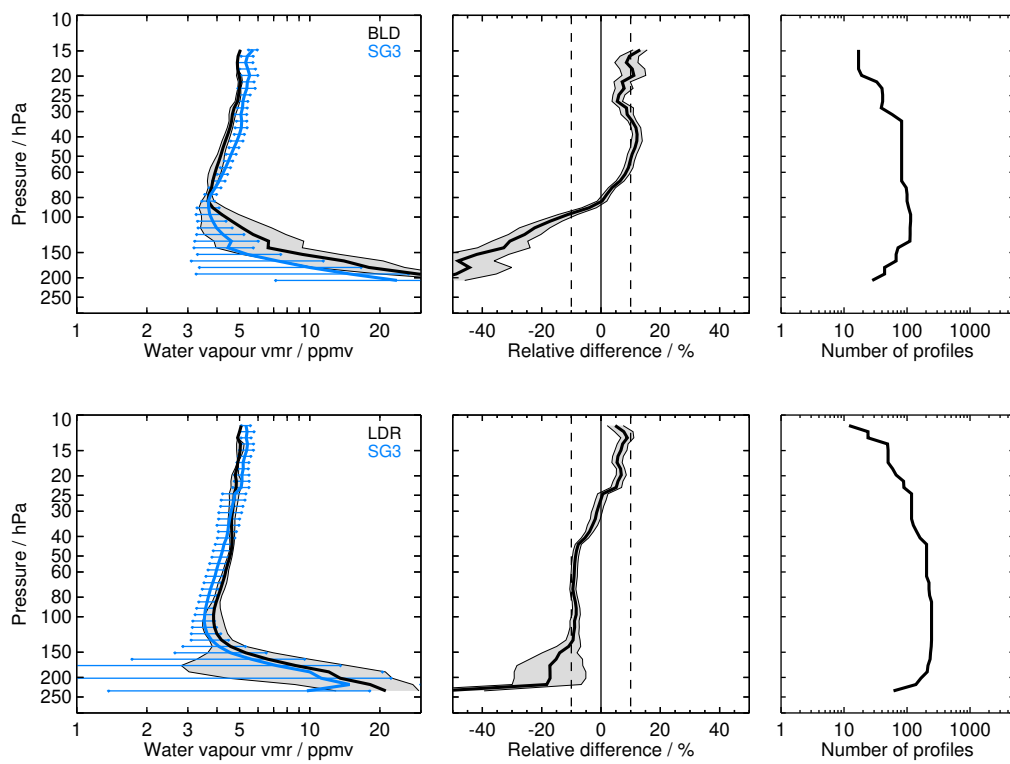


Figure S22: Continued.

2.23 SCIAMACHY H2O_LO_V1.0 (SCL)

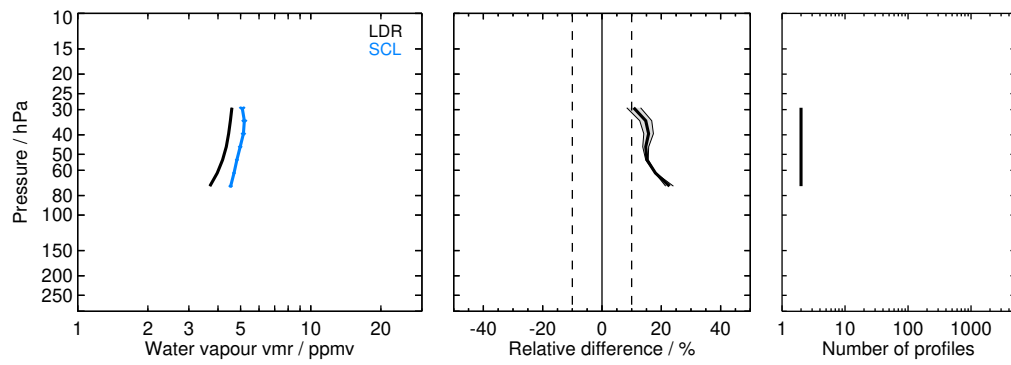


Figure S23: Same as Fig. S1 but for SCL and the LDR, and LDR balloon sites.

2.24 SCIAMACHY H₂O_SOOE_V1.0 (SC1)

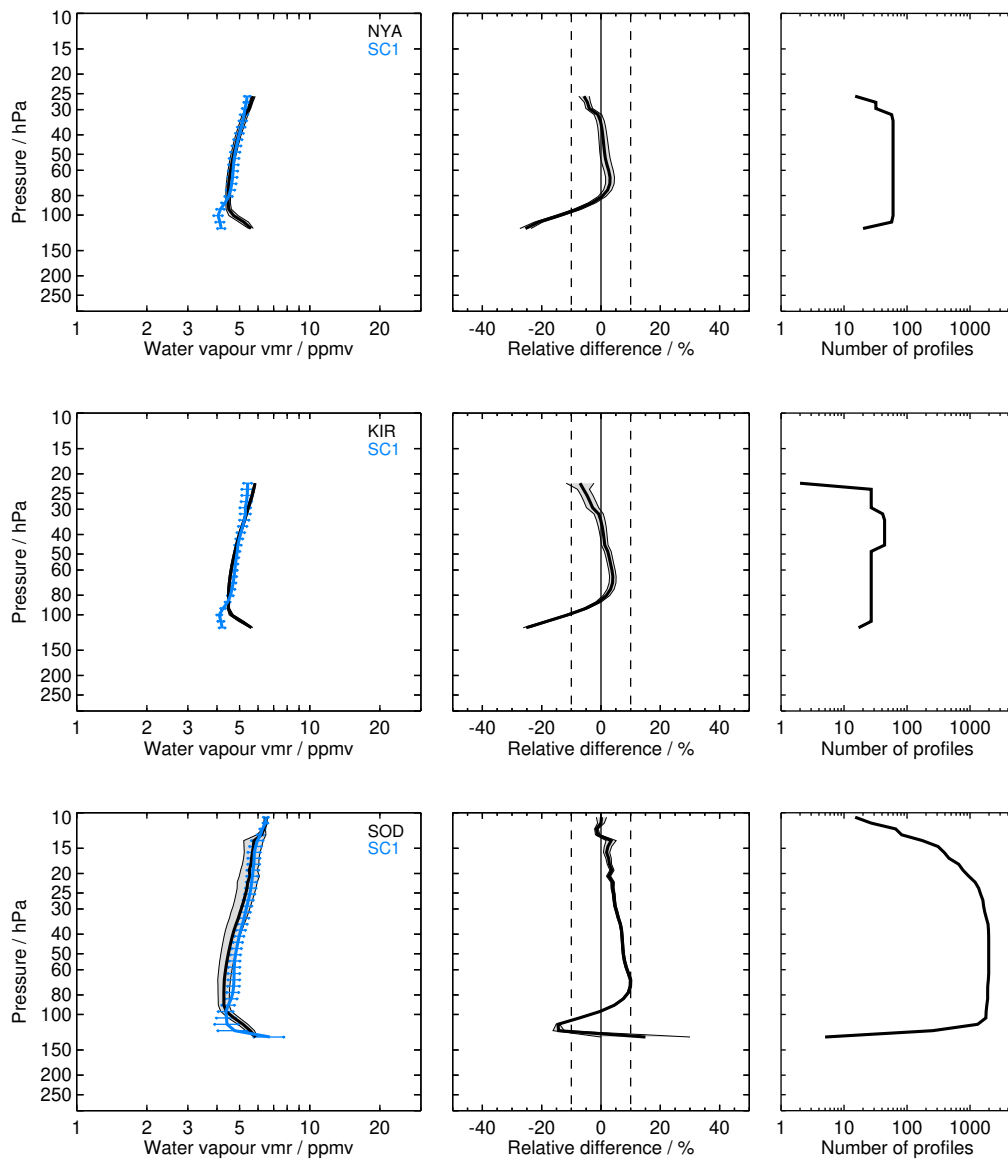


Figure S24: Same as Fig. S1 but for SC1 and the NYA, KIR, SOD, LIN, BLD, BEL, and BEL balloon sites.

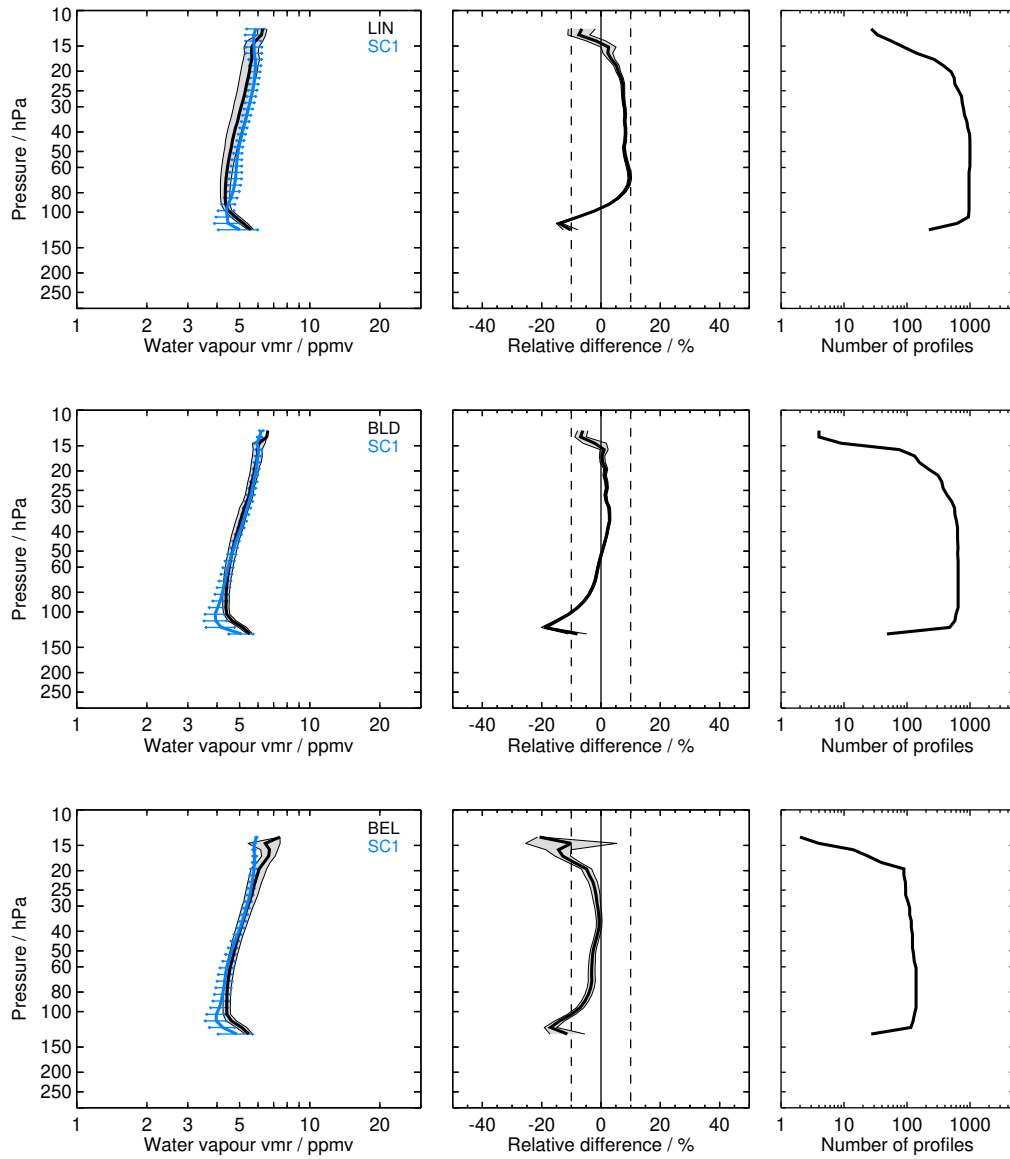


Figure S24: Continued.

2.25 SCIAMACHY H₂O_SOOP_V4.21 (SC4)

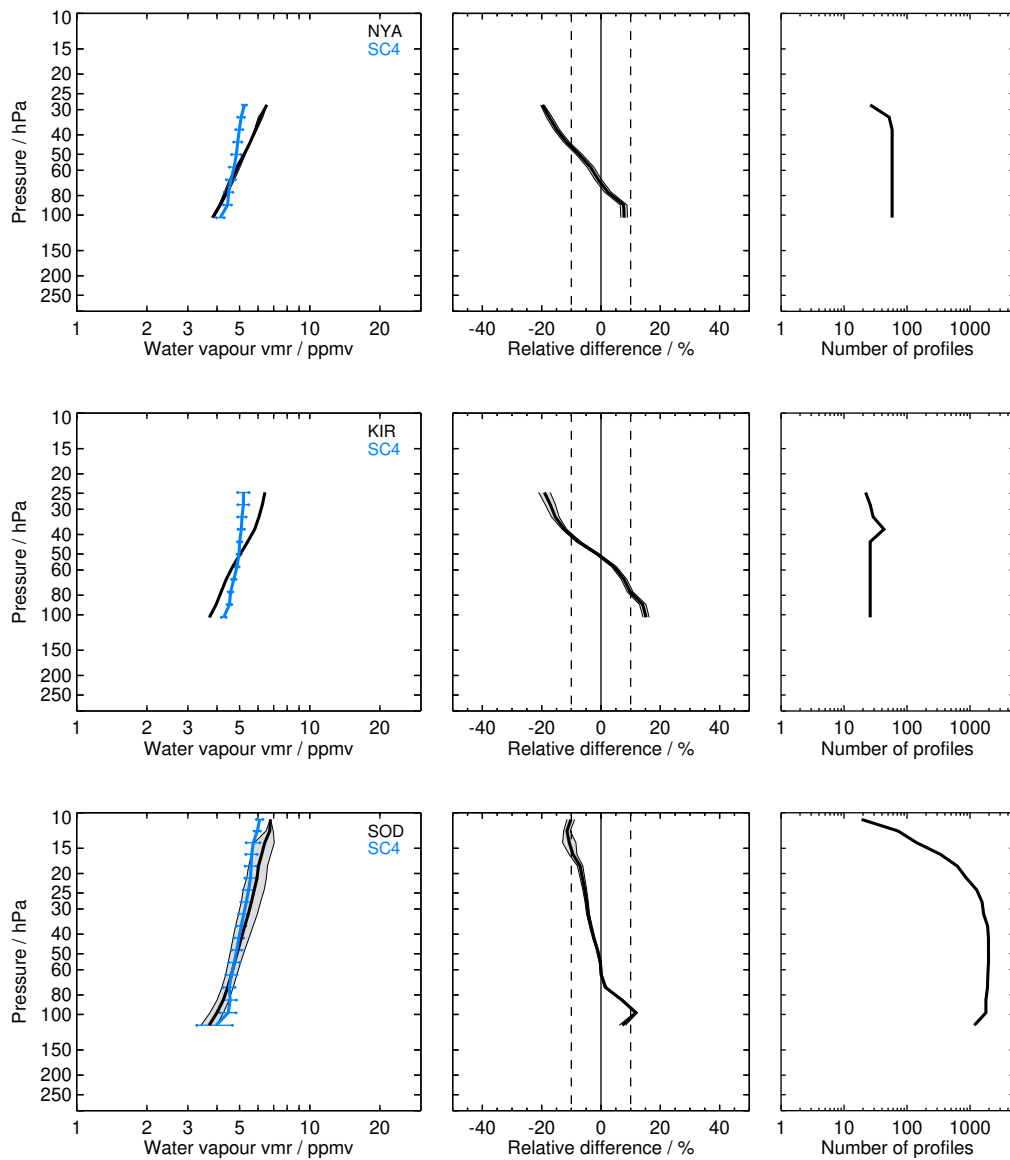


Figure S25: Same as Fig. S1 but for SC4 and the NYA, KIR, SOD, LIN, BLD, BEL, and BEL balloon sites.

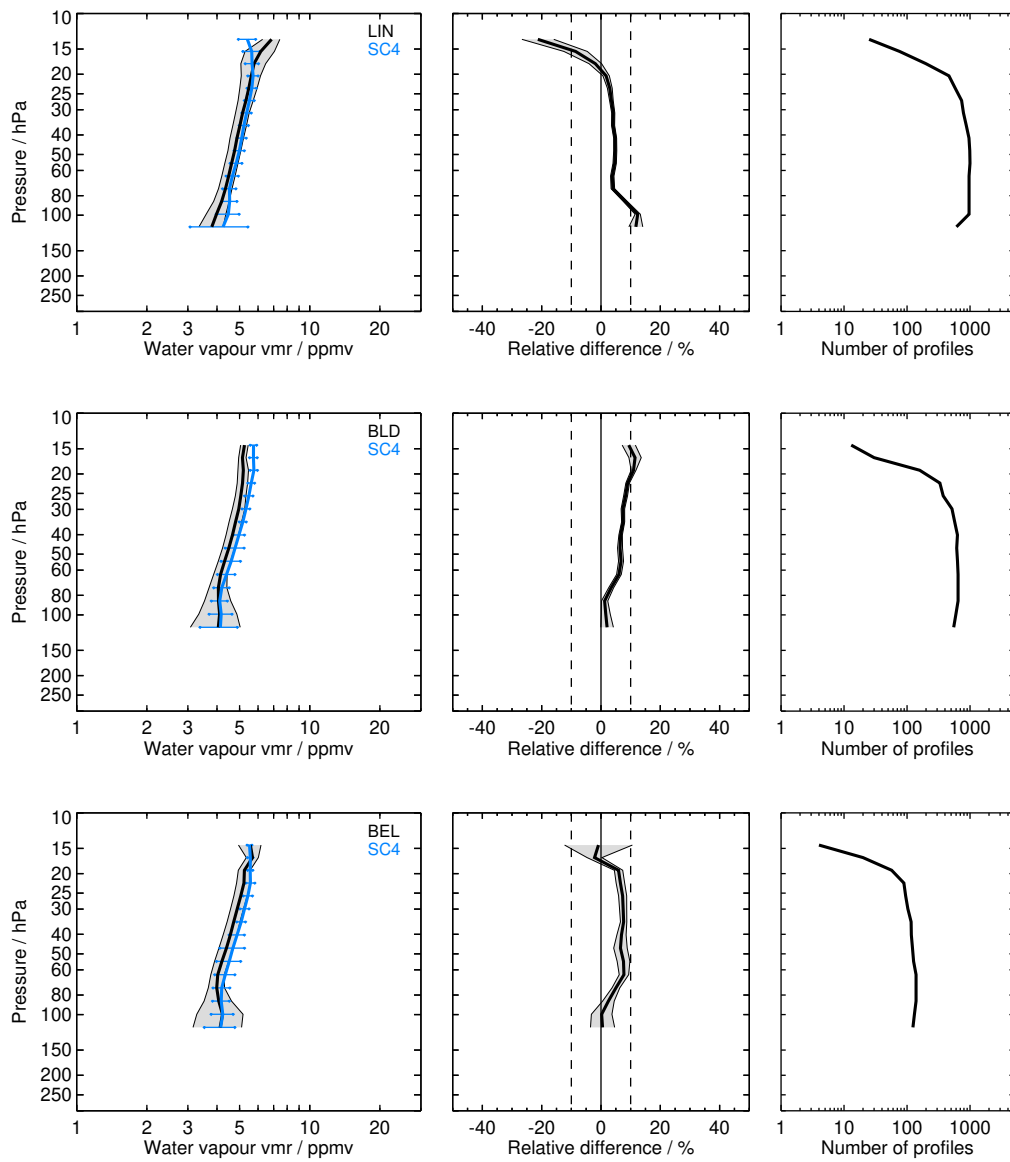


Figure S25: Continued.

2.26 SCIAMACHY H₂O_V3.01 (SC3)

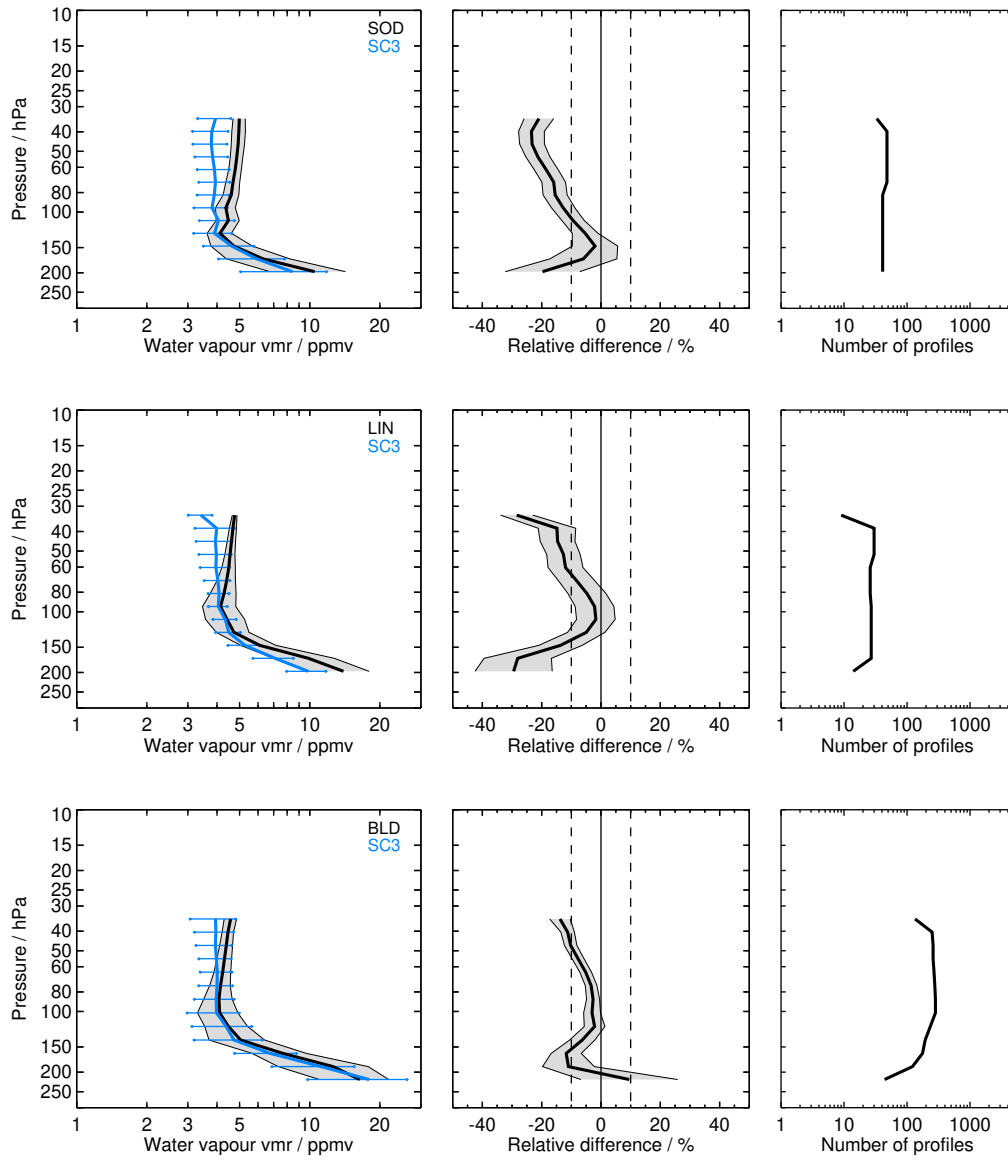


Figure S26: Same as Fig. S1 but for SC3 and the SOD, LIN, BLD, BEL, SGP, FTS, TMF, LSA, HOU, YAN, HAN, HIL, SJC, TRW, KTB, BIK, RVM, LRN, LDR, and LDR balloon sites.

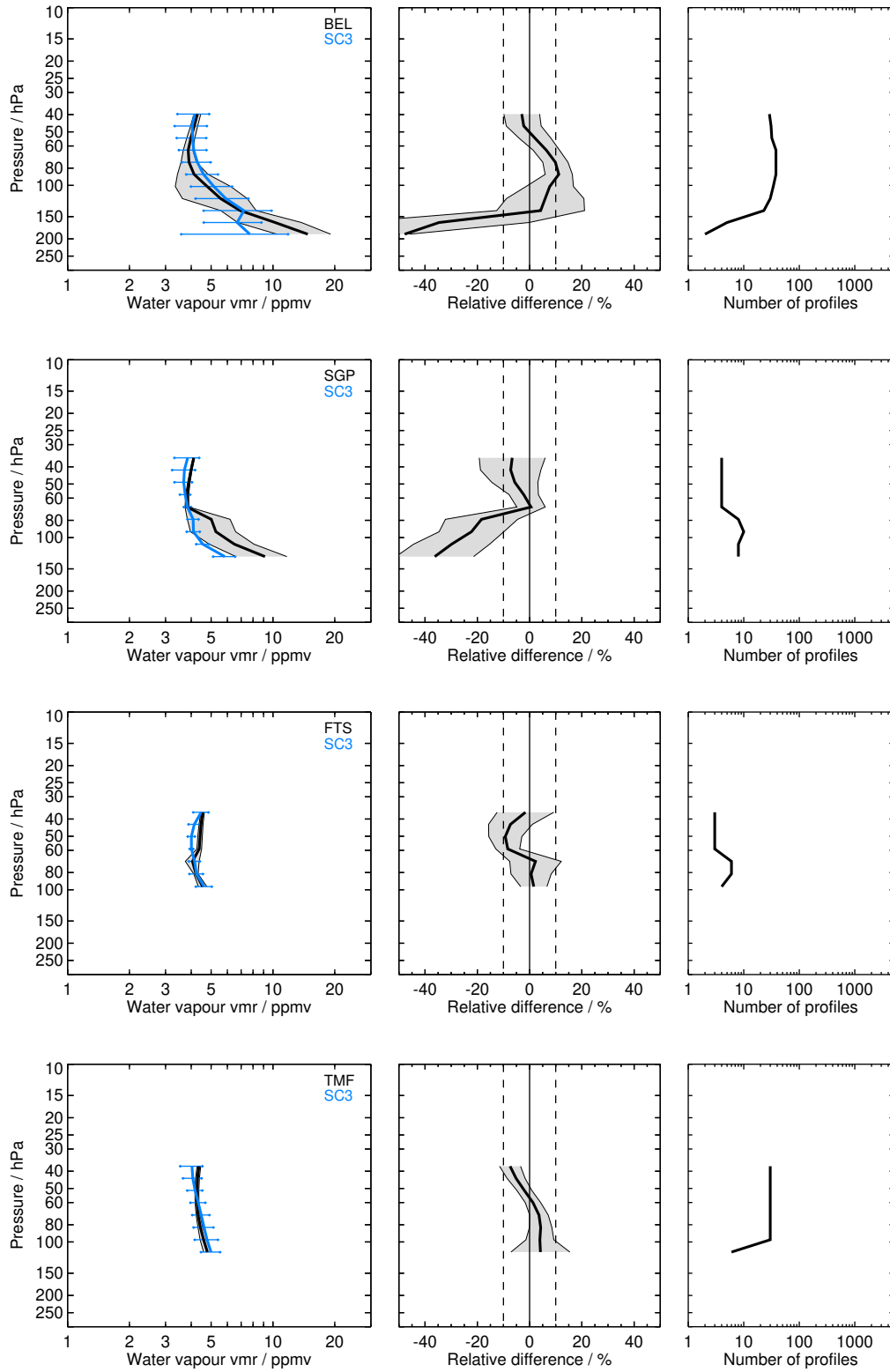


Figure S26: Continued.

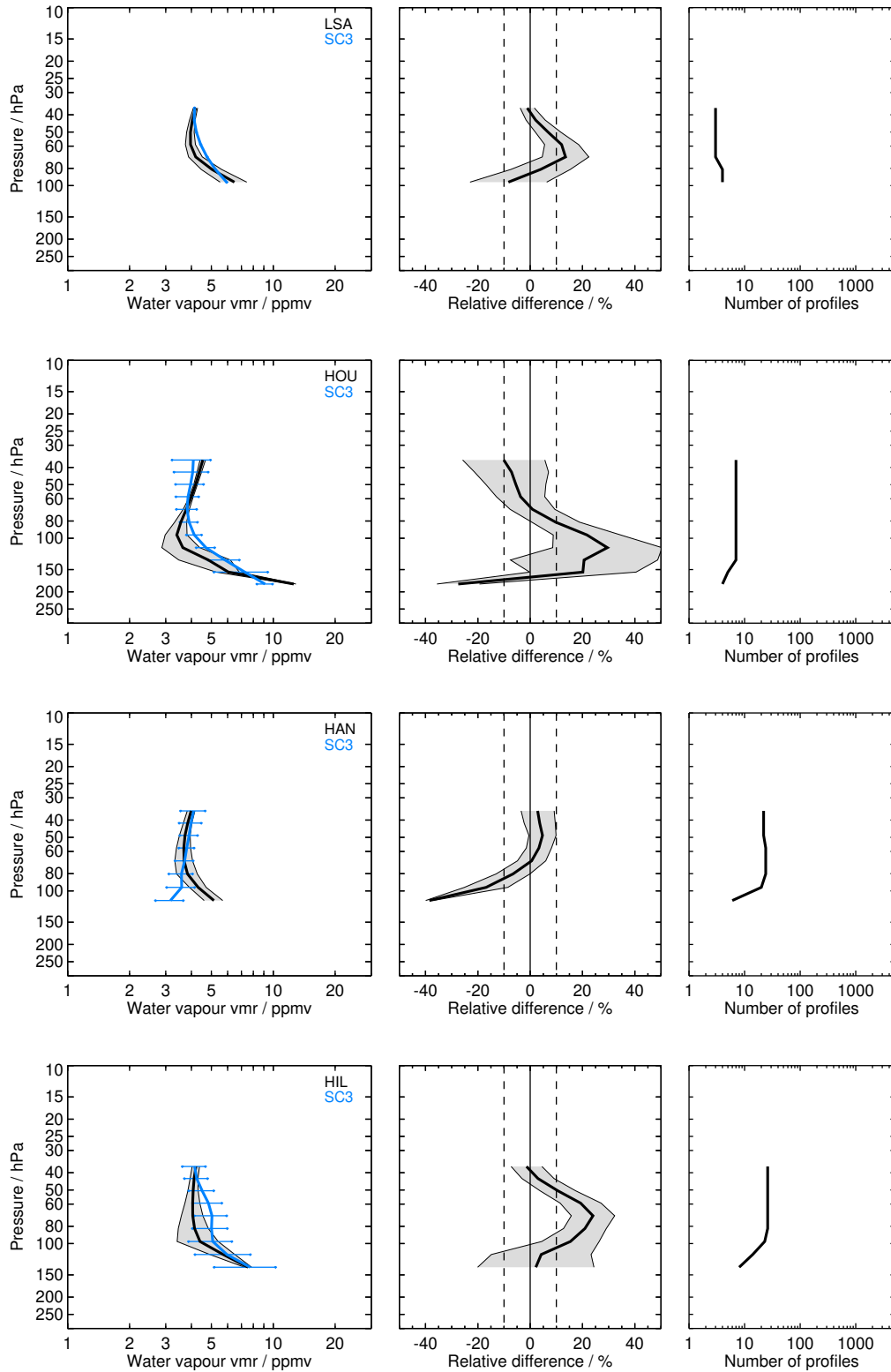


Figure S26: Continued.

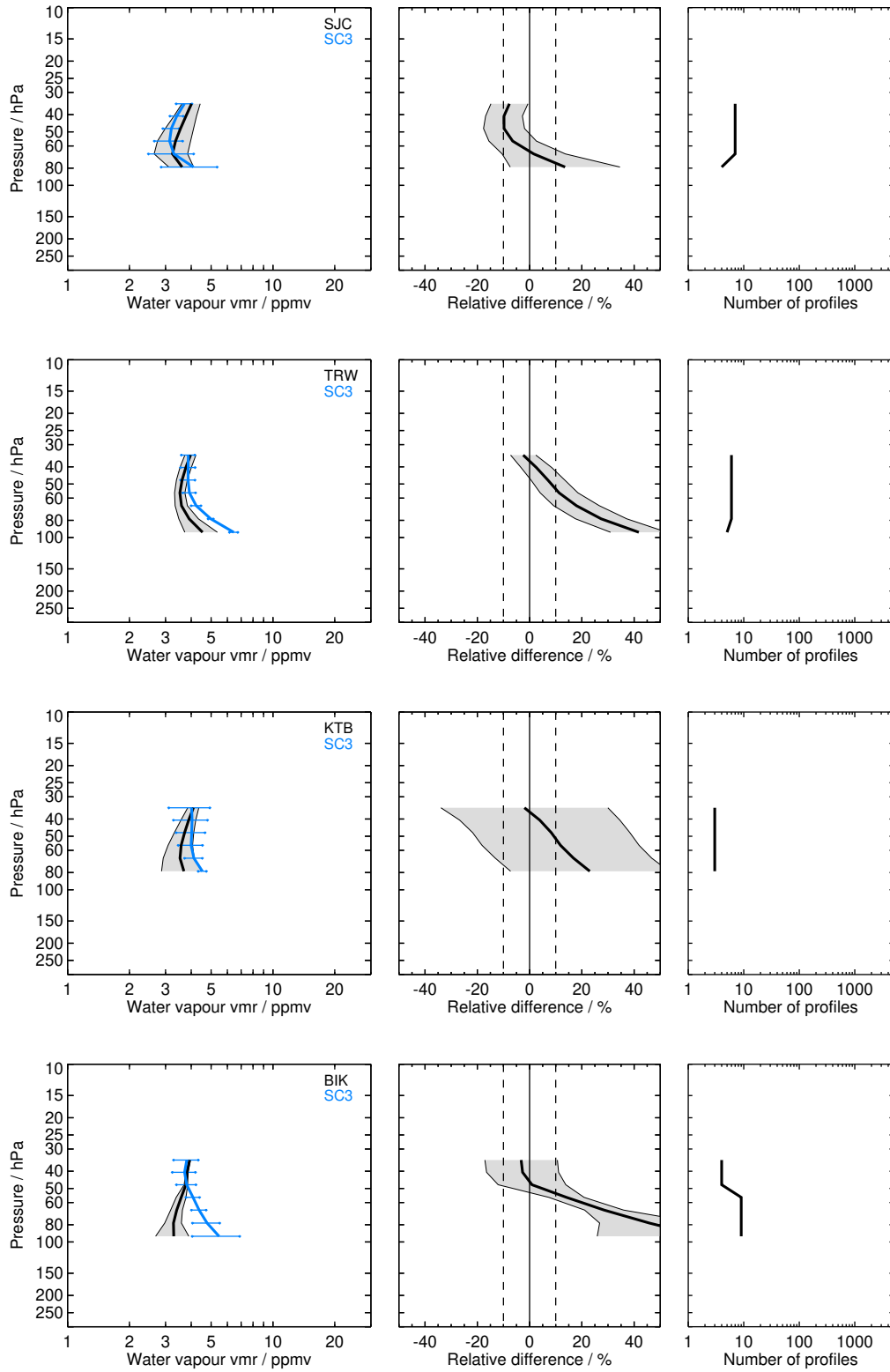


Figure S26: Continued.

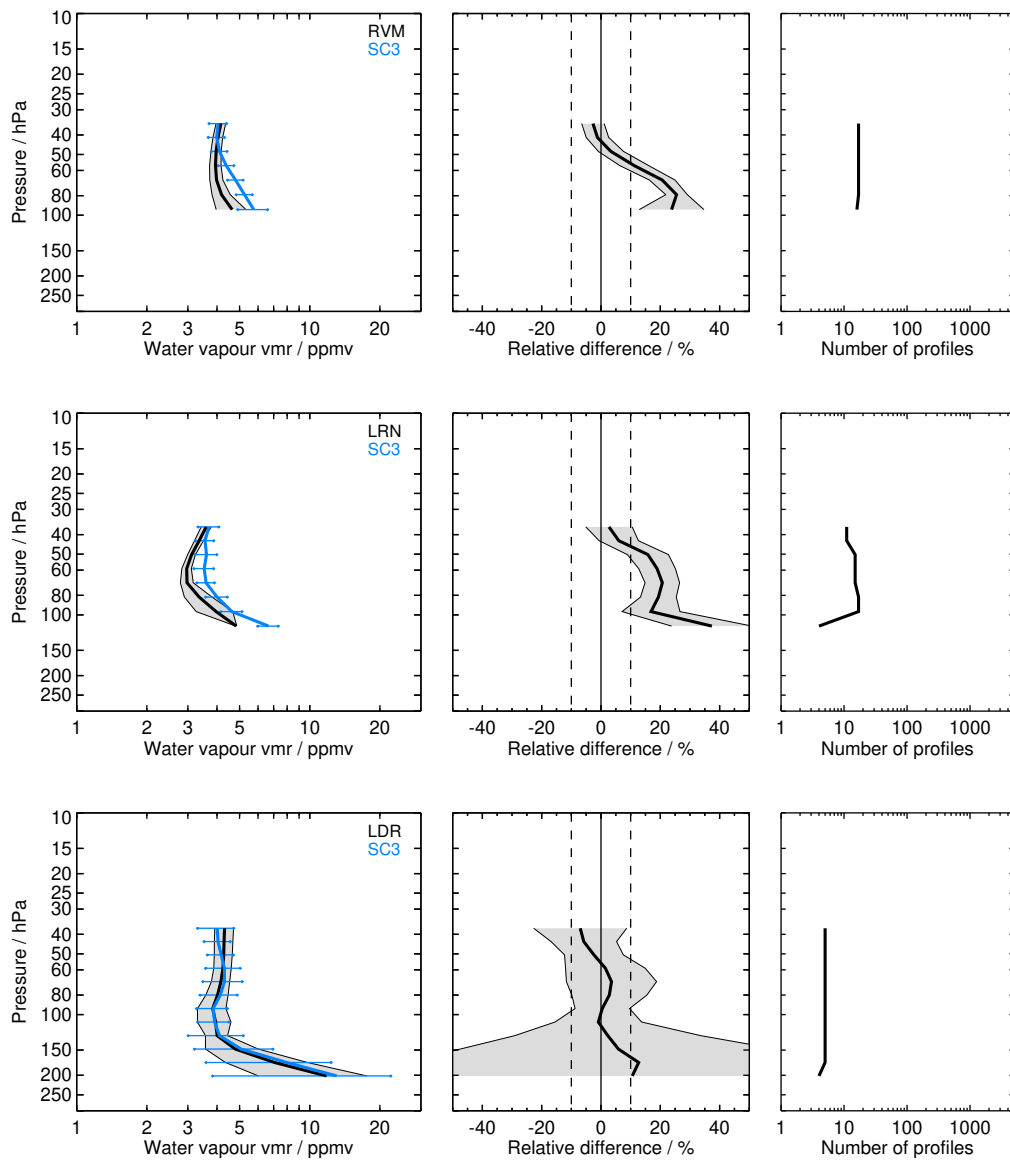


Figure S26: Continued.

2.27 SMILES H2O_A_2.9.2 (SLA)

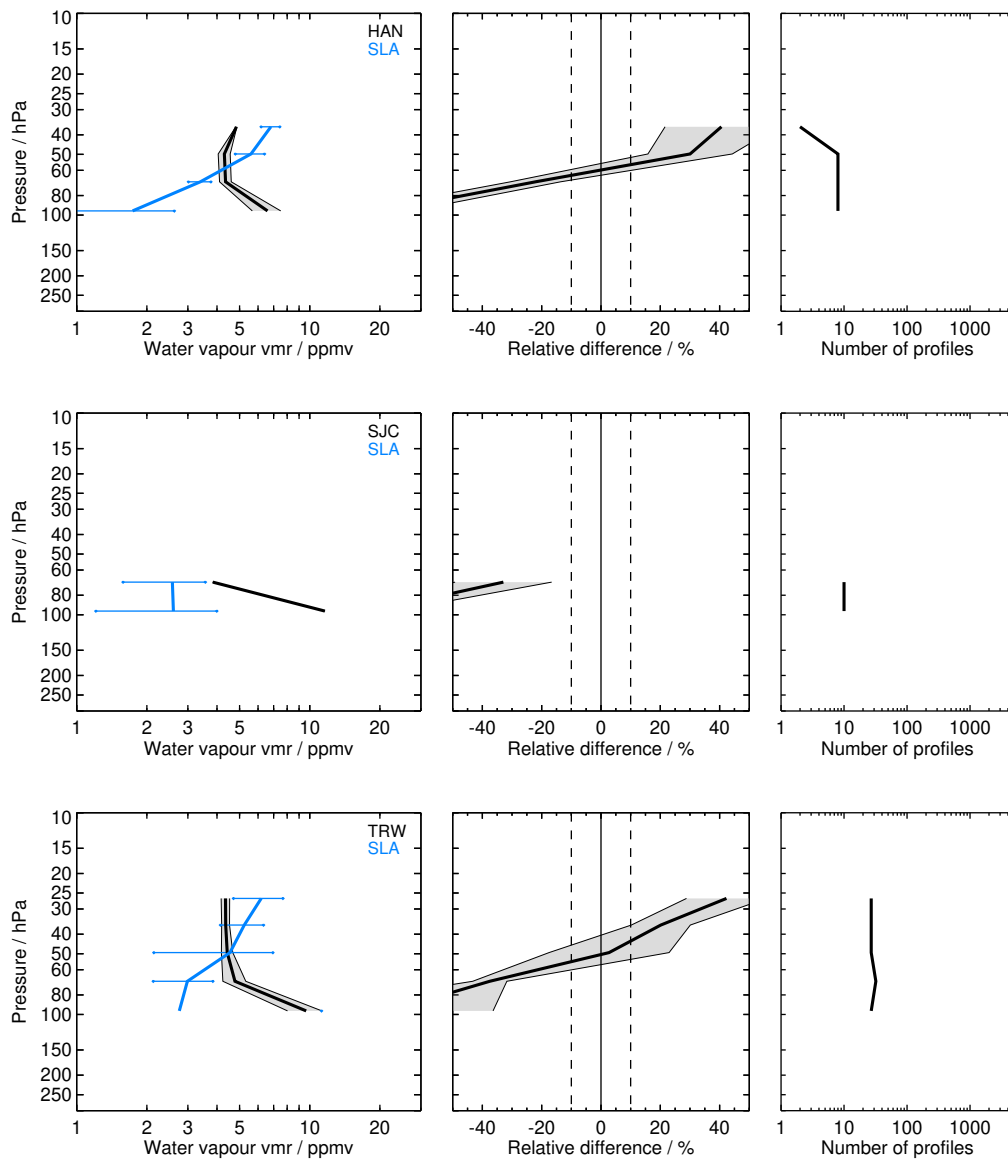


Figure S27: Same as Fig. S1 but for SLA and the HAN, SJC, TRW, BIK, and BIK balloon sites.

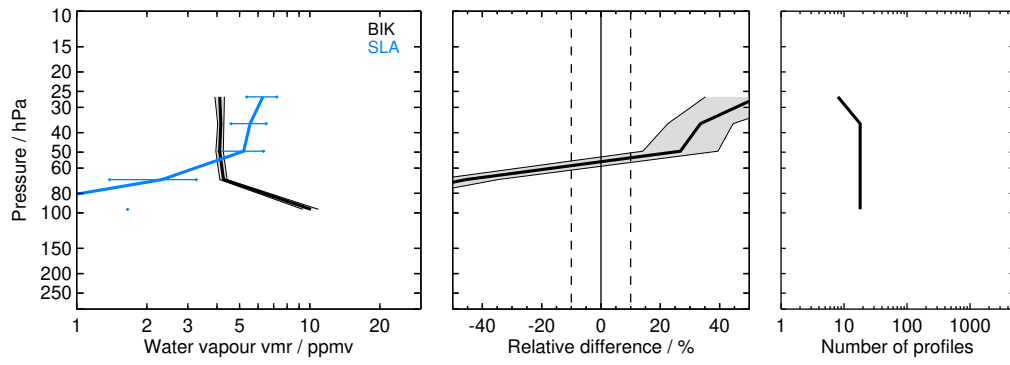


Figure S27: Continued.

2.28 SMILES H2O_B_2.9.2 (SLB)

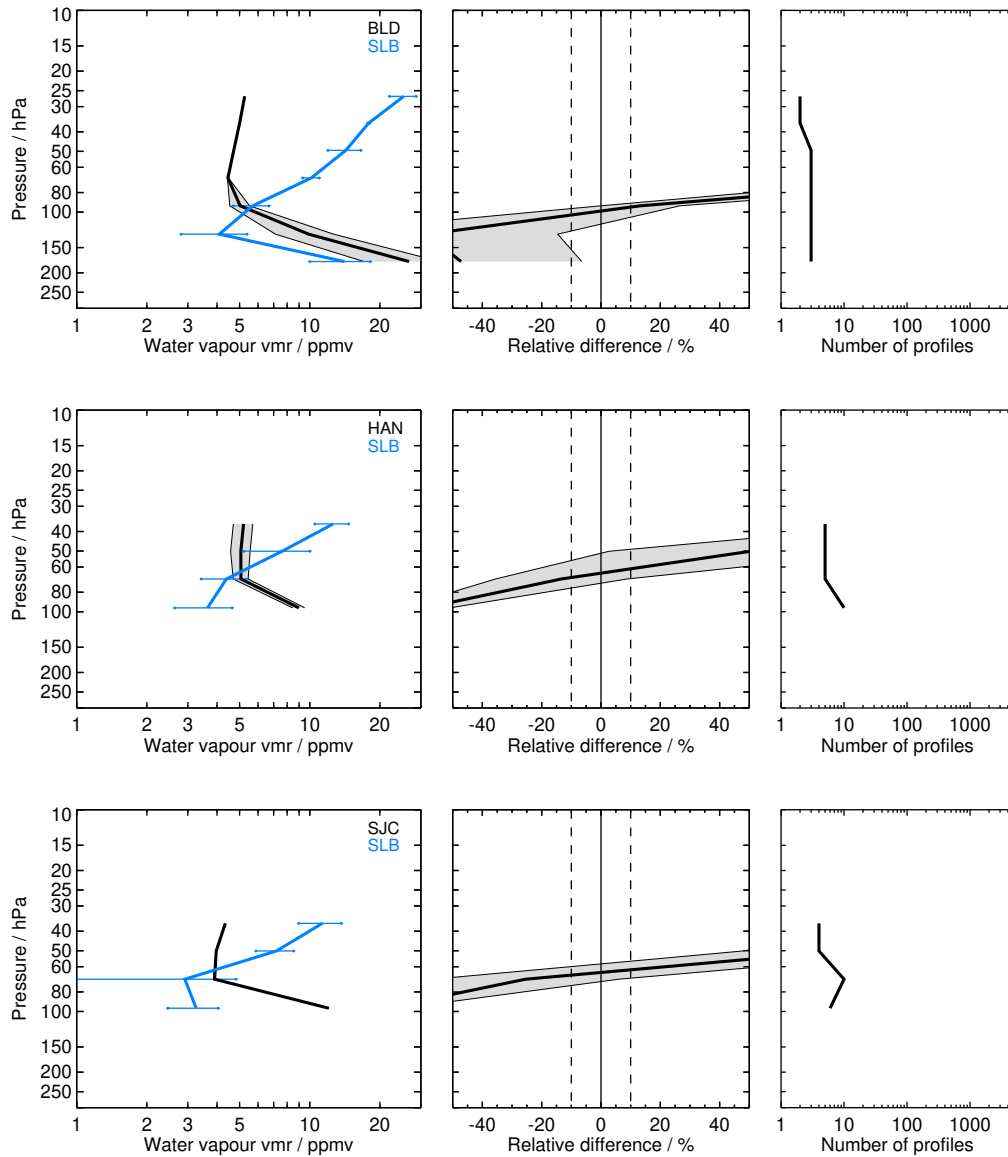


Figure S28: Same as Fig. S1 but for SLB and the BLD, HAN, SJC, TRW, BIK, and BIK balloon sites.

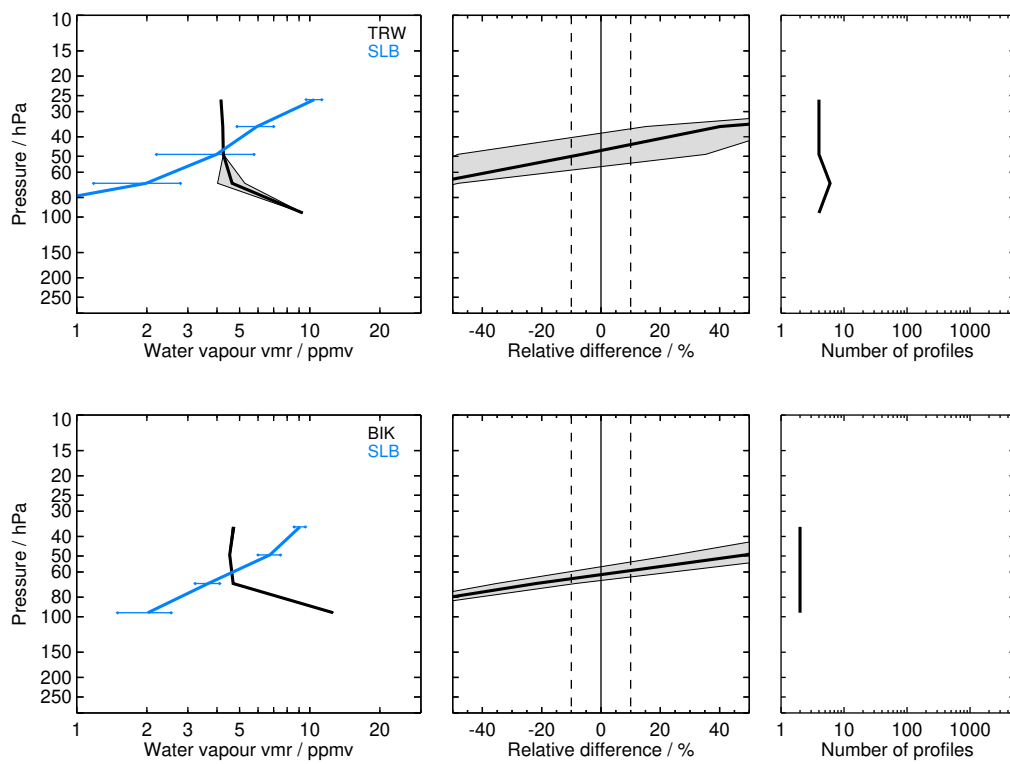


Figure S28: Continued.

2.29 SMR H2O_020_544 (SM5)

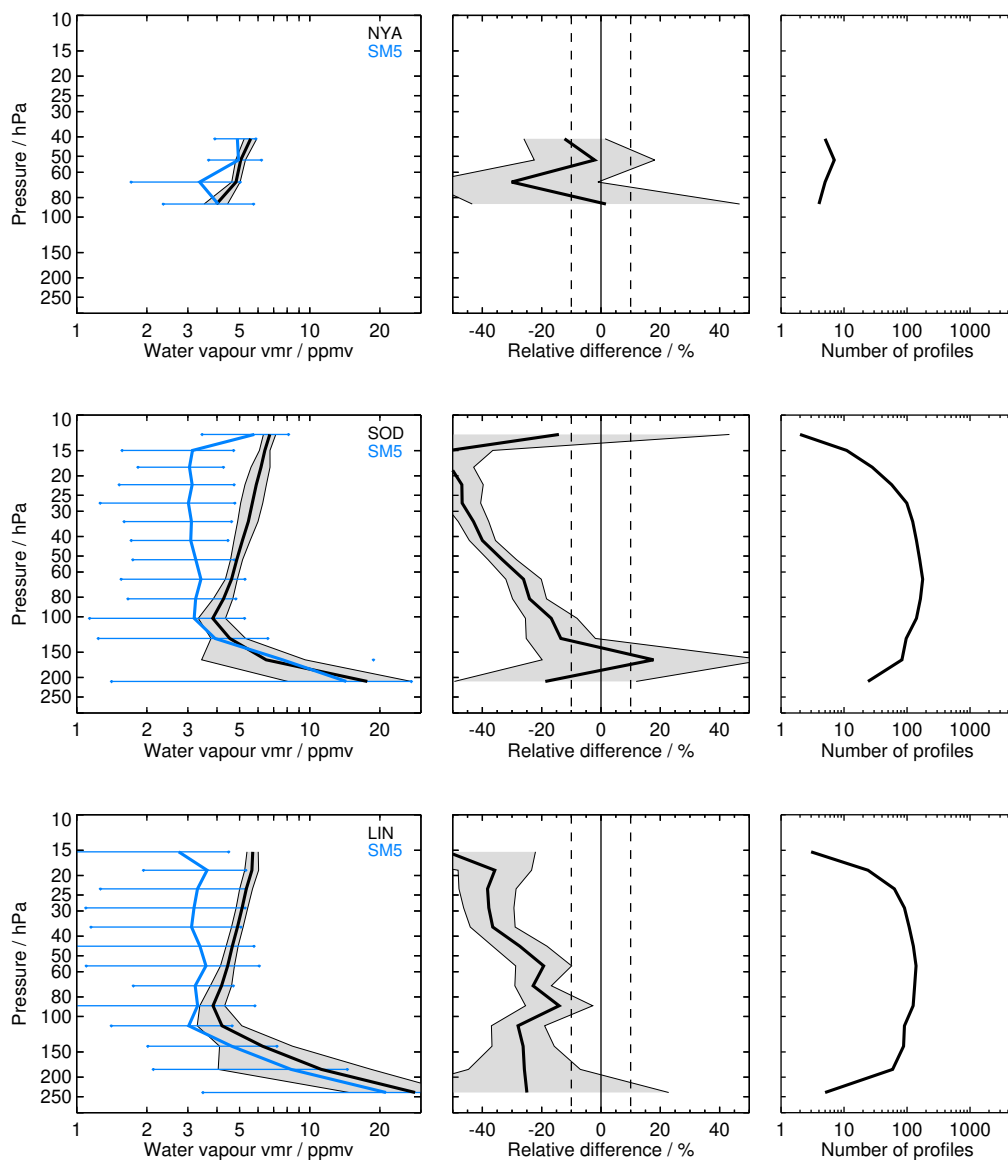


Figure S29: Same as Fig. S1 but for SM5 and the NYA, SOD, LIN, BLD, BEL, SGP, HUN, FTS, TMF, LSA, HOU, TNG, KMG, YAN, HAN, HIL, SJC, TRW, KTB, SCR, BIK, RVM, LRN, LDR, and LDR balloon sites.

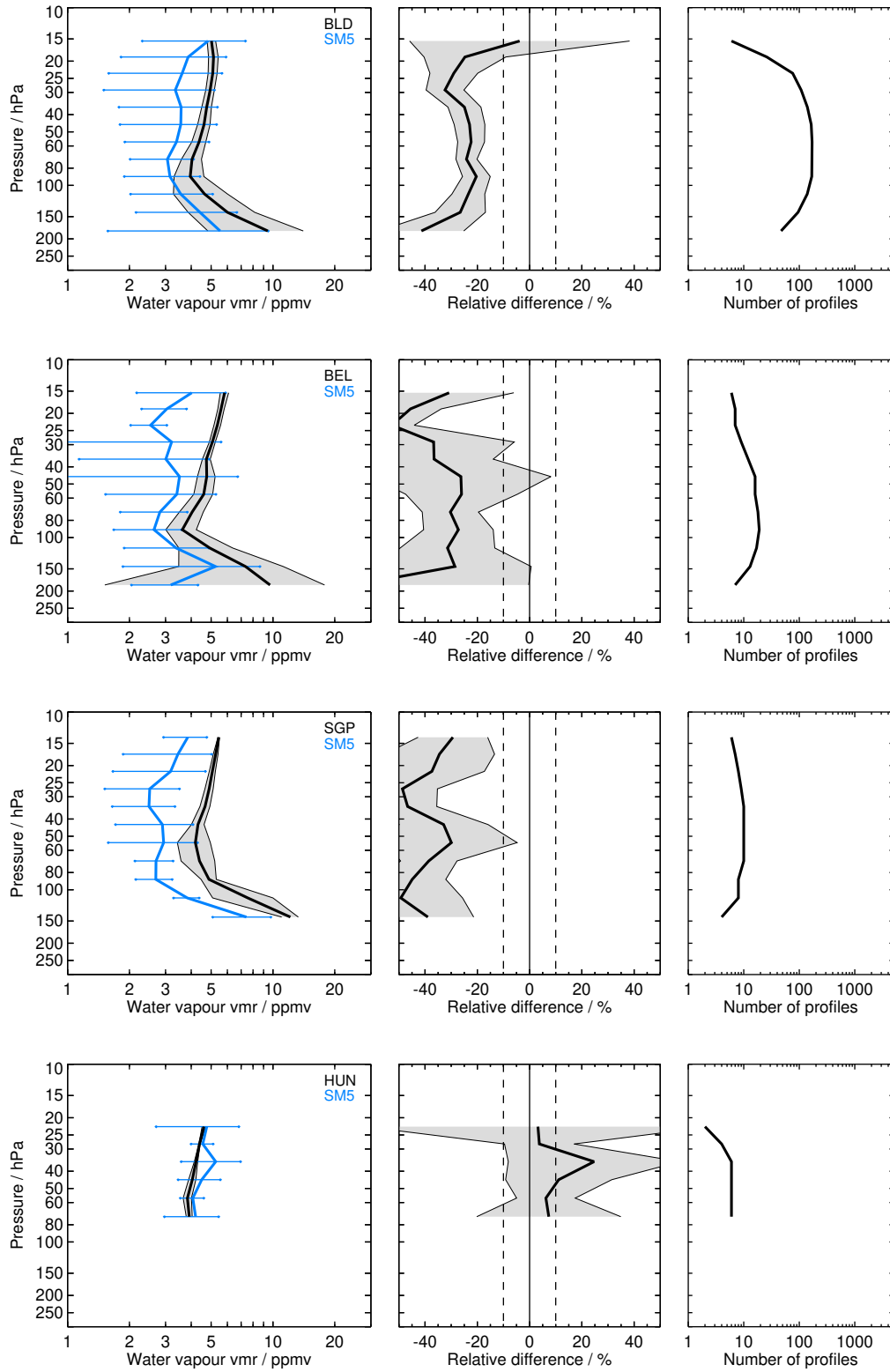


Figure S29: Continued.

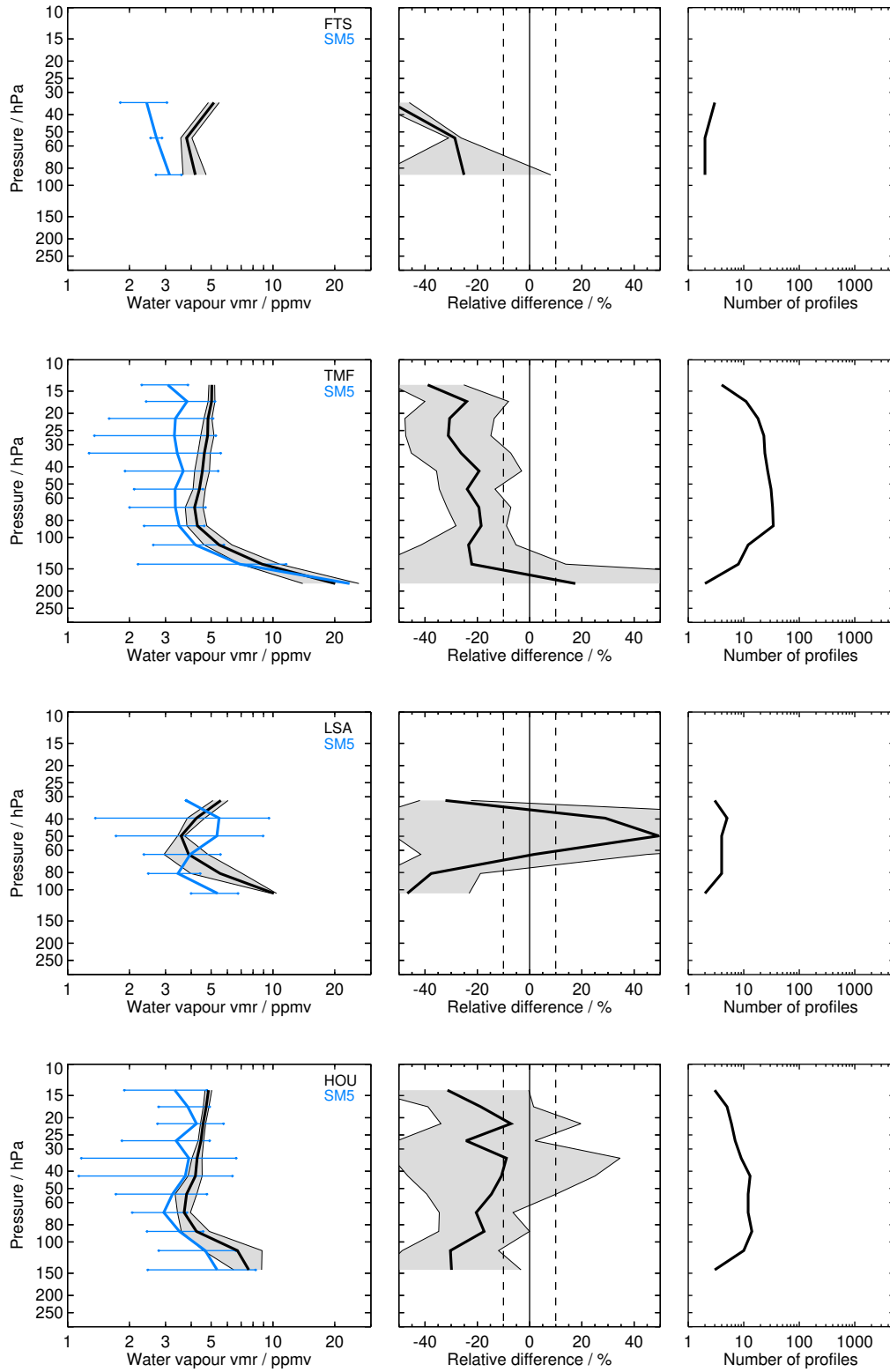


Figure S29: Continued.

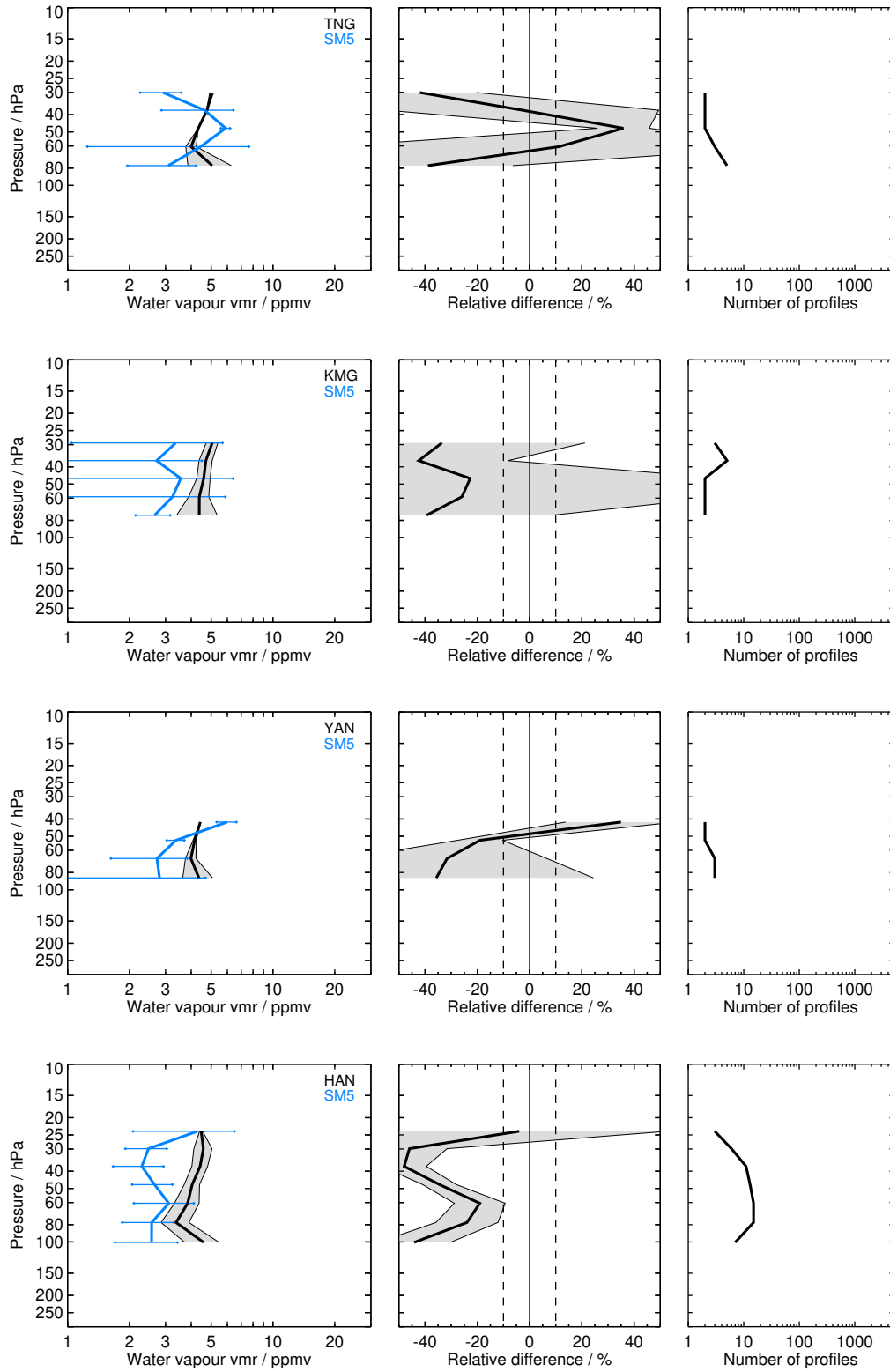


Figure S29: Continued.

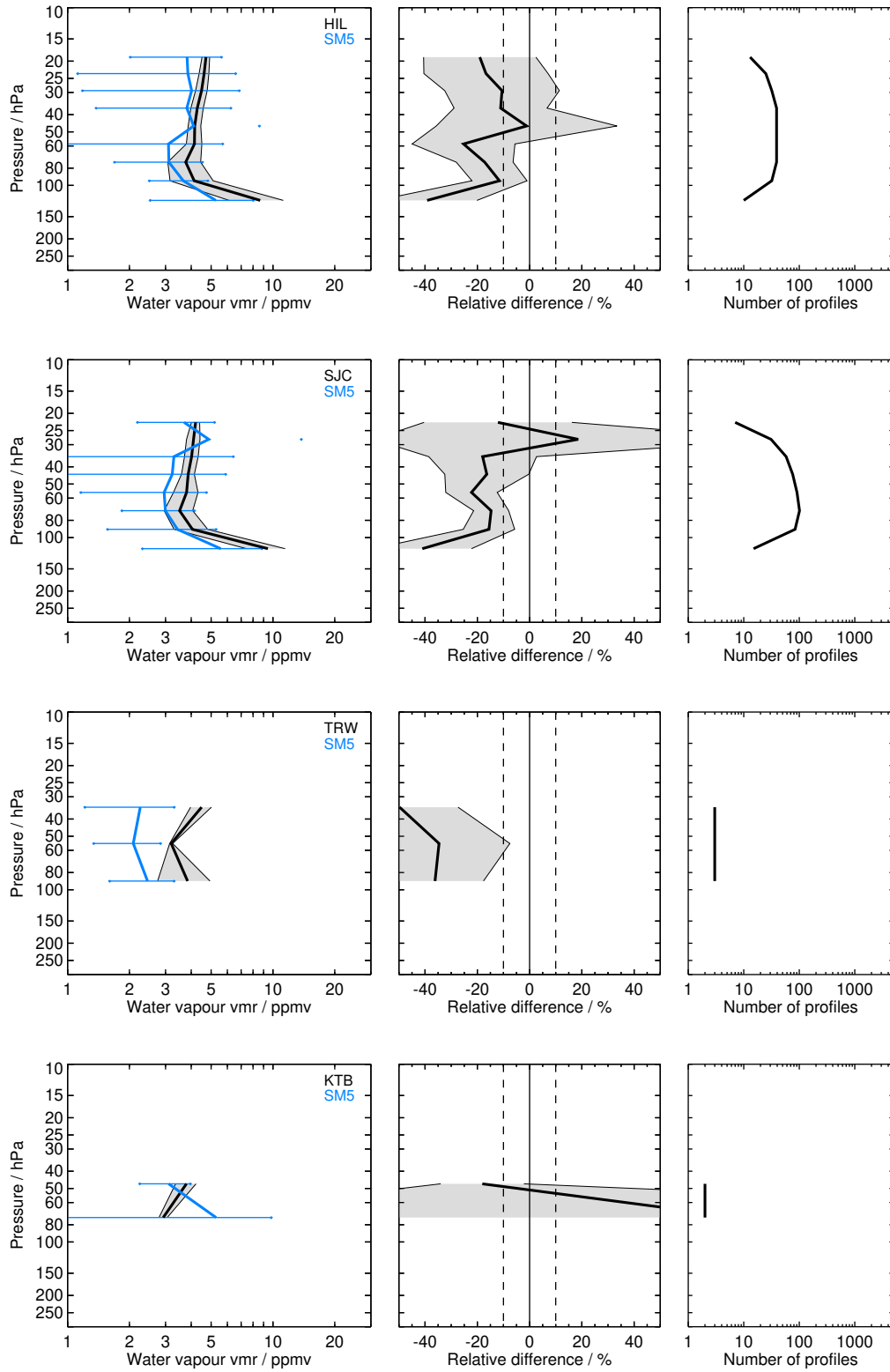


Figure S29: Continued.

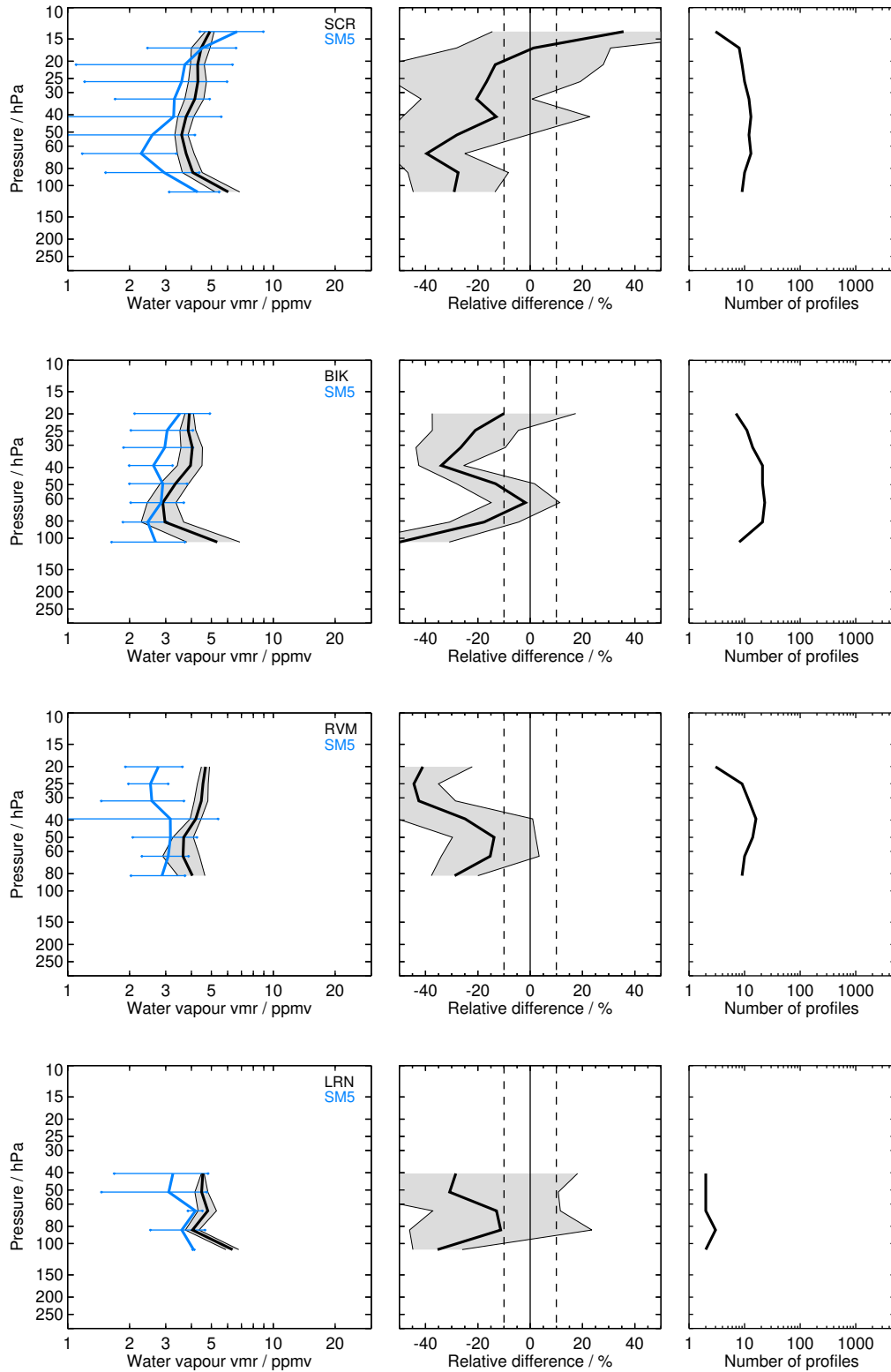


Figure S29: Continued.

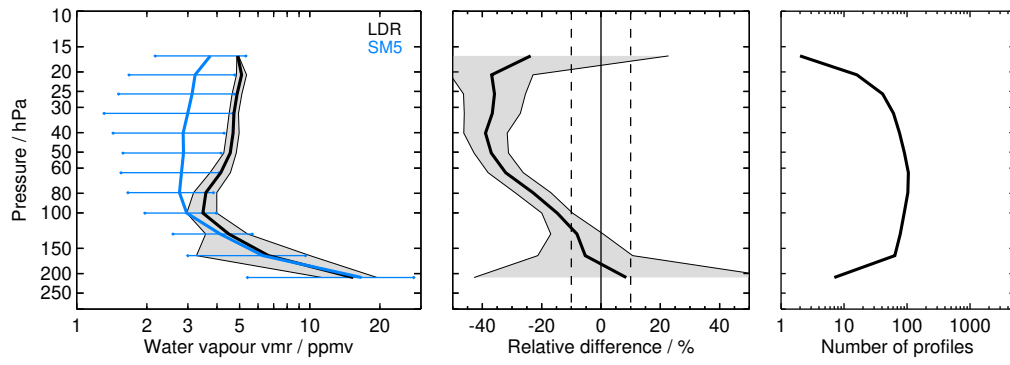


Figure S29: Continued.

2.30 SMR H2O_021_489 (SM4)

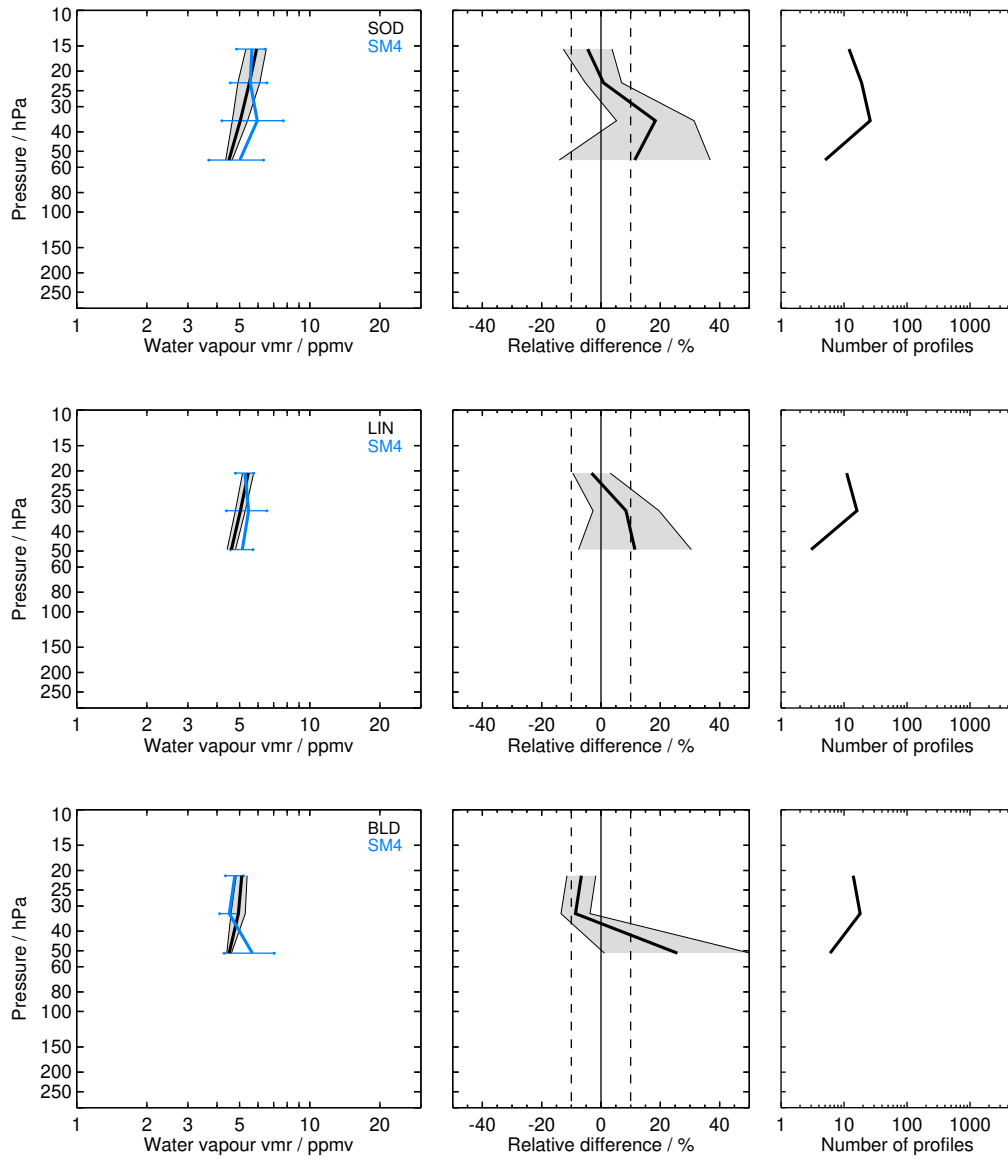


Figure S30: Same as Fig. S1 but for SM4 and the SOD, LIN, BLD, BEL, TMF, HAN, HIL, SCR, LDR, and LDR balloon sites.

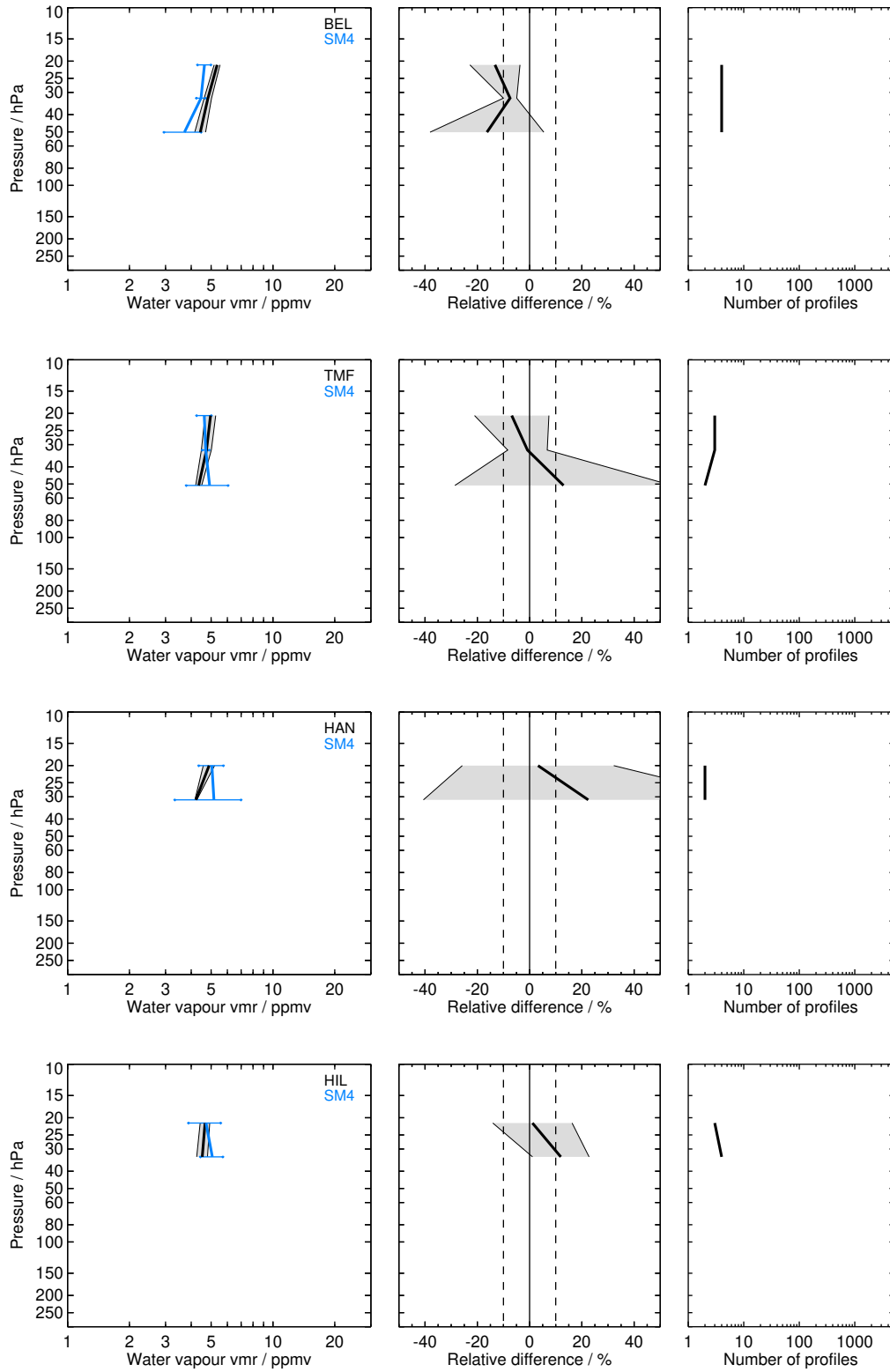


Figure S30: Continued.

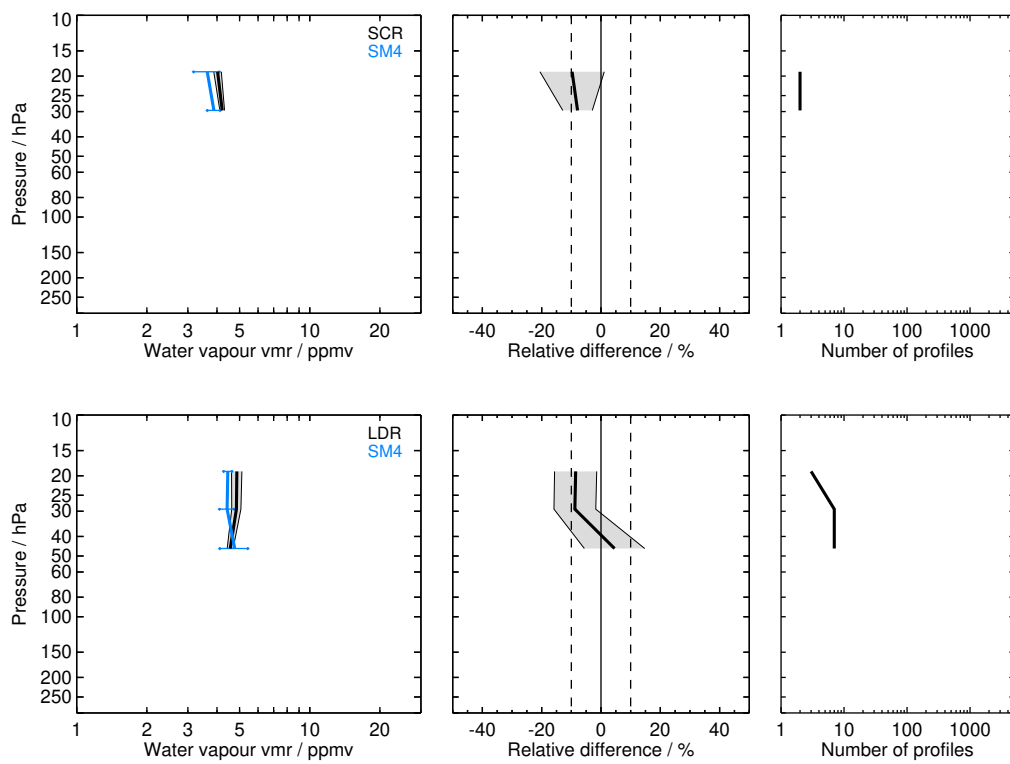


Figure S30: Continued.

2.31 SOFIE H2O_v01.3 (SOF)

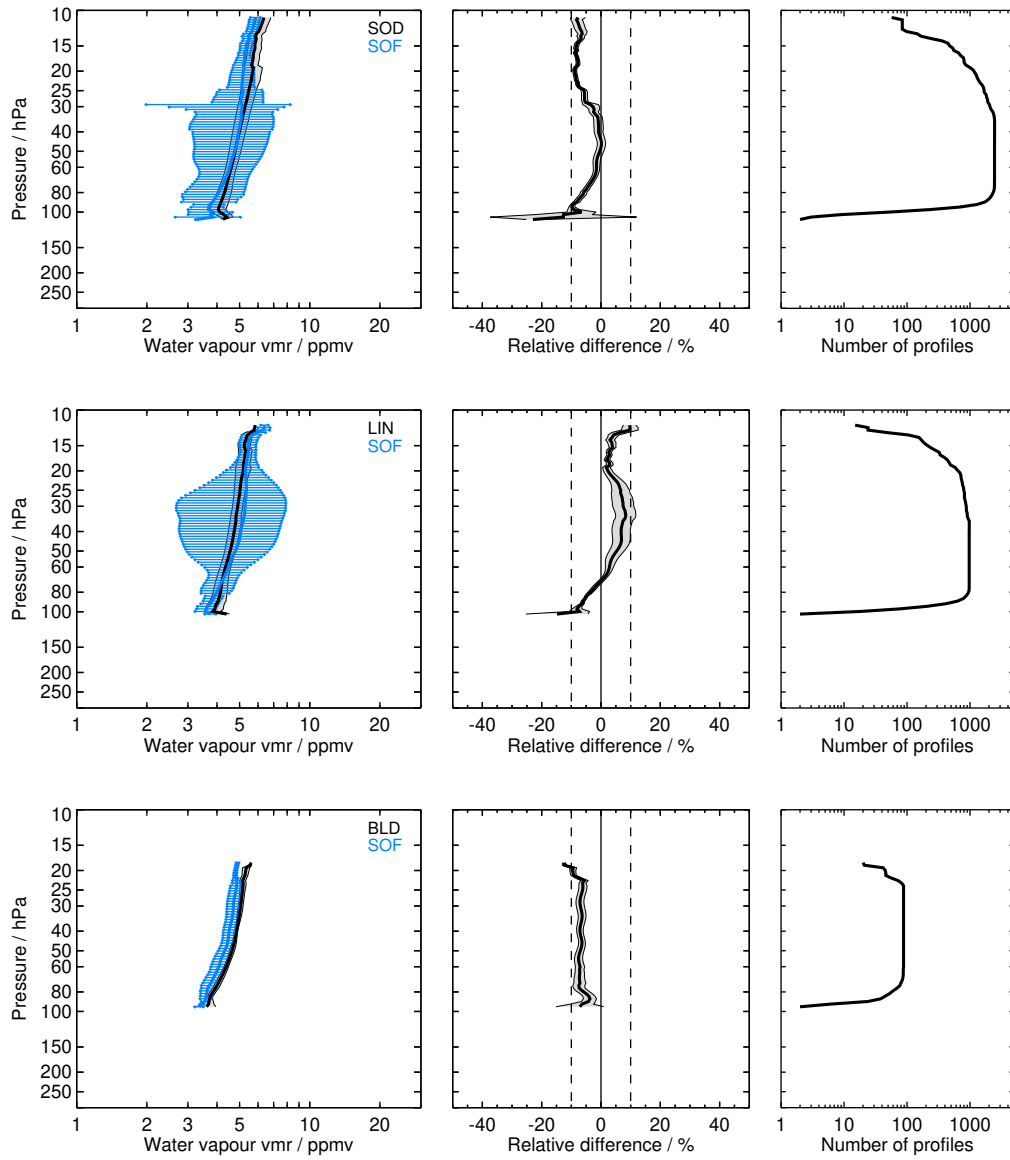


Figure S31: Same as Fig. S1 but for SOF and the SOD, LIN, BLD, HIL, SJC, LDR, and LDR balloon sites.

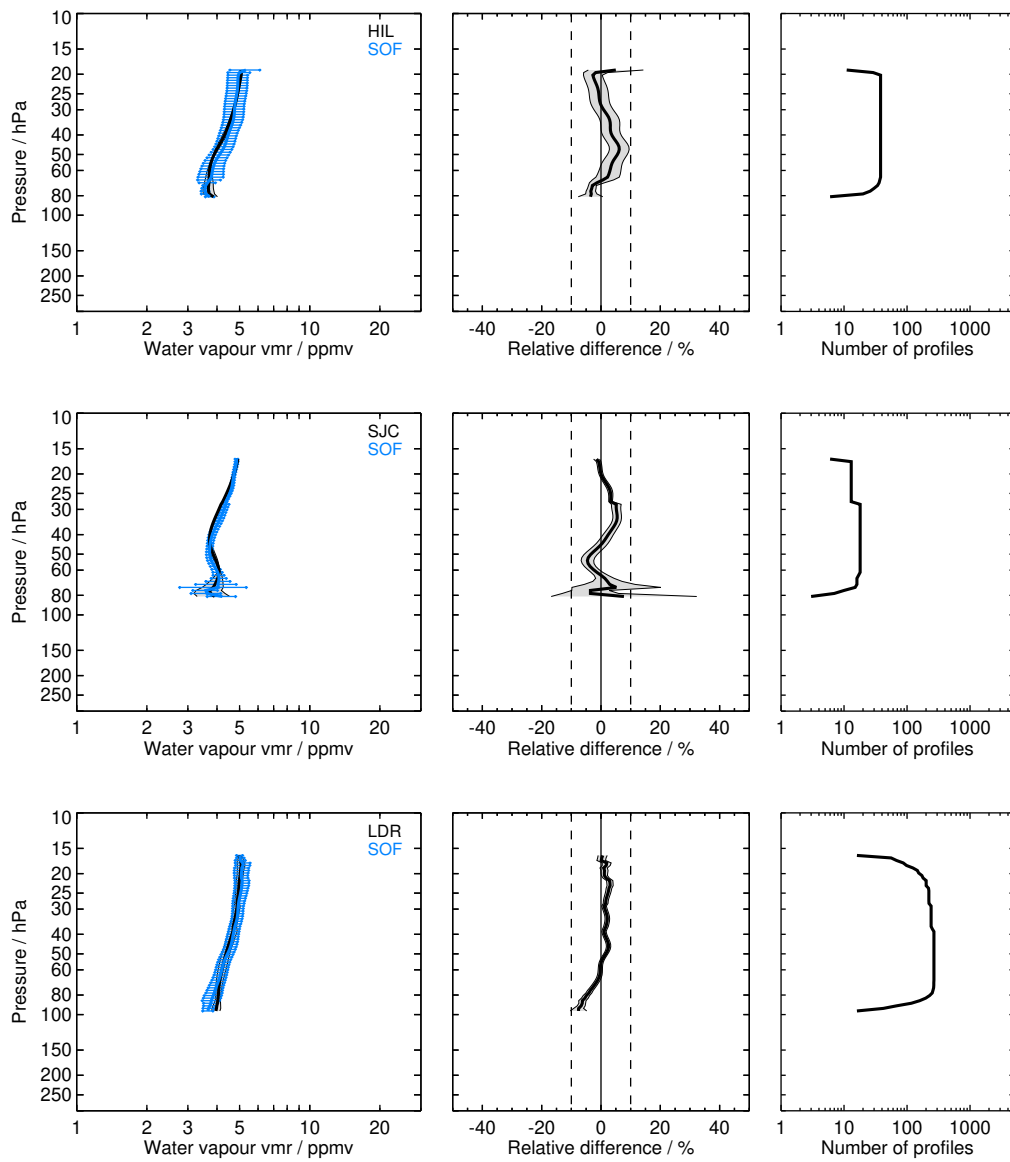


Figure S31: Continued.